



ECONOMIC GEOLOGY RESEARCH INSTITUTE HUGH ALLSOPP LABORATORY

**University of the Witwatersrand
Johannesburg**

**SCIENTIFIC CONTRIBUTIONS BY STAFF AND
STUDENTS OF THE SCHOOL OF GEOSCIENCES,
UNIVERSITY OF THE WITWATERSRAND,
JOHANNESBURG**

**11TH Quadrennial IAGOD Symposium and Geocongress
2002, Windhoek, Namibia
22-26 July, 2002**

C.R.ANHAEUSSER

• INFORMATION CIRCULAR No. 362

UNIVERSITY OF THE WITWATERSRAND
JOHANNESBURG

**SCIENTIFIC CONTRIBUTIONS BY STAFF AND STUDENTS OF THE SCHOOL OF
GEOSCIENCES, UNIVERSITY OF THE WITWATERSRAND, JOHANNESBURG**

**11th Quadrennial IAGOD Symposium and Geocongress 2002,
Windhoek, Namibia**

22-26 JULY, 2002

Compiled by

C.R. ANHAEUSSER

*(Economic Geology Research Institute-Hugh Allsopp Laboratory,
School of Geosciences, University of the Witwatersrand,
Private Bag 3, P.O. Wits 2050, Johannesburg, South Africa)*

**ECONOMIC GEOLOGY RESEARCH INSTITUTE
INFORMATION CIRCULAR No. 362**

September, 2002

SCIENTIFIC CONTRIBUTIONS BY STAFF AND STUDENTS OF THE SCHOOL OF GEOSCIENCES, UNIVERSITY OF THE WITWATERSRAND, JOHANNESBURG

CONTENTS	Page
1. SOUTHERN AFRICAN ARCHAEOAN TERRANES	
ULTRAMAFIC COMPLEXES ALONG THE NORTHERN FLANK OF THE BARBERTON GREENSTONE BELT, SOUTH AFRICA: REMNANTS OF OCEANIC LITHOSPHERE ALONG AN ARCHAEOAN SUTURE ZONE?	<i>C.R. ANHAEUSSER</i> 1
ARCHAEOAN GRANITOIDS ROCKS OF THE MAKOPPA DOME, LIMPOPO PROVINCE, SOUTH AFRICA: PRELIMINARY PETROLOGICAL AND GEOCHEMICAL RESULTS.....	<i>C.R. ANHAEUSSER</i> 6
TECTONIC CONTROLS ON GOLD MINERALISATION IN THE ZIMBABWE CRATON.....	<i>P.H.G.M. DIRKS</i> and A. MIKHAIEV 10
GEOLOGY AND MINERALISATION MODEL FOR THE ABELSKOP BIF-HOSTED LODE GOLD DEPOSIT – AMALIA GREENSTONE BELT, SOUTH AFRICA	<i>ROBERT KIEFER</i> 12
ARCHAEOAN CRUSTAL EVOLUTION OF THE CENTRAL PARTS OF THE KAAPVAAL CRATON: EVIDENCE FROM THE VREDEFORT DOME, SOUTH AFRICA.....	<i>C. LANA, R.L. GIBSON AND W.U. REIMOLD</i> 16
2. CENTRAL AFRICAN COPPERBELT	
CONTRIBUTIONS TO THE GEOLOGY AND MINERALIZATION OF THE CENTRAL AFRICAN COPPER-BELT: I. NATURE AND GEOCHRONOLOGY OF THE PRE-KATANGAN BASEMENT.....	<i>C. RAINAUD, R. A. ARMSTRONG, S. MASTER, L. J. ROBB</i> and P.A.C.C. MUMBA* 19
CONTRIBUTIONS TO THE GEOLOGY AND MINERALIZATION OF THE CENTRAL AFRICAN COPPER-BELT: II. NEOPROTEROZOIC DEPOSITION OF THE KATANGA SUPERGROUP WITH IMPLICATIONS FOR REGIONAL AND GLOBAL CORRELATIONS.....	<i>S. MASTER, C. RAINAUD, R. A. ARMSTRONG, D. PHILLIPS</i> and <i>L. J. ROBB</i> 24
CONTRIBUTIONS TO THE GEOLOGY AND MINERALIZATION OF THE CENTRAL AFRICAN COPPER-BELT: III - NATURE OF METAMORPHIC AND EPIGENETIC FLUIDS.....	<i>L.N. GREYLING, Y. YAO, L.J. ROBB</i> and <i>S. MASTER</i> 29
CONTRIBUTIONS TO THE GEOLOGY AND MINERALIZATION OF THE CENTRAL AFRICAN COPPER-BELT: IV. MONAZITE U-Pb DATING AND ^{40}Ar - ^{39}Ar THERMOCHRONOLOGY OF METAMORPHIC EVENTS DURING THE LUFILIAN OROGENY.....	<i>C. RAINAUD, S. MASTER, R. A. ARMSTRONG, D. PHILLIPS</i> and <i>L. J. ROBB</i> 33
CONTRIBUTIONS TO THE GEOLOGY AND MINERALIZATION OF THE CENTRAL AFRICAN COPPER-BELT: V. SPECULATIONS REGARDING THE ‘SNOWBALL EARTH’ AND REDOX CONTROLS ON STRATABOUND Cu-Co AND Pb-Zn MINERALIZATION.....	<i>L. J. ROBB, S. MASTER, L. N. GREYLING, Y. YAO</i> and <i>C. L. RAINAUD</i> 38
3. PGE-BEARING LAYERED INTRUSIONS - CHINA	
PGE-BEARING LAYERED INTRUSIONS IN THE SOUTHWEST SICHUAN PROVINCE, PEOPLE'S REPUBLIC OF CHINA.....	<i>Y. YAO, M. J. VILJOEN, R. P. VILJOEN, A. H. WILSON, H. ZHONG, B. G. LIU, H. L. YING, G. Z. TU</i> and <i>Y. N. LUO</i> 44
XINJIE LAYERED INTRUSION IN THE SICHUAN PROVINCE, SW CHINA: A GEOCHEMICAL, PETROLOGICAL AND PGE MINERALIZATION STUDY.....	<i>Y. YAO, H. ZHONG, S. A. PREVEC, M. J. VILJOEN, R. P. VILJOEN, A. H. WILSON, B. G. LIU, H. L. YING</i> and <i>Y. N. LUO</i> 48

Note: Names of Wits University staff and students in bold italics

TRACE ELEMENT GEOCHEMISTRY OF THE HONGGE LAYERED INTRUSION IN THE PAN-XI AREA, SOUTHWESTERN CHINA.....	<i>H. ZHONG, Y. YAO, X. H. ZHOU, B. G. LIU, M. SUN, M. F. ZHOU, M. J. VILJOEN and R. P. VILJOEN</i>	52
---	---	----

4. BUSHVELD COMPLEX AND OTHER INTRUSIONS

A RE-EVALUATION OF THE LINK BETWEEN CHROMITITE FORMATION AND PGE ENRICHMENT IN THE BUSHVELD COMPLEX.....	<i>JUDITH A. KINNAIRD, F. JOHAN KRUGER , PAUL A.M. NEX and R. GRANT CAWTHORN</i>	57
PLAGIOCLASE-RICH CYCLIC UNITS IN THE BUSHVELD COMPLEX.....	<i>L. SPIES and R.G. CAWTHORN</i>	63
BIFURCATING CHROMITITES IN THE BUSHVELD COMPLEX, SOUTH AFRICA: MAGMATIC ANALOGUES OF SAND VOLCANOES.....	<i>P.A. NEX</i>	66
THE MOCHILA LAYERED COMPLEX-VENEZUELA : A PGE EXPLORATION CASE STUDY.....	<i>R. P. VILJOEN</i>	72
THE FOY OFFSET DYKE, AN ORE-BEARING IMPACT GENERATED FRACTURE, SUBDURY STRUCTURE, ONTARIO, CANADA	<i>M. G. TUCHSCHERER and J. G. SPRAY</i>	76

5. WITWATERSRAND

SEDIMENTOLOGICAL MODEL AND RE- EVALUATION OF THE MAIN REEF LEADER, CENTRAL RAND GOLDFIELD.....	<i>M.J. VILJOEN and R.P. VILJOEN</i>	79
MINERALIZATION ASSOCIATED WITH IMPACT STRUCTURES, WITH SPECIAL REFERENCE TO THE VREDEFORT-WITWATERSRAND SYSTEM.....	<i>WOLF UWE REIMOLD</i>	83
ENVIRONMENTAL ASPECTS ASSOCIATED WITH THE PAST, PRESENT AND FUTURE MINING OF THE CENTRAL RAND.....	<i>N.F. MPHEPHU and M.J. VILJOEN</i>	86

6. OTHER MINERALIZATION

GEOLOGY OF THE “ROUND MOUNTAIN” GOLD MINE IN NEVADA, UNITED STATES OF AMERICA, AND POTENTIAL FOR EXPLORATION OF SIMILAR DEPOSITS IN THE ANDES.....	<i>ALBERTO LOBO-GUERRERO</i>	89
GEMSTONES OF SOMALILAND: SUSTAINABLE DEVELOPMENT OF THE SMALL-SCALE MINING SECTOR.....	<i>JUDITH A. KINNAIRD</i>	94
PLATINUM-GROUP MINERALOGY IN THE KATINNIQ AND ZONE 2 OREBODIES, RAGLAN NI-CU (PGE) SULPHIDE DEPOSIT, CAPE SMITH, CANADA.....	<i>CHARLIE L. SEABROOK, HAZEL M. PRICHARD and P. C. FISHER</i>	99

7. GENERAL

H ₂ O: A FUNCTIONAL ANALOGUE FOR CONTINENTAL Margin RIFT TECTONICS?	<i>STEPHEN A. PREVEC</i>	102
JIGSAW BRECCIAS AN INTRODUCTION TO HYDROTHERMAL BRECCIAS.....	<i>ALBERTO LOBO-GUERRERO</i>	105
GEOLOGY AND STRUCTURAL SETTING OF THE JAMIESON WINDOW, MT USEFUL SLATE BELT, VICTORIA AUSTRALIA.....	<i>F. WIELAND</i>	110
REUNITING LOST CONTINENTS – FOSSIL REPTILES FROM THE ANCIENT KAROO AND THEIR WANDERLUST.....	<i>BRUCE S. RUBIDGE</i>	112

ACKNOWLEDGEMENTS

Staff and senior students in the School of Geosciences, University of the Witwatersrand, Johannesburg, in collaboration with colleagues locally and abroad, contributed the papers that are presented in this Information Circular at the 11th Quadrennial IAGOD Symposium and Geocongress 2002, held in Windhoek, Namibia from 22-26 July, 2002. The papers, together with others presented at the Windhoek meeting, were refereed by a Review Panel whose names appear on the CD ROM of Extended Abstracts published by the Geological Survey of Namibia and made available to delegates registered at the conference. Richard Montjoie contributed greatly with his computer skills to the successful production of both the CD ROM and this Information Circular.

oOo

**Published by the Economic Geology Research Institute
(incorporating the Hugh Allsopp Laboratory)**
School of Geosciences
University of the Witwatersrand
1 Jan Smuts Avenue
Johannesburg
South Africa

HTTP://WWW.WITS.AC.ZA/EGRU

ISBN 1-86838-314-8

1. SOUTHERN AFRICAN ARCHAean TERRANES

ULTRAMAFIC COMPLEXES ALONG THE NORTHERN FLANK OF THE BARBERTON GREENSTONE BELT, SOUTH AFRICA: REMNANTS OF OCEANIC LITHOSPHERE ALONG AN ARCHAean SUTURE ZONE?

C.R. ANHAEUSSER

Economic Geology Research Institute – Hugh Allsopp Laboratory

School of Geosciences, University of the Witwatersrand,

Private Bag 3, P.O. Wits 2050, Johannesburg, South Africa

e-mail: 065cra@cosmos.wits.ac.za

SYNOPSIS

Geotectonic reconstructions indicate that a number of Archaean layered ultramafic complexes and associated ultramafic-mafic volcanic rocks are developed in a zone, believed to be a suture or oceanic crustal collisional zone, along the northern flank of the Barberton greenstone belt, South Africa. The ultramafic complexes, which resulted from the differentiation of komatiitic parent magma, consist mainly of serpentinized dunite, harzburgite and pyroxenite and minor gabbro. The ultramafic-mafic associations may be likened to oceanic crust or “Layered Series” assemblages of Phanerozoic ophiolites. Serpentinized ultramafic components of ophiolites are, in turn, often encountered in orogenic belts where they commonly mark the positions of suture zones. U-Pb zircon dating suggests that the Barberton greenstone terrane is formed of two principal crustal blocks (ca. 3450 and 3230 Ma old) each of which have been interpreted to comprise an amalgamation of other arc-like crustal blocks. Thus convergence of the early oceanic crust appears to have occurred in stages, being responsible for successive episodes of calc-alkaline volcanism (Upper Onverwacht Group) and accompanying TTG granitoid plutonism. Age relationships in Archaean greenstone belts are generally constrained by dating TTG igneous and volcanic events. Accurate age constraints have yet to be provided for the oceanic lithosphere conveyed to sites of subduction and which, in turn, constitute protoliths for the ensuing TTG magmatism.

INTRODUCTION

Ultramafic and related rocks are of widely differing types and occur in a broad range of geological and geotectonic environments (Wyllie, 1967). Some occur in variably sized stratiform intrusions like the Bushveld, Skaergaard, Stillwater, Great Dyke and Muskox intrusions (Eales and Cawthorn, 1996; Irvine and Smith, 1967; McCallum, 1996; McBirney, 1996; Wilson, 1996), whilst others occur as alkalic ring complexes or kimberlite intrusives (Gold, 1967; Dawson, 1967). Close scrutiny worldwide, however, reveals that most ultramafic rocks occur as remnants of oceanic crust and upper mantle caught up and emplaced in Phanerozoic orogenic belts as a result of plate tectonic processes. These include the Alpine-type peridotite-serpentinite bodies distributed along deformed mountain chains and island arcs (Thayer, 1967) and the concentrically zoned dunite-peridotite intrusive complexes of southeastern Alaska and the Ural Mountains of Russia (Irvine, 1967; Taylor, 1967). Most Alpine-type ultramafic-mafic associations are regarded as being synonymous with ophiolite suites, the latter considered to be slices of oceanic crust and mantle tectonically emplaced in orogenic belts. Some of the best-known ophiolite occurrences include those of Troodos in Cyprus (generally regarded as the classic type example – Moores and Vine, 1971; Robertson and Xenophontos, 1993), and the ophiolites of the Oman Tethys (Semail Ophiolite along the coastline of the Gulf of Oman – Lippard et al., 1986).

Dewey and Bird (1970, 1971) described the ophiolite suite as having been generated at oceanic ridges, and by slow spreading in marginal basins behind and within island-arc complexes. They showed that many ophiolites in orogenic belts (e.g., the Alpine orogenic belt), occur in a variety of tectonic settings, including those found as severely deformed and serpentinized bodies in suture zones, in sutured mélange terranes, and as thrust wedges. Because serpentinized ultramafic rocks are a common feature of most early Archaean greenstone belts there have also been attempts to equate these rock associations with Phanerozoic ophiolite complexes (de Wit et al., 1987). However, adherence to the GSA Penrose Conference definition of an ophiolite (Anonymous, 1972), shows several important differences (one of these being the complete absence of mafic sheeted dyke complexes in Archaean

terranes) making direct comparison untenable. The presence of ophiolites in Archaean or even Proterozoic terranes has thus proved to be controversial (Bickle et al., 1995; Hamilton, 1998). If the strict definition of ophiolite is disregarded it could be argued that greenstone belts contain slices of Archaean oceanic lithosphere produced as a prototype to present day plate tectonic-related oceanic crust. Furthermore, theoretical and actualistic models are increasingly pointing to an Archaean tectonic regime not fundamentally different from that of today (Lowe, 1999).

BARBERTON GREENSTONE BELT

Ultramafic and mafic rocks are extensively developed in the Barberton greenstone belt (BGB), South Africa, and comprise volcanic outpourings of komatiite, komatiitic basalt and high-Mg tholeiite, as well as numerous layered ultramafic complexes (Viljoen and Viljoen, 1969; Anhaeusser, 1985). Recent interpretations suggest that the ultramafic-mafic lava successions are similar to modern oceanic plateau assemblages (Cloete, 1999; Dann, 2000). By contrast the Archaean layered ultramafic complexes have been regarded as penecontemporaneous sill-like intrusive bodies formed in shallow-seated magma chambers following the differentiation of komatiitic parent magmas (Anhaeusser, 1985). This contribution examines the possibility that the ultramafic complexes form part of the oceanic crust in existence early in the evolution of the BGB and that these rocks were emplaced along a primitive consuming plate boundary today manifest along the northern flank of the BGB..

Anhaeusser (1985) recorded the presence of 27 ultramafic complexes in the BGB, most of which show pronounced magmatic differentiation and the common development of cyclically repeated layering consisting dominantly of dunite, orthopyroxenite, and harzburgite and volumetrically subordinate websterite and anorthositic gabbro-norite units. Although Archaean ultramafic complexes are known from around the world, most are considerably less magnesian than the Barberton examples, which appear to have developed from parental komatiite magmas with about 28% MgO. It has been estimated that dunite, harzburgite and lherzolite constitute as much as 80% by volume of some of the complexes, the remainder consisting of ortho- and clinopyroxenites and minor gabbro-norite phases. Most of the ultramafic rocks have been extensively serpentinized and steatized to various talc ± tremolite ± chlorite ± carbonate schists or massive rock assemblages.

Field studies undertaken along the northern flank of the BGB (Anhaeusser, 1969, 1972) indicated that 19 ultramafic complexes occurred in the region (Fig.1A) and may once have formed either a single continuous, sheet-like intrusion, or a series of related, but probably discontinuous sill-like bodies.

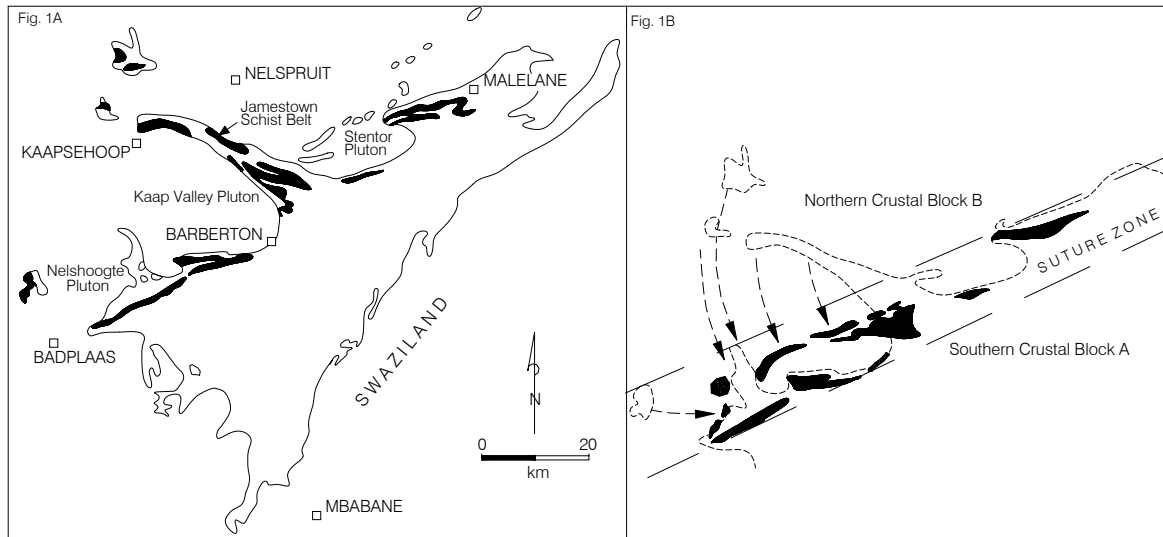


Figure 1: (A) Simplified map showing the present distribution of layered ultramafic complexes along the northern flank of the Barberton greenstone belt. (B) Schematic reconstruction - minus the influence of the Kaap Valley, Nelshoogte and Stentor granitoid plutons - showing the alignment of the ultramafic complexes along a possible suture or convergence zone separating a southern crustal block (ca. 3445 Ma) from a northern block (ca. 3227 Ma).

These bodies were shown to extend from Malelane in the northeast, towards Badplaas in the southwest – a distance of approximately 110km, almost the length extent of the BGB. A reconstruction of their likely disposition prior to the emplacement of the Kaap Valley tonalite pluton at 3227 ± 1 Ma (Kamo and Davis, 1994) is shown in Figure 1B. It was envisaged (Anhaeusser, 1969) that prior to emplacement of the Kaap Valley pluton the rocks comprising the Jamestown Schist Belt, as well as the belt of massive and schistose ultramafic and mafic rocks southwest of Barberton (see Wuth, 1980), may have formed a contiguous stratigraphic zone. Field evidence supporting this notion includes the close similarity of the various components of the Onverwacht Group rocks present in both regions, and the presence of a series of chrysotile asbestos and verdite-buddstone deposits as well as occurrences of stichtite-barbertonite unique to these two localities.

The reconstruction (Fig.1B) envisages removing the diapiric Kaap Valley pluton and swinging the arcuate Jamestown Schist Belt into a position parallel to the NE-SW regional trend of the BGB, in much the same manner as the jaws of a closing pair of scissors. In so doing the various layered ultramafic complexes occupy an almost continuous zone along the northwest flank of the greenstone belt. Embayments by other intrusive TTG granitoid bodies (Stentor and Nelshoogte plutons) also produce local disruption to the continuity of the ultramafic-mafic rock exposures along the zone.

CONCLUSIONS

A number of studies have demonstrated that the BGB is a compound terrane formed through long-term magmatic activity and late-stage tectonic accretion. Evidence available suggests that the BGB represents a compound crustal block constructed of a number of amalgamated crustal blocks formed over a time-span variously placed at between 330-490Ma (de Ronde and de Wit, 1994; Lowe, 1999). It has been argued further that collision-like processes were responsible for the late-stage tectonism reflected in the amalgamation and suturing of the earlier-formed protocontinental blocks. Given this scenario it is suggested here that the zone occupied by the ultramafic complexes described earlier may represent a further manifestation of convergence of two separate crustal blocks in a manner akin to obducted oceanic crust commonly found in orogenic suture zones and in sutured mélange terranes. Precise dating techniques now clearly identify an older southern crustal domain (> 3445 Ma) from a younger (ca. 3227 Ma) northern domain (Kamo and Davis, 1994). It is suggested, therefore, that the ultramafic-mafic wedge separating these two crustal blocks reflects a consuming margin along and into which were emplaced TTG granitoids following subduction-related arc-like volcanism. Figure 2 indicates schematically the possible nature of the collisional interface, with the Fig Tree and Moodies sediments as well as earlier calc-alkaline volcanic rocks (Upper Onverwacht assemblages) occurring to the south and representing products of the subduction event. This could imply that the poorly time-constrained ultramafic-mafic zone in the north as well as the Onverwacht type-locality komatiitic assemblages on the southern side of the BGB may be part of the same oceanic crust and lithosphere upon which the later arc-like events of volcanism and magmatism were developed.

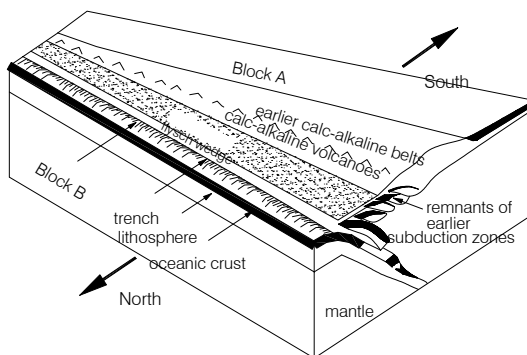


Figure 2: Schematic block diagram showing the collisional interface or suture zone along which the oceanic crust and ultramafic complexes were emplaced on the northern flank of the the Barberton greenstone belt. Fig Tree and Moodies Group sediments (the flysch wedge) and calc-alkaline, arc-like volcanics (Upper Onverwacht) occupy the area to the south on amalgamated crustal block A. Oceanic crust subducted along the trench led eventually to the emplacement of the Kaap Valley, Nelshoogte and Stentor granitoid plutons (Fig.1A), which intruded into the younger crustal block B (diagram modified after Dewey and Bird, 1971).

REFERENCES

- Anhaeusser, C.R. (1969). The stratigraphy, structure and gold mineralization of the Jamestown and Sheba Hills area of the Barberton Mountain Land. PhD thesis (unpubl.), Univ. Witwatersrand, Johannesburg, 322pp.
- Anhaeusser, C.R. (1972). The geology of the Jamestown Hills area of the Barberton Mountain Land, South Africa. *Trans. Geol. Soc. S. Afr.*, 75 (3), 225-263.
- Anhaeusser, C.R. (1985). Archaean layered ultramafic complexes in the Barberton Mountain Land, South Africa, 281-301. In: Ayres, L.D., Thurston, P.C., Card, K.D. and Weber, W (eds.), *Evolution of Archean Supracrustal Sequences*. Spec. Paper Geol. Assoc. Canada, 28, 380pp.
- Anonymous (1972). Ophiolites. *Geotimes*, 17, 24-25.
- Bickle, M.J., Nisbet, E.G. and Martin, A. (1995). Archaean greenstone belts are not oceanic crust. *J. Geol.*, 102, 121-138.
- Cloete, M. (1999). Aspects of volcanism and metamorphism of the Onverwacht Group lavas in the southwestern portion of the Barberton greenstone belt. *Mem. Geol. Surv. S. Afr.*, 84, 232pp.
- Dann, J.C. (2000). The 3.5Ga Komati Formation, Barberton greenstone belt, South Africa, Part I: new maps and magmatic architecture. *S. Afr. J. Geol.*, 103(1), 47-68.
- Dawson, J.B. (1967). A review of the geology of kimberlite, 241-251. In: Wyllie, P. J. (ed.), *Ultramafic and Related Rocks*. John Wiley & Sons, New York, 464pp..
- Dewey, J.F. and Bird, J.M. (1970). Mountain belts and the new global tectonics. *J. Geophys. Res.*, 75 (14), 2625-2647.
- Dewey, J.F. and Bird, J.M. (1971). Origin and emplacement of the ophiolite suite: Appalachian ophiolites in Newfoundland. *J. Geophys. Res.*, 76 (14), 3179-3206.
- de Ronde, C.E.J. and de Wit, M. J. (1994). Tectonic history of the Barberton greenstone belt, South Africa: 490 million years of Archean crustal evolution. *Tectonics*, 13 (4), 983-1005.
- de Ronde, C.E.J. and Kamo, S. (2000). An Archaean arc-arc collisional event:a short-lived (ca 3Myr) episode, Weltevreden area, Barberton greenstone belt, South Africa. *J. Afr. Earth Sci.*, 30, 219-248.
- de Wit, M.J., Hart, R.A. and Hart, R.J. (1987). The Jamestown Ophiolite Complex, Barberton mountain belt: a section through 3.5Ga oceanic crust. *J. Afr. Earth Sci.*, 6 (5), 681-730.
- Eales, H. V. and Cawthorn, R.G. (1996). The Bushveld Complex, 181-231. In: Cawthorn, R.G.(ed.) *Layered Intrusions*, Elsevier, Amsterdam, 531pp.
- Gold, D.P. (1967). Alkaline ultrabasic rocks in the Montreal area, Quebec, 288-302. In: Wyllie, P. J. (ed.), *Ultramafic and Related Rocks*. John Wiley & Sons, New York, 464pp.,
- Hamilton, W.B. (1998). Archaean magmatism and deformation were not products of plate tectonics. *Precambrian Res.*, 91, 143-179.
- Irvine, T.N. (1967). The Duke Island ultramafic complex, southeastern Alaska, 84-97. In: Wyllie, P. J. (ed.), *Ultramafic and Related Rocks*. John Wiley & Sons, New York, 464pp.
- Irvine and Smith (1967). The ultramafic rocks of the Muskox intrusion Northwest Territories, Canada, 38-49. In: Wyllie, P. J. (ed.), *Ultramafic and Related Rocks*. John Wiley & Sons, New York, 464pp.
- Kamo, S. and Davis, D.W. (1994). Reassessment of Archaean crustal development in the Barberton Mountain Land, South Africa based on U-Pb dating. *Tectonics*, 13, 167-192.
- Lippard, S. J., Shelton, A.W. and Gass, I.G. (1986). The Ophiolite of Northern Oman. *Mem. Geol. Soc. Lond.*, 11, 178pp.
- Lowe, D.R. (1999). Geologic evolution of the Barberton greenstone belt and vicinity. *Geol. Soc. Amer. Spec. Paper* 329, 287-312.
- McBirney (1996). The Skaergaard intrusion, 147-180. In: Cawthorn, R.G. (ed.) *Layered Intrusions*, Elsevier, Amsterdam, 531pp.
- McCallum (1996). The Stillwater Complex, 441-483. In: Cawthorn, R.G. (ed.) *Layered Intrusions*, Elsevier, Amsterdam, 531pp.
- Moores, E. M. and Vine, F.J. (1971). Troodos Massif, Cyprus and other ophiolites as oceanic crust: evaluation and implications. *Phil.Trans. Roy. Soc.Lond.*, A268, 443-466.
- Robertson and Xenophontos (1993). Development of concepts concerning the Troodos ophiolite and adjacent units in Cyprus, 85-119. In: Prichard, H. M., Alabaster, T., Harris, N.B.W. and Neary, C. R. (eds.), *Magmatic Processes and Plate Tectonics*. Spec. Publ. Geol. Soc. Lond., 76, 526pp.
- Taylor, H.P. (1967). The zoned ultramafic complexes of southeastern Alaska, 97-121. In: Wyllie, P.J. (ed.), *Ultramafic and Related Rocks*, John Wiley & Sons, New York, 464pp.

- Thayer, T.P. (1967). Chemical and structural relations of ultramafic and feldspathic rocks in Alpine intrusive complexes, 222-239. In: Wyllie, P.J. (ed.), Ultramafic and Related Rocks, John Wiley & Sons, New York, 464pp.
- Viljoen, M.J. and Viljoen, R.P. (1969). The geology and geochemistry of the Lower Ultramafic Unit of the Onverwacht Group and a proposed new class of igneous rock. Spec. Publ. Geol. Soc. S. Afr., 2, 55- 85.
- Wilson, A.H. (1996). The Great Dyke of Zimbabwe, 365-402. In: Cawthorn, R.G. (ed.) Layered Intrusions, Elsevier, Amsterdam, 531pp.
- Wuth, M. (1980). The geology and mineralization potential of the Oorschot-Weltevreden schist belt, south-west of Barberton – Eastern Transvaal. MSc thesis (unpubl.), Univ. Witwatersrand, Johannesburg, 185pp.
- Wyllie, P.J. (1967). Ultramafic and ultrabasic rocks, 1-7. In: Wyllie, P.J. (ed.), Ultramafic and Related Rocks, John Wiley & Sons, New York, 464pp.

oOo

ARCHAEOAN GRANITOIDS ROCKS OF THE MAKOPPA DOME, LIMPOPO PROVINCE, SOUTH AFRICA: PRELIMINARY PETROLOGICAL AND GEOCHEMICAL RESULTS

C.R. ANHAEUSSER

Economic Geology Research Institute – Hugh Allsopp Laboratory
School of Geosciences, University of the Witwatersrand,
Private Bag 3, P.O. Wits 2050, Johannesburg, South Africa
e-mail: 065cra@cosmos.wits.ac.za

SYNOPSIS

Preliminary field observations, together with petrological and geochemical (major, trace and REE) analyses have led to the recognition of at least three granitoid varieties intruded into Archaean metavolcanic greenstone remnants developed on the Makoppa Dome, Limpopo Province, South Africa. Trondhjemite grey gneisses appear to represent the oldest granitoids (Vaalpenskraal-type), followed by homogeneous, coarse-grained, reddish-coloured, porphyritic granodiorites (Makoppa-type), the latter intruded by dykes of pegmatite and aplite also having a deep red colour. The third granitoid variety consists of homogeneous, medium-grained, greyish-pink granodiorites (Rietkuil-type). The granitoid rocks display chemical characteristics consistent with those produced in volcanic-arc or syn-collisional geotectonic settings. These findings add support to a recent proposal suggesting that the Kaapvaal Craton formed about an older nucleus (ca. 3600-3200 Ma), onto which annealed younger segments of the craton, the latter events being facilitated by the development, at ca. 3100-3000 Ma, of a major crescent-shaped juvenile arc extending around the northern and western margins of the evolving Kaapvaal Craton.

INTRODUCTION

The Makoppa Dome, located northwest of Thabazimbi in the Limpopo Province, South Africa, occupies an ovoid-shaped area over 5000km² in extent, which is largely rimmed by outward-dipping Neoarchaean and Eoproterozoic volcanic and sedimentary rocks of the Ventersdorp and Transvaal Supergroups in the southeast and Palaeoproterozoic Waterberg sediments in the north. The Makoppa Dome, which also extends across the border into neighbouring southeastern Botswana, represents a poorly exposed remnant of Archaean granite-greenstone basement on the northwestern rim of the Kaapvaal Craton, the region being extensively covered by Tertiary-to-Quaternary soil, gravel, limestone and Kalahari sand (Jansen, 1974). Because of the generally poor exposure and, more recently, the subdivision of the terrain into game farms that have restricted access, the area has not received much geological attention.

The Makoppa Dome occupies an important link between Archaean basement exposures of the northwest-trending Kraaipan terrane (ca. 3250-2791 Ma) on the western edge of the Kaapvaal Craton and the northeast-trending Murchison granite-greenstone terrane (ca. 3200-2874 Ma) on the northeastern edge of the craton (Poujol et al., 1996; 2001; 2002).

GENERAL GEOLOGY

Archaean granitoid rocks, according to Jansen (1974), underlie most of the Makoppa Dome. Scattered greenstone remnants have also been recorded and occur mainly in the northeastern sector of the dome, northeast of the Crocodile River, and in the southern sector, between Dwaalboom and Thabazimbi. The greenstone occurrences, which are undifferentiated, consist mainly of various amphibole and talc schists and serpentinite, together with metasediments consisting of banded iron formation, arkose and quartzite. The granitoid rocks, also undifferentiated, were described by Jansen (1974) as consisting of granite and granite-gneiss with some granulite and diorite/norite.

Aeromagnetic data (CFG, 1975) suggests that numerous dykes intrude the Makoppa Dome, but these are rarely exposed. In the south a prominent NW-SE dyke swarm is indicated, but further north a lesser number of preferentially WNW-ESE striking dykes are present.

THIS STUDY

During the present study reconnaissance field investigations, particularly along the Crocodile River and regions to the northeast, have led to the recognition of three granitoid varieties. These include: (1) grey, medium-to-coarse grained, in places weakly foliated or weakly banded, gneissic granitoids, mostly seen with a subhorizontal foliation; (2) reddish, coarse-grained, homogeneous, porphyritic granitoids intruded by fine-grained, reddish-coloured aplitic dykes and coarse-grained pegmatite dykes; and (3) grey-to-pinkish-grey, medium-to-fine grained, homogeneous, in places porphyritic granitoids. The relationships of the three granitoid varieties to one another could not be established directly in the field - hence reliance will have to be placed on future isotopic age determinations.

The *banded and foliated grey gneisses* are, most likely, the oldest of the granitoids and consist of trondhjemites (category I or Vaalpenskraal-type gneisses) containing quartz, albitic plagioclase and biotite (some with rutile needles), as well as accessory amounts of microcline, perthite, apatite, zircon, magnetite and ilmenite. The plagioclase is variably saussuritized and sericitized to epidote, sericite and muscovite. Table 1(column 1) lists an average composition of the trondhjemites, which are distinguished by their high Na₂O, Sr and Ba and low K₂O and Rb contents. Rare earth element (REE) plots (Fig.1A) show the trondhjemites to be relatively enriched in LREE and depleted in HREE with no Eu anomaly.

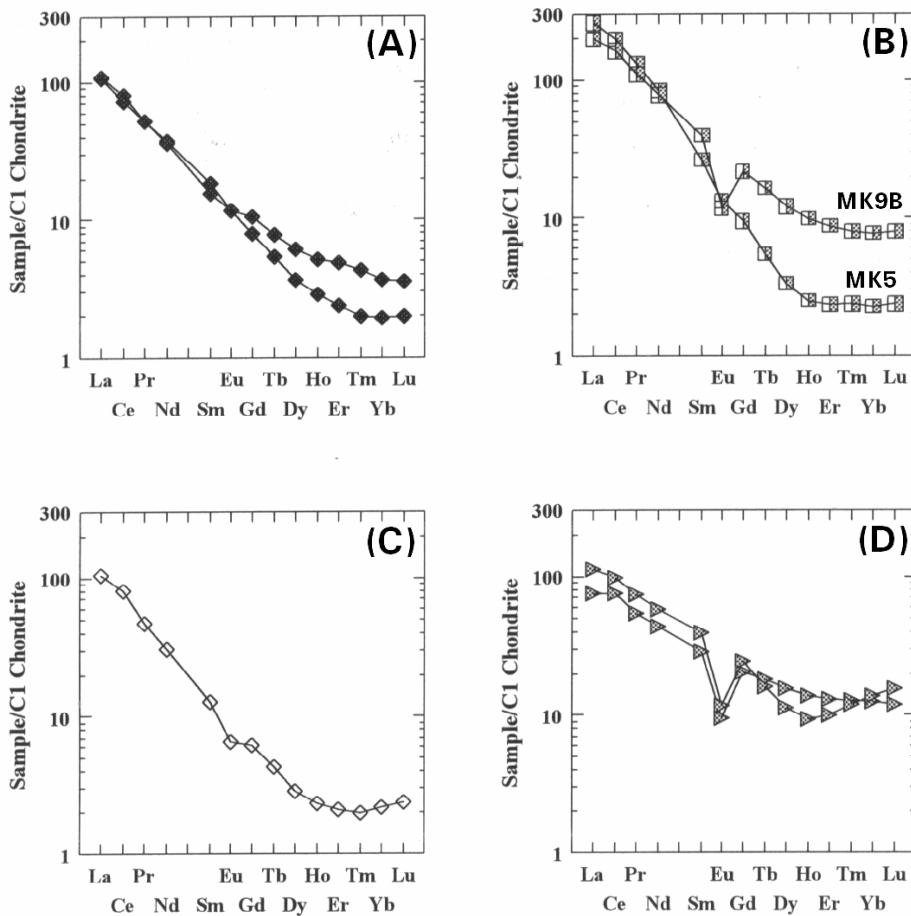


Figure 1: Diagrams showing the REE distribution patterns of the granitoid rocks encountered on the Makoppa Dome. A. Trondhjemitic grey gneisses (Vaalpenskraal-type); B. Homogeneous, coarse-grained, reddish porphyritic granodiorite (Makoppa-type); C. Aplite dyke intruded into granodiorite (B, sample MK5); and D. Homogeneous, medium-grained, grey-to-pink granodiorite (Rietkuil-type).

The *homogeneous, coarse-textured, reddish, porphyritic granitoids* (category II or Makoppa-type granodiorites) contain prominent amounts of K-feldspar (microcline, perthite) and quartz, with lesser biotite, plagioclase (albitic), epidote, muscovite, sericite, ilmenite and leucoxene. The plagioclase

generally displays sericitic alteration and vermicular quartz (myrmekite) replaces K-feldspar. Reddish, fine-grained, generally homogeneous, *aplitic dykes* (usually less than 50cm in width) intrude the porphyritic granitoids but, in places, may show a weak foliation parallel to the dyke margins. The aplites consist of finely crystalline quartz, feldspar (plagioclase and microcline) and epidote, with accessory amounts of biotite, magnetite, apatite and sericite. An average composition of this porphyritic granodiorite variety is listed in Table 1 (column 2) and shows an increase in K₂O, Rb and Zr and a corresponding decrease in Na₂O, CaO, Sr, and Ba, relative to the trondhjemites. Figure 1B shows one sample (MK9B) with a negative Eu anomaly, LREE enrichment and a moderate HREE pattern, and a second sample (MK5) with LREE enrichment, no Eu anomaly and depleted HREEs. This sample has a similar REE pattern to that of the aplite dyke shown in Figure 1C although the LREEs are somewhat depleted in the aplite. The aplite dyke (Table 1, column 4) also shows lower SiO₂ and higher Al₂O₃ and Na₂O contents than the other Makoppa granitoid varieties as well as different trace elements contents.

Table 1: Average major and trace element abundances of an aplitic dyke and three varieties (I-III) of granitiod rocks recognized in the Makoppa Dome

	I	II	III	IV
SiO ₂	72.07	72.99	73.39	68.89
TiO ₂	0.26	0.26	0.24	0.11
Al ₂ O ₃	15.42	14.53	14.02	17.88
Fe ₂ O ₃	1.86	1.97	1.85	1.14
MnO	0.03	0.02	0.04	0.03
MgO	0.34	0.31	0.1	0
CaO	2.03	0.95	1.18	1.22
Na ₂ O	5.58	4.22	4.15	6.19
K ₂ O	2.27	4.68	4.04	4.49
P ₂ O ₅	0.09	0.08	0.11	0.02
ppm				
Ba	763	485	890	720
Rb	65	328	150	162
Sr	497	127	186	211
Y	10	40	14	10
Zr	109	136	157	98
Nb	6	20	8	5
Co	11	10	10	11
Ni	9	9	11	9
Cu	2	2	3	2
Zn	31	31	24	16
V	21	15	20	19
Cr	10	9	16	10

Analyst: S. Farrell, Department of Geology, University of the Witwatersrand, Johannesburg

* Category I or Vaalpenskraal-type (trondhjemite) = Mean of Samples
MK9C, MK10, MK11, MK12 (unpubl. data)

* Category II or Makoppa-type (granodiorite) = Mean of samples
MK5, MK8B, MK9B (unpubl. data)

* Category III or Rietkuil-type (granodiorite) = Mean of samples
MK1, MK2, MK3 (unpubl. data)

* Column IV is an aplitic granitoid dyke (MK4) intruded into II

The *homogeneous, grey-to-pink, medium-grained granodiorites* (category III or Rietkuil-type granodiorites) consist mainly of quartz, microcline and sericitized albitic plagioclase, together with biotite, chlorite, muscovite, epidote, sphene and magnetite. Some large K-feldspar megacrysts poikilitically enclose crystals of quartz and plagioclase and myrmekite is also in evidence. Table 1 (column 3) gives an average composition for this granodiorite variety and shows roughly equal proportions of alkali elements Na₂O and K₂O and Rb and Sr. The contents of Ba and Zr are also greater than in the coarser, red granodiorites. A REE plot for this granitoid variety (Fig. 1D) reflects an overall flatter pattern, with relative enrichment in LREE, moderate HREE abundances and a conspicuous negative Eu anomaly.

CONCLUSIONS

The granitoid rocks on the Makoppa Dome appear to have intruded older greenstone remnants represented by a variety of poorly exposed amphibolitic schists (tremolite- or hornblende-bearing varieties) and banded iron formations. Preliminary geochemical investigations suggest the mafic schists represent metamorphosed tholeiites and high-magnesian basalts.

Reconnaissance field investigations have also led to the recognition of at least three granitoid varieties on the Makoppa Dome. Confirmation of the relative ages of these granitoid rocks awaits future isotopic age dating. The distinctive field characteristics of the three types could, however, be verified both petrologically as well as geochemically using major, trace and REE analytical techniques.

In a manner similar to the ca. 3250-2790 Ma Kraaipan granitic terrane on the western margins of the Kaapvaal Craton (Anhaeusser and Walraven, 1999; Poujol et al., 2001) the three granitic varieties on the Makoppa Dome appear to consist of : (1) early trondhjemitic granitic gneisses that in places show banding and a sub-horizontal layering and foliation (Vaalpenskraal-type); (2) very coarse-grained, homogeneous, in places porphyritic and distinctively reddish granodiorites (Makoppa-type) - the latter intruded by very fine-grained, reddish aplite dykes as well as coarse-textured pegmatitic dykes; and (3) medium-grained, homogeneous, pink-to-grey granodiorites (Rietkuil-type).

Discrimination diagram plots (following Pearce et al., 1984 and Rollinson, 1998, but not presented here) have also shown that the Makoppa granitoids fall within the field of volcanic-arc granites or syn-collisional granites. This oceanic arc or convergent geotectonic setting adds support to the concept, recently outlined by Poujol et al. (2002), that the central core of the Kaapvaal Craton (ca. 3600-3200 Ma) formed a nucleus onto which annealed the younger segments of the craton, both in a northerly and westerly direction. The model further envisaged that cratonic growth was facilitated by the development, at ca. 3100-3000 Ma, of a major crescent-shaped, juvenile arc extending around the northern and western margins of the craton from the Murchison-Giyani-Pietersburg granite-greenstone terrane, westward towards Botswana, and then southwards through the Kraaipan-Amalia granite-greenstone terrane towards Kimberley and beyond.

REFERENCES

- Anhaeusser, C. R. and Walraven, F. (1999). Episodic granitoid emplacement in the western Kaapvaal Craton: evidence from the Archaean Kraaipan granite-greenstone terrane, South Africa. *J. Afr. Earth Sci.*, 28 (2), 289-309.
- Council for Geoscience (CFG) (1975). 1:250 000 Total magnetic field intensity map 2426 Thabazimbi. Regional Aeromagnetic Series, Council for Geoscience, Pretoria.
- Jansen, H. (1974). Explanatory notes. 1:250 000 Geological Series map 2426 Thabazimbi. Geological Survey of South Africa.
- Pearce, J. A., Harris, N. B. W. and Tindle, A. G. (1984). Trace element discrimination diagrams for the tectonic interpretation of granitic rocks. *J. Petrol.*, 25, 956-983.
- Poujol, M., Robb, L.J., Respaut, J.P. and Anhaeusser, C. R. (1996). 3.07-2.97 Ga greenstone belt formation in the northeastern Kaapvaal Craton: implications for the origin of the Witwatersrand basin. *Econ. Geol.*, 91(8), 1455-1461.
- Poujol, M., Anhaeusser, C. R. and Armstrong, R. A. (2001). Episodic granitoid emplacement in the Archaean Amalia-Kraaipan terrane, South Africa: confirmation from single zircon U-Pb geochronology. *J. Afr. Earth Sci.*, 33 (2), 435-449.
- Poujol, M., Robb, L.J., Anhaeusser, C.R. and Gericke, B. (2002). Geochronological constraints on the evolution of the Kaapvaal Craton, South Africa. *Inform. Circ. Econ. Geol. Res. Inst., Univ. Witwatersrand, Johannesburg*, 360, 33pp.
- Rollinson, H.R. (1998). Using Geochemical Data: Evaluation, Presentation, Interpretation. Longman, UK, 352pp.

TECTONIC CONTROLS ON GOLD MINERALISATION IN THE ZIMBABWE CRATON

¹DIRKS, P.H.G.M., and ²MIKHAILOV, A.,

¹School of Geosciences, Univ. of the Witwatersrand, PO Box 3 Wits 2050, Johannesburg;

²SRK Zimbabwe, 28 Kennedy Drive, Greendale., Harare, Zimbabwe.

SYNOPSIS

Zimbabwe has a long and rich mining history, with underground mining dating back to the 12th century. Total historical production from the country amounts to ~2700 tons and current production levels are ~ 25 tons annually (excluding production by the informal sector) making it the third largest producer in Africa and the 14th largest worldwide. Gold has been largely produced from the late-Archaean Zimbabwe Craton, and especially from sheared greenstone sequences within it (the craton hosts a large variety of other minerals as well including nickel, chrome, copper, asbestos, gemstones etc). Further gold occurrences are located in the Archaean Zambezi and Limpopo orogenic belts, to the north and the south of the craton, the 1900 Ma Magondi belt to the west of the craton, and in alluvial deposits.

Records of over 6000 gold occurrences within the Archaean Zimbabwe Craton have been compiled on a computer database, which includes details on production, host rock type, structural associations and associated veining and sulphides (>1000000 entries). Combined with new tectonic concepts and operated within a GIS environment, this database offers an invaluable tool for identifying critical controls on mineralisation, which will be of use to gold exploration.

Historically the largest production comes from extensively altered shear zone hosted deposits (~38%) and quartz veins (~31%), both of which tend to be high-grade (ave. ~ 8.3 g/t). Low-grade deposits (3.5-5 g/t) associated with stock works and disseminated mineralisation in intrusive rocks have produced a modest amount of gold in the past (~6%), but currently present the main exploration targets (e.g. Freeda-Rebecca, Eureka, Indarama). Stratabound BIF hosted deposits (4% at 4.9 g/t) can be best categorized as a special group of disseminated shear zone deposits, since the majority of mineralised BIF's are tectonic in nature.

Traditionally Archaean gold mineralisation has been linked to secondary structures along late-tectonic discontinuities within Archaean greenstone terrains. Many such discontinuities can be easily identified on satellite imagery, and they generally represent strongly foliated mylonite zones that originated as accretionary thrusts. Many of the thrusts were reactivated as strike-slip zones during the later stages of the cratonic evolution, when most of the gold appears to have been deposited. Although the identification of secondary structures and associated stress fields may be successful in predicting mineralised geometries on a mining-scale, such structures can not explain the distribution pattern of deposits on a 3-50 km scale. Alignments and especially clustering of deposits on this scale occurs along trends that bear no-immediate relationship with upper-crustal structural geometries.

Using the database it can be shown that major, deep-seated lineaments exert a profound (i.e. larger-scale) control on the distribution of gold-mineralisation. The existence of preferentially mineralized lineaments, can be well demonstrated with gritted gold production maps of the craton that have been filtered using spatial dimensions derived from fractal and cluster analyses. These lineaments not only control mineralisation, but also appear to influence the distribution pattern of greenstones, and represent fundamental tectonic breaks in the Archaean lithosphere.

The lineaments probably originated in the brittle upper mantle, as sets of shear fractures. Movements along them resulted in secondary "Riedel"- "Anti-Riedel"- "Extension vein" arrays in the overlying upper crust. Many of these secondary structures are discrete and different from the older accretionary geometries, although reactivations of the latter are common. Trapping of gold-bearing fluids occurred in older and younger structures, as well as in suitable geometries created by late tectonic intrusions, especially those emplaced within the greenstone pile. An analysis of all extension vein related gold deposits suggests that the dominant lineaments originated in a conjugate array of NW and NE trending structures that were activated due to E-W compression (or N-S relaxation).

The distribution pattern of gold occurrences, and their close spatial association with greenstone lithologies indicate that gold was locally derived and concentrated. Significant mobilization of gold appears to have only occurred along the deep seated lineaments in certain orientations (NW, NE and E-W trending). It is suggested that a critical component necessary to mobilize and transport gold (e.g. S or Cl as well as certain metals) was mantle-derived and released into the lower crust along the lineaments. Trapping of these fluids in the upper crust (typically 2-4 Kbar; 250-350°C) was controlled by changes in physio-chemical conditions and took place in any suitably dilatant geometry.

GEOLOGY AND MINERALISATION MODEL FOR THE ABELSKOP BIF-HOSTED LODE GOLD DEPOSIT – AMALIA GREENSTONE BELT, SOUTH AFRICA

ROBERT KIEFER

Centre of Applied Mining and Exploration Geology (CAMEG),
University of the Witwatersrand, Private Bag 3, P.O. WITS 2050,
Johannesburg, South Africa

SYNOPSIS

The Blue Dot Gold Mine is situated in the northern part of the Amalia Greenstone Belt, which is one of four N-S trending belts of the Kraaipan Group, North West Province, South Africa. The mine consists of three small BIF-hosted lode gold deposits, of which one is named Abelskop Section. The metavolcanic rocks of the Abelskop Section originated from high-magnesium basalts, tholeiites and tuffs with intercalated banded iron formations (BIF). At least three deformation phases D_{n+1} to D_{n+3} are found, which has resulted in steeply dipping BIF with a sub-parallel alignment of the foliation, formation of small-scale, parasitic S-type fold structures and refolding of the parasitic small-scale folds. Economic gold mineralisation is found in one siliceous BIF unit where an ore shoot plunges at 45 - 50° to the SE. Alteration zonation is present around the orebody, which involves mineralogical changes adjoining the mineralised zone. Fuchsite-quartz-carbonate schist is associated with quartz and carbonate veining and envelopes the main mineralised BIF unit at Abelskop. Quartz-carbonate-chlorite schists occur further away from the mineralization and change progressively to tremolite-bearing quartz-carbonate-chlorite schists. Gold occurs in sulphidized magnetite-hematite BIF layers adjacent to white quartz veins that crosscut the BIF along joints and brecciated zones.

INTRODUCTION

The Blue Dot Gold Mine lies 30km west of the town of Schweizer-Reneke and about 10km southwest of Amalia, in the North West Province, South Africa. The gold mine consists of three small banded iron formation - (BIF) hosted lode gold deposits located on the farms Abelskop 75HO, and Goudplaats 96 HO situated in the Amalia Greenstone Belt, one of four N-S trending belts of the Archaean Kraaipan Group. Three other greenstone belts (viz., the western Stella belt, the central Kraaipan belt and the eastern Madibe belt), are exposed approximately 70km further to the north and disappear under thick Kalahari sand cover near the Botswana border (Fig.1). Alluvial diamonds are also recovered in the region of the Amalia gold occurrences, but are associated with Recent sediments deposited in and adjacent to the upper Harts River, which traverses the area.

The main lithologies of the Amalia Greenstone Belt are metavolcanics, which originated from high-magnesium basalts, tholeiites and tuffs with intercalated BIF and subordinate metasediments (metaarkoses). Whole-rock Pb-Pb data from BIF of the Kraaipan Group indicated an age of 3410 +61-64 Ma (Anhaeusser and Walraven, 1997). Zircons derived from two felsic schists from the eastern Madibe Greenstone Belt yielded ages of 3082.5 ± 5.9 and 3098.4 ± 7.6 Ma (Hirner, 2001), which represent the best estimate for the extrusion of the volcanic rocks. U-Pb single zircon ages from a lapilli tuff band and a volcanic tuff intercalated and deformed together with BIF in the north-eastern part of the Amalia Belt have been dated at 2754 ± 5 and 2740 ± 13 Ma, respectively (Poujol, et al. in prep.). This age suggests that the Amalia belt is the youngest greenstone belt yet dated on the Kaapvaal Craton. The Amalia belt is surrounded by a variety of granitoids, which comprise tonalitic, granodioritic and trondhjemitic gneisses to the west and adamellites and granodiorites to the east. The western intrusive rocks demonstrate episodic granitoid emplacement events, which occurred over a time-span of approximately 70 Ma (Poujol et al., 2000) and yielded U-Pb single zircon ages of 3008 ± 4 Ma and 2938.6 ± 9.6 Ma. The eastern potassic granitoids (adamellites and granodiorites) range in age between 2880 ± 2 and 2846 ± 22 Ma (zircon evaporation age) (Anhaeusser and Walraven, 1997).

The Amalia Greenstone Belt is poorly exposed, consisting of a number of isolated, low ridge outcrops mainly of steeply dipping oxide-facies BIF layers, which are intercalated with weathered, carbonate-altered schists. These are overlain to the north by shallow-dipping Ventersdorp lavas and Tertiary and Kalahari cover sequences. On the farm Abelskop 75HO the longest continuous BIF succession is exposed with a N-S extent of over 4km and is composed of 10 to 13 closely spaced, steeply NE-dipping individual BIF layers. The entire sequence forms a large S-shape structure. The BIF units disappear to the south under thick soil cover of the Harts River. In the kink of the S-shaped ridge the BIF's are structurally thickened, resulting in the formation of a topographic high – the Abelskop Hill.

The southern end of the northern limb is faulted by an inferred wrench fault, which has a horizontal displacement of approximately 200m (Fig.1).

At least three deformational ages affected the rocks. Early contractional deformation that resulted in thrust faulting and associated isoclinal recumbent folding appears to have been one of the first deformational events, and is often observed in many other greenstone belts of the world (Kusky and Vearncombe, 1997). These structures are rarely associated with penetrative metamorphic fabrics and are thus difficult to identify, especially in an environment of strong carbonate alteration and poor surface exposure. The first identifiable deformational event is an episode of large, upright, tight-to-isoclinal folding with associated foliation and metamorphism of the metavolcanics to form schists. This event D_{n+1} brings the BIF into a steep NE-dipping attitude with a subparallel alignment of the foliation. D_{n+2} is a small-scale, parasitic S-type folding in BIF, with a plunge direction to the SE. This deformation event is well developed in the northern and southern limbs of the large S-fold structure. The Abelskop Hill region represents a further tectonic domain, where the N-S trending BIF units are folded over the Abelskop Hill, creating the large-scale S-type fold structure. This might have been formed by a postulated N-S orientated sinistral strike-slip shear, which caused structural thickening of the BIF units of the Abelskop Hill together with refolding of the parasitic small-scale folds (fold plunge direction to the NE and SE) along the short E-W trending limb (D_{n+3}). The absence of any mineral elongation lineation or any preserved foliation makes it difficult to structurally interpret the Abelskop Hill region.

The main lithologies of Abelskop include schistose, carbonate-altered metavolcanics with tholeiitic affinity, bands of oxide facies BIF's and occasionally intercalations of quartz-chlorite-sericite schist, which are interpreted as metasediments. The BIF units exhibit small-scale, internally disharmonic folding, fracturing and boudinage formation together with variable amounts of chert. One of these BIF bands carries economic gold mineralisation (Abelskop Main BIF unit). A clear alteration zonation is evident around the orebody, which involves mineralogical changes adjoining the mineralised zone. Fuchsite-quartz-carbonate schist is always associated with quartz and carbonate veining and envelops the mineralised Abelskop Main BIF unit. Quartz-carbonate-chlorite schist (\pm talc, sericite and albite) occurs further away from the mineralisation. These rocks change progressively to tremolite-bearing quartz-carbonate-chlorite schist (\pm sericite and plagioclase). To the SE some intercalations of fine-grained, foliated quartz-carbonate-sericite schist occur together with an augen-schist unit that contains carbonated and sericitised, cm-sized feldspar clasts. An S-C fabric is developed in the chlorite matrix surrounding the clasts.

Economic gold mineralization is only found at the southern end of the northern BIF limb, in one siliceous BIF unit, where an ore shoot plunges to the SE at about 45 to 50° (Fig. 2). To the SE the orebody is terminated by a N-S striking fault, which dips about 35 to 40° to the east. The result is a widening along strike of the ore shoot at depth. At surface the ore shoot has a strike length of about 25m, which increases steadily at depth (at 60m on 2-level the mineralisation extends over 50m). The hangingwall and footwall BIF units locally contain subeconomic mineralization. Figure 2 shows a longitudinal section of the Main BIF unit with the borehole intersection points and the interpreted ore shoot pattern.

Gold occurs only in sulphidised magnetite-hematite layers of BIF, adjacent to white quartz veins which crosscut the BIF along joints and brecciated zones. The veins carry only minor gold mineralization (0.1-0.5g/t). The prevailing sulphide mineral is pyrite with microscopically small inclusions of chalcopyrite and pyrrhotite. Gold occurs as μm -sized inclusions in the pyrite or is attached along mutual grain boundaries of pyrite cubes. Sulphidation, and consequently gold mineralization, is highest directly at the contact of the BIF and a quartz vein. Here gold values as high as 79g/t have been encountered. This zone of massive sulphidation extends for only around 10 to 20cm into the BIF and decreases constantly with increasing distance from the vein contact, producing an extremely erratic gold distribution pattern. Changes of up to 40g/t gold within one metre are common.

REFERENCES

- Anhaeusser C.R. and Walraven F., 1997. Polyphase crustal evolution of the Archaean Kraaipan granite-greenstone terrane, Kaapvaal Craton, South Africa. Information Circular, Economic Geology Research Unit, University of the Witwatersrand, Johannesburg, 313, 27pp.
- Hirner, A.J., 2001. Geology and gold mineralization of the Madibe Greenstone Belt, eastern part of the Kraaipan Terrain, Kaapvaal Craton, South Africa. Unpublished PhD thesis, University of the Witwatersrand, Johannesburg.

Kusky, T.M., Vearncombe, J.R., 1997. Structural Aspects. In: de Wit, M.J., Ashwal, L.D. (eds.), Greenstone Belts, Oxford Monographs on Geology and Geophysics, 35, 1st edition; p. 91-124.
 Poujol, M., Kiefer, R., Anhaeusser, C.R., Armstrong, R.A. (in preparation). The Amalia greenstone belt, Kaapvaal Craton, South Africa: A late Archaean (2.75Ga) greenstone belt?

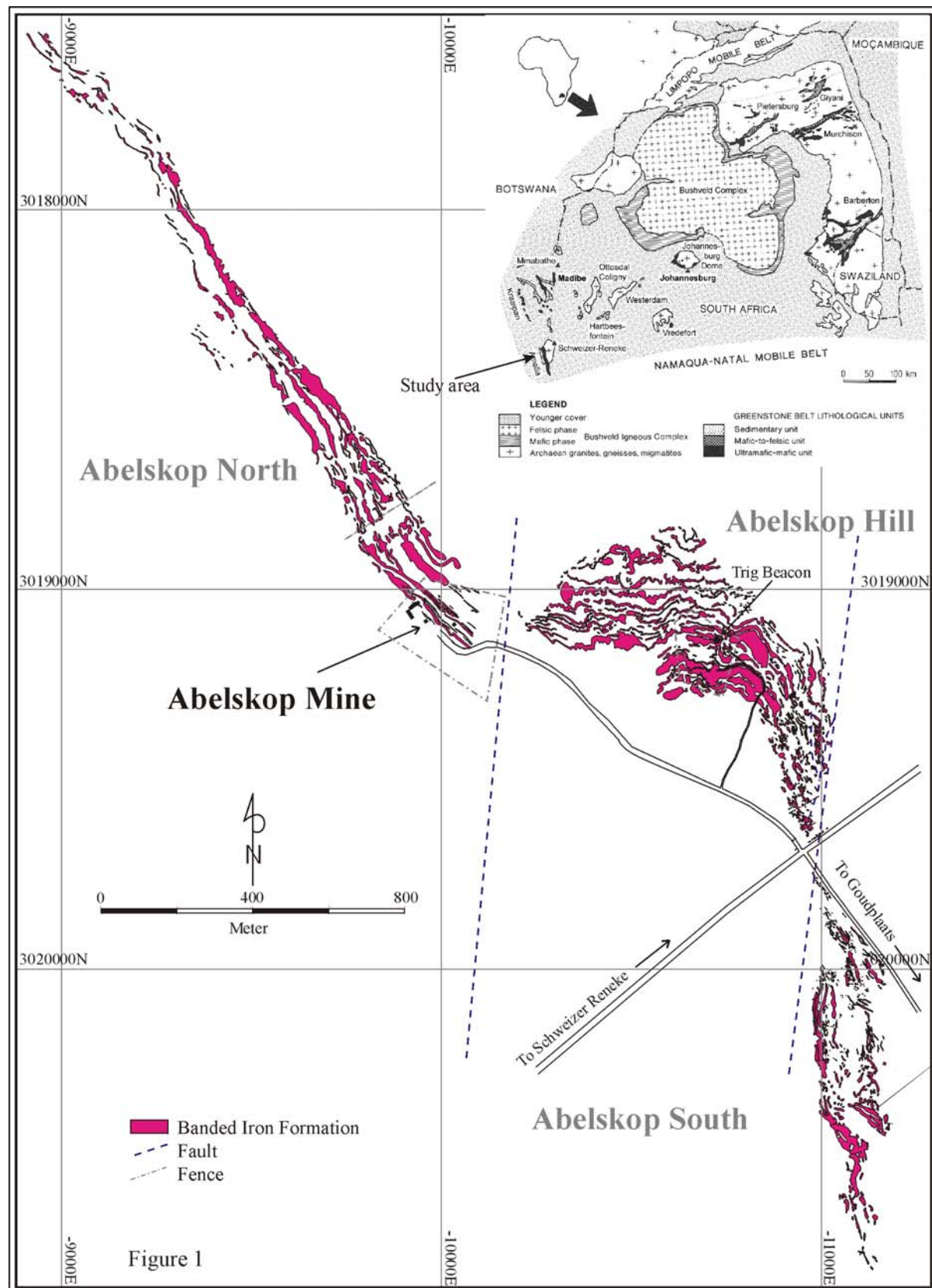


Figure 1: Simplified geological map showing the BIF outcrops in the vicinity of the Abelskop Section of the Blue Dot Gold Mine, Amalia Greenstone Belt, North West Province, South Africa.

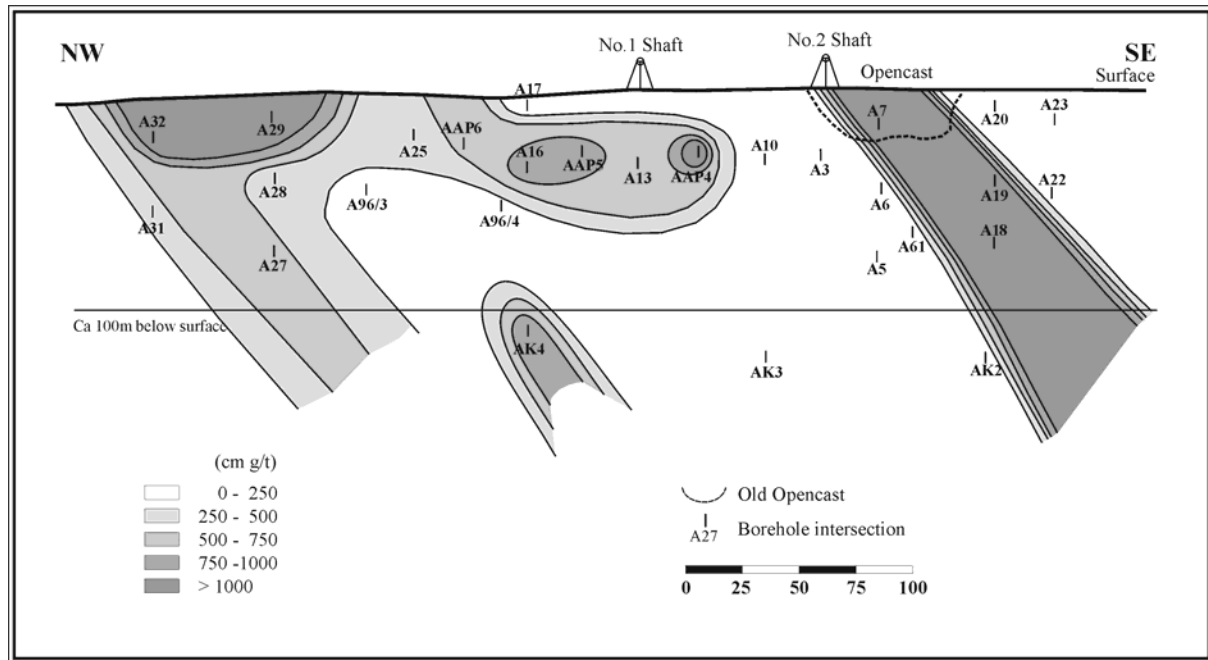


Figure 2: Longitudinal NW-SE section through the Abelskop Section of the Blue Dot Gold Mine, Amalia Greenstone Belt. The distribution of the BIF-hosted mineralization is shown together with gold values, reef thicknesses and interpreted gold content.

ARCHAean CRUSTAL EVOLUTION OF THE CENTRAL PARTS OF THE KAAPVAAL CRATON: EVIDENCE FROM THE VREDEFORT DOME, SOUTH AFRICA

C. LANA, R.L. GIBSON AND W.U. REIMOLD

Impact Cratering Research Group, School of Geosciences,
University of the Witwatersrand, Private Bag 3, P.O. Wits 2050,
Johannesburg, South Africa
e-mail: lanac@science.pg.wits.ac.za

SYNOPSIS

Lithological and structural mapping, combined with geochemical studies, in the Archaean Basement Complex in the Vredefort Dome has revealed a complex history of intrusions, polyphase deformation and metamorphism in the central parts of the Kaapvaal Craton prior to 3.1 Ga. An ~10 km thick mid-crustal section, exposed as a result of a large meteorite impact event, is interpreted as being the root zone of an Archaean magmatic arc. Contrary to previously published models, our results suggest that this section does not expose the Moho, nor is there evidence for a major mid-crustal tectonic boundary.

INTRODUCTION

The Archaean Basement Complex (ABC) of the Vredefort Dome, located some 120 km southwest of Johannesburg, consists of a 45-50 km wide core of Archaean basement gneisses, surrounded by a 15-20 km wide collar of subvertical- to- overturned Late Archaean to Palaeoproterozoic supracrustal rocks. The basement lithologies comprise polydeformed Archaean migmatitic gneisses and subsidiary metasedimentary and metavolcanic xenoliths that experienced upper amphibolite- to- granulite facies metamorphism at ~ 3.1 Ga. Published geochemical and geophysical models have suggested that the ABC comprises three concentrically arranged crustal levels, exposed as a result of quasi-diapiric uplift [1]. Modification to these models proposed that three major crustal domains - the Outer Granite Gneiss (OGG), the Inlandsee Leucogranofels (ILG) and the Greenlands Greenstone Complex (GGC) - were tectonically juxtaposed between 2.5-2.8 Ga [2, 3]. The models also proposed that ultramafic rocks exposed near the centre of the Dome represent upper mantle and, thus, that the entire crustal section through the central Kaapvaal Craton is exposed in the Vredefort Dome. However, this crust-on-edge hypothesis is effectively a two-dimensional model, which is based largely on two geochemical traverses across the ABC [2]. To date, no comprehensive lithological or structural mapping of the core of the Dome has been completed.

THIS STUDY

Field-based lithological and structural mapping of the ABC was undertaken with the aim of elucidating the evolution of these rocks in the light of: (a) their Archaean magmatic and tectonometamorphic history; and (b) the effects of the 2.02 Ga Vredefort impact event. The lithological mapping, combined with geochemical studies, established a complex distribution of rock types that does not support the simplified concentric models. The dominant rocks are tonalitic- to- trondhjemetic gneisses that grade into trondhjemetic- to- granitic stromatic migmatites. The migmatites, in turn, have been intruded by syntectonic porphyritic granodiorites and granites. Locally, the migmatites exhibit xenoliths of pre-migmatitic trondhjemetic gneisses.

GEOCHEMISTRY

The geochemical results from the basement lithologies indicate that the linear geochemical traverses across the Dome performed previously do not fully account for the heterogeneous character of the rocks in the ABC. Major element results for different lithologies fall along a single trend in Harker diagrams. Most oxides, with the exception of K_2O , show negative linear correlation with SiO_2 . The trace element data display trends that are less clearly defined and most likely reflect small-scale heterogeneities of the basement lithologies resulting from migmatisation. No significant difference between lithologies from the outer and inner parts of the Dome could be identified – again contradicting earlier models suggesting that the OGG and ILG are distinct terranes. Results of REE analysis display similar trends in normalising diagrams. Small variations in REE content, such as positive and negative Eu anomalies, reflect differences in mineralogical composition between different migmatitic bands, rather than bulk-scale crustal differentiation as previously proposed by Hart et al. [2].

All lithologies analysed in this work display a flat REE pattern when normalised to the average upper-crustal composition [4] and are more fractionated with respect to the average lower-crustal composition. This confirms previous geophysical and metamorphic models for the Dome [6], which suggest that only upper and mid-crustal levels are exposed. Combined REE patterns and major and trace element data indicate that the basement lithologies are chemically similar to modern arc-related granitoids.

STRUCTURAL OBSERVATIONS

The stromatic migmatitic gneisses in the ABC show well-defined migmatitic banding (S1). Close to the collar-basement contact this banding defines a vertical- to- subvertical circular trend that is parallel to the supracrustal strata. Away from the contact dips are subhorizontal. The subvertical orientation is, thus, related to formation of the Dome at 2.02 Ga. Throughout the Dome the S1 fabric is transposed by NW-trending high-strain shear zones (S2). The S2 fabric is clearly truncated by the collar-basement contact and it defines a major Archaean crustal shear zone. Like S1, S2 is largely defined by migmatitic banding. This indicates that D1 and D2 occurred under similar high-grade metamorphic conditions associated with crustal melting. Conjugate pairs of D2 shear bands crosscutting S2 (cf. [5]) indicate subhorizontal S2-parallel extension during the latter stages of D2. Retrograde mylonitic shear zones, such as the Broodkop shear zone in the GGC [1], crosscut relatively late pegmatitic veins, which, in turn, post-date the migmatitic bands. The mylonitic zones were produced during a third deformation event (D3) that affected the core of the Dome under much lower-grade metamorphic conditions than the earlier deformation events. The D3 shear zones are crosscut by pseudotachylites formed during the 2.02 Ga impact event.

IMPLICATIONS FOR KAAPVAAL CRATON EVOLUTION

Based on the Hart et al. [2] interpretation of the ABC in the Vredefort Dome, de Wit et al. [3] suggested that tectonic stacking of large crustal slabs played an important role in the evolution of the central parts of Kaapvaal Craton. They envisaged the “alleged mantle rocks” [2] in the central part of the Dome represented part of an Archaean oceanic lithosphere. They further speculated on a series of collision events, with the “alleged ophiolitic rocks” having been subducted under the ILG. The ILG, in turn, was seen as having been tectonically emplaced beneath the OGG. De Wit et al. [3] also proposed that the GGC and ILG are “geochemically and structurally unrelated continental slabs” that collided between 2.5 and 2.8 Ga ago. However, lithological, geochemical and structural mapping has failed to distinguish any substantial differences between the evolution of the so-called OGG and ILG. Furthermore, detailed mapping along the “alleged terrane boundaries” has failed to identify any evidence that these are tectonic in origin. These terranes record a single, shared, tectonothermal history, which culminated in widespread crustal melting during a regional NE-SW- directed crustal shortening event at ~ 3.1 Ga.

Structures in the core of the Dome tie D1/D2 to the anticlockwise P-T-t loop proposed for the high-grade metamorphic event in the core of the Dome [6]. An ~ 3.1 Ga age for the high-grade metamorphic event [7], together with geochemical data, indicate that the crustal thickening was related to the ~ 3.1 Ga arc-related granodioritic magmatism [8, 9] in the Johannesburg Dome at ~ 3.1 Ga.

DOMING-RELATED DEFORMATION EFFECTS

The Vredefort Dome represents an area of extreme structural uplift caused by the Vredefort impact event. At the current level of exposure, the supracrustal-basement contact is uplifted by a minimum of 8-10 km [cf. 10]. The concentric, vertical- to- overturned orientation of the collar strata indicates extreme rotation accompanying doming. However, with the exception of S1 in the outer parts of the core, pre-impact Archaean structures do not show a concentric arrangement and are thus not consistent with the two-dimensional, overturned crustal section proposed in the crust-on-edge model [2]. Only in the central 5 km of the core is there evidence for the effects of widespread impact-related melting [11] that may have assisted with the accommodation of the space problem that developed during doming. It is clear that the collar strata indicate significant inward and upward movement of rocks to form the Dome, but the core lithologies show only limited structural evidence as to how they were uplifted.

CONCLUSIONS

- (1) Available field data indicate that much, if not all, of the observed ductile deformation in the ABC is Archaean in age. The D1/D2 deformation event is associated with intense crustal melting and most likely reflects a significant ~ 3.1 Ga event involving crustal thickening in an arc-related magmatic environment.
- (2) The GGC, OGG and ILG display similar deformational histories, contrary to the model proposed by Hart et al. [2] suggesting tectonic juxtaposition of disparate terranes with distinct crustal histories.
- (3) The geochemical results from the basement lithologies indicate that they cannot be grouped into different terranes and that rocks from the central parts of the Dome do not represent material from the lower crust.

- (4) The present orientation of the Archaean tectonic fabrics is not consistent with the uniformly overturned crustal section of the crust-on-edge model. The mechanism for the basement uplift remains, however, unclear.

REFERENCES

- [1] Stepto, D., (1990). Tectonophysics, 171, 75-103.
- [2] Hart, R. et al., (1990). Chem. Geol., 82, 21-50.
- [3] de Wit, M. et al. (1992). Nature, 357, 553-562.
- [4] Taylor, S. and McLennan, M., (1985). Continental Crusts. Oxford, Blackwell.
- [5] Colliston, W. and Reimold, W. (1990). EGRU Inf. Circ. No. 229.
- [6] Stevens, G. et al. (1997). Pre. Res., 61, 113-132.
- [7] Hart, R. et al., (1999). Geology, 23, 277-280.
- [8] Anhaeusser, C.R. (1999). S. Afr. J. Geol., 102, 303-322.
- [9] Poujol, M. and Anhaeusser, C.R. (2001). Pre. Res., 108, 139-157.
- [10] Gibson, R. and Reimold, W. (2000). Lect. and notes in Earth Science, 91, 249-278.
- [11] Gibson, R. et al., Geology (in press).

2. CENTRAL AFRICAN COPPERBELT

CONTRIBUTIONS TO THE GEOLOGY AND MINERALIZATION OF THE CENTRAL AFRICAN COPPERBELT: I. NATURE AND GEOCHRONOLOGY OF THE PRE-KATANGAN BASEMENT

C. RAINAUD¹, R. A. ARMSTRONG², S. MASTER¹, L. J. ROBB¹
and P.A.C.C^{1,3} MUMBA*

¹Economic Geology Research Institute/ Hugh Allsopp Laboratory, School of Geosciences, University of the Witwatersrand, Pvt. Bag 3, WITS 2050, South Africa.

²Research School of Earth Sciences, Australian National University, Canberra, ACT 0200, Australia.

³School of Technology, Copperbelt University, Kitwe, Zambia. *Deceased

SYNOPSIS

U-Pb SHRIMP zircon age data from the basement of the Katangan Sequence in the Central African Copperbelt show the existence of Neoproterozoic, Paleoproterozoic and Mesoarchaean terranes. The Nchanga red granite showed an age of emplacement of 887 ± 11 Ma. The calc-alkaline metavolcanic Lufubu schists from Zambia and the Democratic Republic of Congo have been dated respectively at 1968 ± 9 and 1873 ± 8 Ma. Fertile granitoids intercepted in drill cores located in the Zambian Copperbelt yield ages ranging from 1952 to 1994 Ma. Granitic gneiss from the Mkushi copper mine south of the Zambian Copperbelt has an age of 2049 ± 6 Ma. The Mulungushi bridge gneiss gives an age of 1976 ± 5 Ma. Zircons from the Mkushi aplites have xenocrystic cores (2035 ± 22 Ma) and rims dated at 1088 ± 159 Ma. Quartzite from the Muva Supergroup, which unconformably overlies the crystalline basement, exhibits a broad range of detrital zircon ages from 3180 Ma down to 1941 Ma. Furthermore, a population of xenocrystic zircons from a Katangan lapilli tuff has ages of c. 3200 Ma and provides, together with the data from the Muva quartzite, the first evidence of a cryptic Mesoarchaean basement beneath the Central African Copperbelt.

INTRODUCTION

The Central African Copperbelt, hosted by the Neoproterozoic metasediments of the Katangan Sequence is located in Zambia and the Katanga Province of the Democratic Republic of Congo (D.R.C.). The Copperbelt is one of the great metallogenic provinces of the world, being a leading producer of Cu and Co, as well as lesser amounts of Pb, Zn, Ge, Ga, U, Au and PGE (Master, 1998). It has long been recognised that the basement to the Katangan Sequence in the Copperbelt contains abundant copper mineralization, and many authors have regarded this as having an important bearing on the origin of the Copperbelt ores. This pre-Katangan basement consists of schists of the Lufubu Group, which are intruded by a variety of granitoids, both of which are unconformably overlain by metaquartzites and schists of the Muva Supergroup. This study provides new geochronological insight on this basement.

Although the Central African Copperbelt has a strike length of 500 km in the Lufilian Arc of Katanga (D.R.C) and Zambia, the pre-Katanga basement is mainly exposed in the Zambian Copperbelt and in immediately adjacent areas of Katanga. About half of this basement consists of granitoids, and the rest comprises mainly Lufubu schists with subordinate areas of Muva quartzite.

The Lufubu schists consist mainly of biotite or muscovite and quartz-bearing micaceous schists and quartzites, with minor accessory plagioclase, tourmaline, sphene, zircon, calcite and pyrite. Previously regarded as of metasedimentary origin (Mendelsohn, 1961), the Lufubu schists are calc-alkaline metavolcanics ranging from trachyandesite to rhyodacite and rhyolite (Rainaud et al., 1999).

The granitoids are commonly seen as intruding into the Lufubu schists. Their composition range from biotite granites to quartz monzonites, granodiorites and tonalites (Mendelsohn, 1961). Previous work on these granitoids yielded imprecise ages (Cahen et al, 1984; Ngoyi et al, 1991). The Muva Supergroup unconformably overlies the Lufubu schists and comprises mainly quartzites with minor conglomerates and argillaceous beds (Garlick, 1961).

GEOCHRONOLOGY

We present zircon U-Pb ages of the intermediate to felsic metavolcanic Lufubu schists from both the D.R. Congo and Zambia, several granitoids including the Mkushi gneiss, the Samba porphyry, a granite intersected in boreholes through the Chambishi Basin, the Mulungushi Bridge augen gneiss, the Mkushi aplite and the Nchanga Red granite as well as detrital zircons from the Muva Supergroup. Finally, we will present xenocrystic zircon data from a Katangan lapilli tuff located in D.R.C.

15 analyses have been carried out on 15 zircons from the Kinsenda Lufubu schists (D.R.C.). The results are plotted on the concordia diagram in Figure 1. The age is well constrained at 1873 ± 8 Ma and is interpreted as the age of the volcanism in the area. Results of 15 analyses undertaken on one sample of Mufulira Lufubu schists (Zambia) are plotted on the concordia diagram in Figure 2. Three clusters of zircons are discernible. One zircon yields an age of 2174 ± 13 Ma whereas 3 zircons yielded an average mean $^{207}\text{Pb}/^{206}\text{Pb}$ of 2057 ± 9 Ma. These older zircons are interpreted as inherited. The last group of 10 zircons yielded a weighted mean $^{207}\text{Pb}/^{206}\text{Pb}$ of 1968 ± 9 Ma (Figure 3). This age is interpreted as the age of volcanic emplacement of the Mufulira Lufubu Schists. The volcanism of the Lufubu schists thus spanned a period of about 95 Ma.

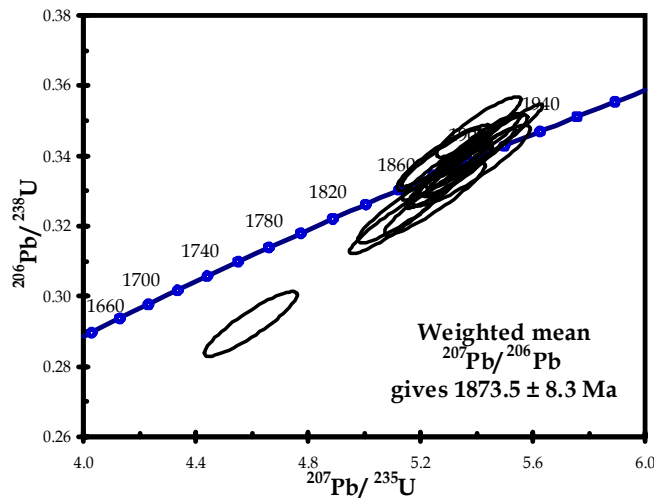


Figure 1: $^{206}\text{Pb}/^{238}\text{U}$ vs $^{207}\text{Pb}/^{235}\text{U}$ concordia plot of ages (Ma) of the Kinsenda Lufubu schists.

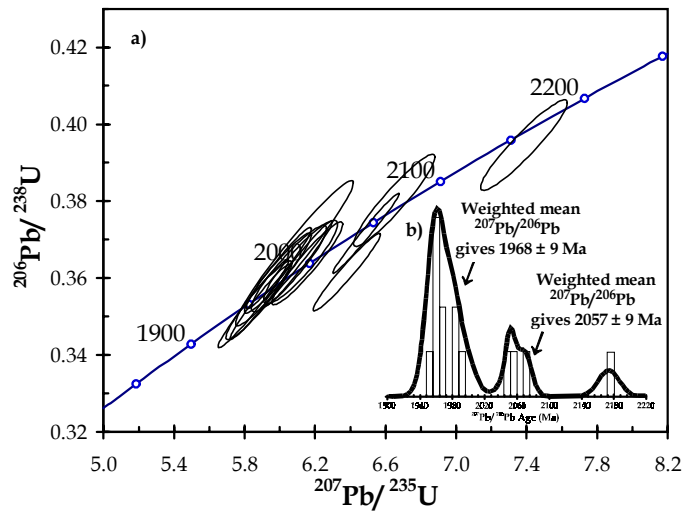


Figure 2: a) $^{206}\text{Pb}/^{238}\text{U}$ vs $^{207}\text{Pb}/^{235}\text{U}$ concordia plot of ages (Ma) of the Mufulira Lufubu schists. b) Histogram plot showing the relative distribution of $^{207}\text{Pb}/^{206}\text{Pb}$ ages of the zircons.

The Mkushi gneiss yielded an emplacement age of 2049 ± 6 Ma (Rainaud et al., 1999), which makes it the oldest dated rock unit in the Palaeoproterozoic basement of the Copperbelt. The Mufulira granite yielded an age of emplacement at 1991 ± 3 Ma. The Mulungushi Bridge megacrystic augen gneiss has an age of 1976 ± 5 Ma. The Samba porphyry is a mineralized granodiorite with copper ore reserves estimated at 50 million tons (Wakefield, 1978). Analyses yielded an age of emplacement of 1964 ± 12 Ma (Figure 3). For the granite underlying the Chambishi basin, 2 different samples from different drill holes (NN75 and BN53) were analysed. They yielded 2 similar ages of emplacement: 1983 ± 5 and 1980 ± 7 Ma respectively (Figures 4). A few zircons from the Mkushi aplites at Mtuga Mine were analysed. Three cores, interpreted as xenocrystic, gave ages of 2036 ± 22 Ma, while two rims were dated at 1088 ± 159 Ma. Recent investigations on the Nchanga red granite gave an age of emplacement of 887 ± 11 Ma (Armstrong et al., 1999).

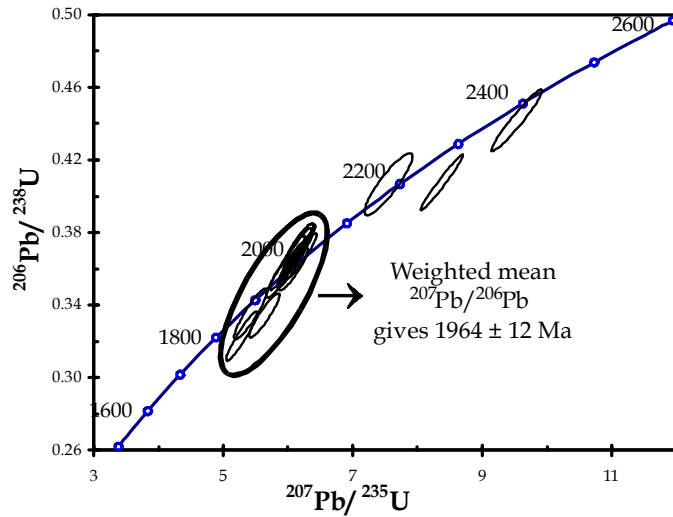


Figure 3: Concordia diagram of the Samba porphyry.

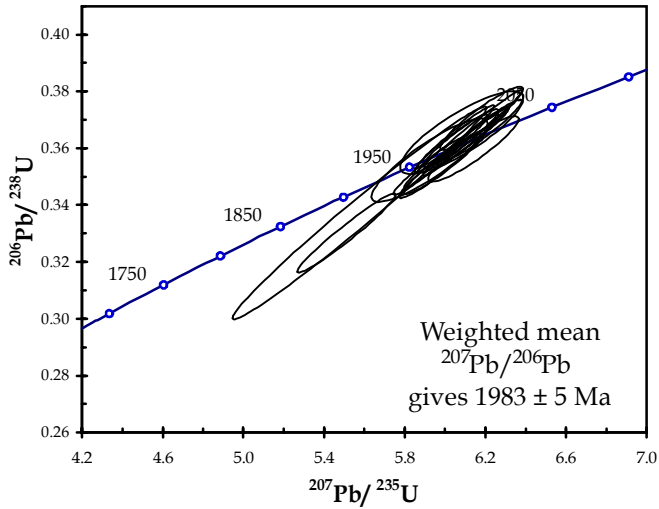


Figure 4: Concordia diagram of the granite beneath the Chambishi basin from borehole NN75.

50 detrital zircons from a Muva quartzite south of Mufulira, Zambia were analysed. The results are plotted on the concordia diagram in Figure 5. An Archaean component is observed with ages clustering at 2550 to 2700 Ma and also at around 3000 to 3180 Ma. Palaeoproterozoic zircons range down to 1941 Ma, the youngest zircon in the population and an indication, therefore, of the maximum age of the deposition for the Muva Supergroup.

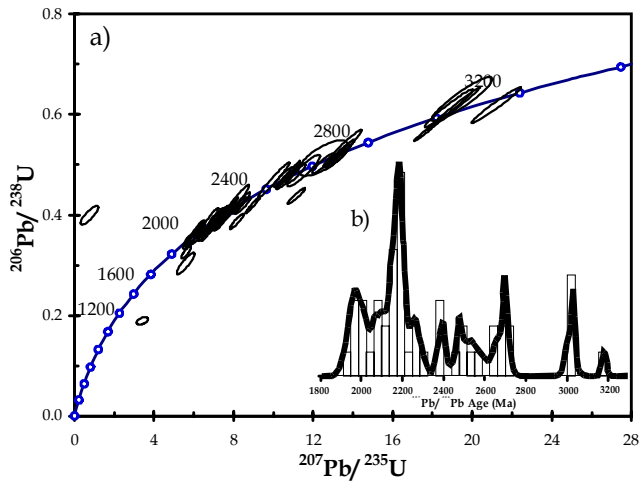


Figure 5: a) $^{206}\text{Pb}/^{238}\text{U}$ vs $^{207}\text{Pb}/^{235}\text{U}$ concordia plot of ages (Ma) of the Muva quartzite. b) Histogram plot showing the relative distribution of $^{207}\text{Pb}/^{206}\text{Pb}$ ages of the zircons.

A Katangan lapilli tuff from the Mwashya Group, Likasi, D. R. C., yielded a population of zircons. Out of 48 analyses undertaken on zircons from this sample, 43 were concordant and older than the maximum age of the deposition of the Katangan Sequence. These zircons were therefore interpreted as xenocrystic. They form several age populations but for the purpose of this paper, the attention will be drawn to the oldest one. 14 zircons yielded ages ranging from 3169 ± 13 Ma to 3225 ± 11 Ma.

These ages are older than that of any rock so far described from Central Africa (Rainaud et al., 2000).

CONCLUSIONS

The basement to the Katangan Sequence in the Central African Copperbelt comprises a Palaeoproterozoic magmatic arc. Tonalite-granodiorite gneisses (Mkushi) together with more evolved granitoids (Mufulira, Mulungushi, Samba and Chambishi) represent the plutonic phases of a major intermediate to acid volcanic province (Lufubu schists) emplaced in the range 2050 to 1865 million years ago. Unconformably overlying this part of the basement is the Muva Supergroup, younger than 1941 Ma, which contains detrital zircons of Palaeoproterozoic to Mesoarchaean age. There are no exposed rocks between 3200 and 3000 Ma in the vicinity of the Muva quartzite. This age range is found as well in xenocrystic zircons located in a Katagan tuff from Likasi. The abundance of c. 3200 Ma xenocrystic zircons in this tuff indicates that a part of the crust beneath the central Lufilian Arc is a Mesoarchaean terrane.

REFERENCES

- Armstrong, R. A., Robb, L. J., Master, S., Kruger, F. J., Mumba, P. A. C. C., 1999. New U-Pb age constraints on the Katangan Sequence, Central African Copperbelt. *J. Afr. Earth Sci.*, 28, 4A, 6-7.
- Cahen, L., Snelling., N. J., Delhal, J., Vail, J. R., Bonhomme, M. & Ledent, D., 1984. *The Geochronology and Evolution of Africa*. Clarendon, Oxford, 512 pp.
- Garlick, W. G., 1961. In: Mendelsohn, F. (Ed.), *Geology of the Northern Rhodesian Copperbelt*: Macdonald, London, 21-54.
- Master, S., 1998a. New developments in understanding the origin of the Central African Copperbelt. *Abstract, Mineral Deposits Studies Group Annual Meeting, University of Greenwich, Chatham Maritime, UK, 5-6 January 1998*.
- Master, S., 1998b. A review of the world-class Katangan metallogenic province and the Central African Copperbelt: tectonic setting, fluid evolution, metal sources and timing of mineralization. *Abstract, Québec 1998, GAC MAC-APGGQ Annual Meeting, Québec, Canada, May 1998*.
- Mendelsohn, F., 1961. *Geology of the Northern Rhodesian Copperbelt*: Macdonald, London, 523 pp.
- Ngoyi, K, Liégeois, J. P., Demaiffe, D. & Dumont, P., 1991. Age tardi-ubendien (protérozoïc inférieur) des dômes granitiques de l'arc cuprifère zaïro-zambien. *C. R. Acad. Sci. Paris*, 313, 83-89.
- Rainaud, C., Armstrong, R. A., Master, S., Robb., L. J., 1999. A fertile Palaeoproterozoic magmatic arc beneath the Central African Copperbelt. In: *Stanley et al. (Eds.), Mineral Deposits: Processes to Processing*, Balkema, Rotterdam, 1427-1430.
- Rainaud, C., Master, S., Armstrong, R. A., Robb, L. J., 2000. A cryptic Mesoarchaean terrane in the basement to the Central African Copperbelt: U-Pb isotopic evidence from detrital and xenocrystic zircons on the Muva and Katangan sequences. *J. Afr. Earth Sci.*, 30 4A, 72-73.
- Wakefield, J., 1978. Samba: a deformed porphyry-type copper deposit in the basement of the Zambian Copperbelt. *Transactions Institution of Mining and Metallurgy*. 87, B43-B52.

CONTRIBUTIONS TO THE GEOLOGY AND MINERALIZATION OF THE CENTRAL AFRICAN COPPERBELT: II. NEOPROTEROZOIC DEPOSITION OF THE KATANGA SUPERGROUP WITH IMPLICATIONS FOR REGIONAL AND GLOBAL CORRELATIONS

S. MASTER¹, C. RAINAUD¹, R. A. ARMSTRONG²,
D. PHILLIPS^{2,3} & L. J. ROBB¹

¹Economic Geology Research Institute, School of Geosciences, University of the
Witwatersrand, P. Bag 3, WITS 2050, South Africa

²PRISE, Research School of Earth Sciences, Australian National University,
Canberra, Australia

³Present Address: University of Melbourne, Melbourne, Victoria, Australia

SYNOPSIS

We present some new data constraining the depositional age of key units within the Neoproterozoic Katanga Supergroup, which hosts the major stratiform Cu-Co deposits of the Central African Copperbelt. The older age limit on basal Roan Group sedimentation is 880 Ma, which is the age of the youngest detrital zircons. The ages of volcanics in the Mwashya Group (760 ± 5 Ma), and a volcanic unit assigned to the Lower Kundelungu (735 ± 5 Ma) bracket the age of the Grand Conglomerat, and allows its correlation with other Neoproterozoic glacial diamictites (e.g., Chuos, Sturtian). Finally, detrital muscovites from Plateau Group siltstones give a maximum age of sedimentation of 565 ± 5 Ma, strongly supporting the idea that the Plateau Group was deposited in a foreland basin of the Lufilian Orogen. Detrital zircon ages indicate a mainly Palaeoproterozoic provenance area for the Katanga basin, with only minor contributions from Archaean and Mesoproterozoic (Kibaran) source regions.

INTRODUCTION

The Neoproterozoic Katanga Supergroup is the host of the major stratiform sediment-hosted Cu-Co deposits, as well as numerous other deposits of Cu, Pb, Zn, U, Au, Fe etc., which constitute the Central African Copperbelt in Zambia and the Democratic Republic of Congo. In spite of its great economic significance there have been, up to now, few age data bearing on the deposition of the Katangan Sequence.

REGIONAL GEOLOGICAL SETTING

In the Central African Copperbelt, the oldest pre-Katangan basement consists of a Palaeoproterozoic magmatic arc sequence, comprising the Lufubu Schists and intrusive granitoids, dated at between 1994 and 1873 Ma. This is overlain unconformably by quartzitic and metapelitic metasediments of the Muva Group (<1941 Ma). The Nchanga Granite is the youngest intrusion in the pre-Katangan basement, and it is nonconformably overlain by the Katangan Sequence, which consists of metasediments traditionally divided into the Roan, Lower and Upper Kundelungu Supergroups. More recently, Wendorff (2001) has proposed a new lithostratigraphic scheme, in which the Katanga Supergroup is subdivided into the Roan, Mwashya and Guba Groups, with two additional lithotectonic units, the Fungurume and Plateau Groups, which were deposited syntectonically in a foreland basin during deformation of the earlier Katangan groups during the Pan-African Lufilian Orogeny.

NCHANGA GRANITE

The Nchanga Granite is an unfoliated coarse-grained peraluminous biotitic alkali granite with A-type geochemical characteristics (Tembo et al., 2000). SHRIMP U-Pb dating of zircons from the

Nchanga Granite has yielded a concordant age of 877 ± 11 Ma, regarded as the age of the intrusion (Armstrong et al., 1999).

KATANGA SUPERGROUP- LOWER ROAN GROUP SEDIMENTS

Conglomeratic and arkosic sediments of the siliciclastic unit in the lower Roan Group at Nchanga Mine nonconformably overlie the Nchanga Granite. Previous studies have indicated that there are pebbles and zircons from the Nchanga Granite in basal Roan conglomerates, suggesting that the lower Roan sediments are derived by erosion of a basement that included the Nchanga Granite. We sampled a suite of detrital zircons from a crossbedded Roan arkose about 10 metres above the contact with the Nchanga Granite in borehole P322 drilled underground at Nchanga Mine. U-Pb SHRIMP dating of these detrital zircons reveals two distinct age populations (Figure 1), one at around 2.0 to 1.8 Ga (corresponding to the age of the Palaeoproterozoic basement), and the other at 880 Ma (coresponding to the age of the Nchanga Granite). This unequivocally proves that the Nchanga Granite provided detritus to the Lower Roan, and sets a firm older limit of c. 880 Ma for the age of the Katanga Supergroup.

Detrital zircons from several other samples of lower Roan Group sediments from Mine de l'Etoile, Musoshi, Konkola, and the Chambishi Basin were U-Pb dated with the SHRIMP. Most of the samples have zircons almost exclusively of Palaeoproterozoic age with a few older and younger ages. Unless otherwise indicated, all ages quoted are $^{207}\text{Pb}/^{206}\text{Pb}$ ages on zircons that are $< \pm 10\%$ discordant on a $^{206}\text{Pb}/^{238}\text{U}$ vs $^{207}\text{Pb}/^{235}\text{U}$ concordia diagram. The sample from Etoile had two zircons of late Archaean age (2831 ± 16 and 2802 ± 36 Ma), and one zircon dated at 1858 ± 24 Ma. Two samples from Musoshi had detrital zircons in the age ranges 1883 ± 21 to 2066 ± 20 Ma (MUS3, 10 analyses) and 1789 ± 35 to 2081 ± 28 Ma (SPOTMU, 46 analyses) respectively. A sample from Konkola (KNS7, 14 analyses) yielded a similar detrital zircon age range to the Musoshi samples, from 1836 ± 26 to 1996 ± 15 Ma. The sample from the Chambishi Basin (RCB2/4, 17 analyses) yielded the following ages of detrital zircons: 908 ± 40 Ma; 891 ± 119 Ma [115% concordant]; 1152 ± 65 Ma; 1301 ± 46 Ma; 1813 ± 28 to 2062 ± 38 Ma. In addition, 42 zircons from the same sample were analysed only for $^{206}\text{Pb}/^{238}\text{U}$, and yielded less reliable $^{206}\text{Pb}/^{238}\text{U}$ ages as follows: 1282 ± 31 Ma; 1711 ± 36 to 2200 ± 48 Ma; 2431 ± 37 Ma; 2840 ± 69 to 2857 ± 60 Ma. These data indicate that the source region for the Lower Roan sediments consisted mainly of Palaeoproterozoic rocks dated between 1790 and 2200 Ma (derived from the Palaeoproterozoic magmatic arc terrain), with minor contributions from older Neoarchaean rocks (c. 2860 to 2800 Ma) (possibly derived from the Kasai Craton) and some younger Mesoproterozoic to early Neoproterozoic rocks (c. 1300 to 900 Ma), possibly derived from the Kibaran Belt.

MWASHYA GROUP

The Mwashya Group, lying above the Roan Group, consists mainly of carbonates and black shales, but contains a thin pyroclastic unit with associated stratiform banded magnetite/haematite iron formations, which form a regional stratigraphic marker. The pyroclastics, mainly mafic lapilli tuffs and agglomerates, are best developed at Shituru Mine near Likasi (D. R. Congo). An attempt was made to date zircons from these pyroclastics (sample S11), but they turned out to be entirely xenocrystic, with ages ranging from 3225 to 1068 Ma (Rainaud et al., 2000). Another sample (S27-S32) of agglomerate from borehole S1 at Shituru Mine yielded three xenocrystic zircon grains with U-Pb SHRIMP ages of 1870 ± 15 , 1047 ± 25 and 983 ± 50 Ma, reflecting inheritance from Palaeoproterozoic and Kibaran rocks. In western Zambia, in the Mwinilunga area, Key and Banda (2000) have mapped a several hundred metres thick volcanic unit within the Mwashya Group, the Lwavu Formation, which consists of basalts and basaltic andesites. These volcanics have been dated at 760 ± 5 Ma, utilising SHRIMP U-Pb dating on zircons (Armstrong, 2000; Liyungu et al., 2001; Key et al., 2001). This is the first accurate date for any Katangan lithological unit.

KUNDELUNGU/ GUBA GROUP

To the southeast of the Mwinilunga area, strongly deformed and poorly differentiated Katangan rocks of the West Lunga Formation, comprising shales, dolomites, siltstones, diamictites, banded iron formations and porphyritic volcanics, have been provisionally correlated with the Kundelungu Supergroup (Liyungu et al., 2001). One of the porphyritic lavas in this area has been dated with the SHRIMP (U/Pb on single zircons) at 735 ± 5 Ma (Armstrong, 2000; Liyungu et al., 2001). We also dated a suite of detrital zircons from the Grand Conglomerat at Kipushi Mine (sample K30-K41, borehole KHI 115034HZ-5, 150-207 m). These detrital zircons have ages ranging from Palaeoproterozoic to Neoproterozoic, as follows: $1945 \pm 15 - 1846 \pm 22$ Ma (6 zircons); and $1025 \pm 86 - 822 \pm 42$ Ma (4 zircons). One zircon gave an age of 729 ± 50 Ma, but it was only 88% concordant.

PLATEAU GROUP

Detrital muscovites from red siltstones of the Plateau Group collected in the Kundelungu Plateau National Park, Katanga, D.R. Congo, were dated using the laser $^{40}\text{Ar}/^{39}\text{Ar}$ technique. The results of laser probe spot fusion of seven individual detrital muscovite grains show a range of $^{40}\text{Ar}/^{39}\text{Ar}$ ages between 635 and 565 Ma, with one age of 1472.4 ± 5 Ma (Figure 2). The youngest detrital muscovite age of 565 ± 5 Ma is regarded as the maximum age for the sediments of the Plateau Group, which are thus constrained to be terminal Neoproterozoic and/or Palaeozoic in age. 50 detrital zircons from the same sample (KPM3) were dated using U-Pb (SHRIMP)- of these, 47 ages were $<\pm 10\%$ discordant. These ages range from $1977 \pm 11 - 1780 \pm 37$ Ma (45 zircons) and $1219 \pm 113 - 1176 \pm 62$ Ma (2 zircons). One zircon had a young age of 463 ± 118 Ma, but it was 144% concordant, and plotted above the concordia curve.

DISCUSSION

The deposition of the Katanga Supergroup started at some time after 880 Ma. The ages of volcanic units in the Mwashya and Lower Kundelungu (Guba) Groups bracket the age of the Grand Conglomerat between 760 ± 5 and 735 ± 5 Ma. This allows the correlation of the Grand Conglomerat with other Neoproterozoic glacial diamictite units such as the Chuos diamictite in the Damara Orogen (Namibia) and the Sturtian diamictites of the Adelaidean Supergroup, South Australia. The age of the Petit Conglomerat is not yet well constrained. The Plateau Group of the Katanga Supergroup now has a maximum age of 575 ± 5 Ma based on laser $^{40}\text{Ar}-^{39}\text{Ar}$ dating of detrital muscovites. The Plateau Group was thus deposited either in the terminal Neoproterozoic, or in the early Palaeozoic, and this timing strongly supports models which regard the Plateau Group as being deposited in a foreland basin to the Pan-African Lufilian orogeny, rather than the earlier models which regarded it as having been deposited in an aulacogen. Detrital zircon ages indicate a mainly Palaeoproterozoic provenance area for the Katanga basin, with only minor contributions from Archaean and Mesoproterozoic (Kibaran) source regions.

ACKNOWLEDGEMENTS

We are grateful to Anglovaal (Zambia) and Klaus Schlegel for supporting this study and for permission to publish this data. We thank ZCCM (Zambia), Gécamines and SODIMICO (D. R. Congo) for access to drillcore.

REFERENCES

- Armstrong, R.A. (2000). Ion microprobe (SHRIMP) dating of zircons from granites, granulites and volcanic samples from Zambia. Unpubl. Rep., ANU, PRISE Job No. A99-160, Canberra.
- Armstrong, R.A., Robb, L.J., Master, S., Kruger, F.J. & Mumba, P.A.C.C. (1999). New U-Pb age constraints on the Katangan Sequence, Central African Copperbelt. J. Afr. Earth Sci., 28(4A), 6-7.
- Key, R. & Banda, J. (2000). The Geology of the Kalene Hills area. Rep. Geol. Surv. Zambia, 107.

Key, R. M., Liyungu, A. K., Njam, F. M., Somwe, V., Banda, J., Mosley, P. N. & Armstrong, R. A. (2001). The Western arm of the Lufilian Arc, NW Zambia and its potential for copper mineralization. *J. Afr. Earth Sci.*, 33 (3-4), 503-528.

Liyungu, A. K., Mosley, P.N., Njam, F.M. & Banda, J. (2001). Geology of the Mwinilunga area. Rep. Geol. Surv. Zambia, 110, 36 pp.

Rainaud, C., Armstrong, R.A., Master, S. & Robb, L.J. (1999). A fertile Palaeoproterozoic magmatic arc beneath the Central African Copperbelt. In: Stanley, C.J. et al. (Eds.), *Mineral Deposits: Processes to Processing*, Volume 2. A.A. Balkema, Rotterdam, 1427-1430.

Rainaud, C., Master, S., Armstrong, R.A. & Robb. L.J. (2000). A cryptic Mesoarchaean terrane in the basement to the Central African Copperbelt: U-Pb isotopic evidence from detrital and xenocrystic zircons in the Muva and Katangan sequences. *J. Afr. Earth Sci.*, 30(4A), 72-73.

Tembo, F., Kampunzu, A.B. & Musonda, B.M. (2000). Geochemical characteristics of Neoproterozoic A-type granites in the Lufilian Belt, Zambia. *J. Afr. Earth Sci.*, 30(4A), p. 85.

Wendorff, M. (2001). New exploration criteria for 'megabreccia'-hosted Cu-Co deposits in the Katangan belt, central Africa. In: Piestrzynski, A. et al. (Eds.), *Mineral Deposits at the Beginning of the 21st Century*. Swets & Zeitlinger Publishers, Lisse, Netherlands, 19-22.

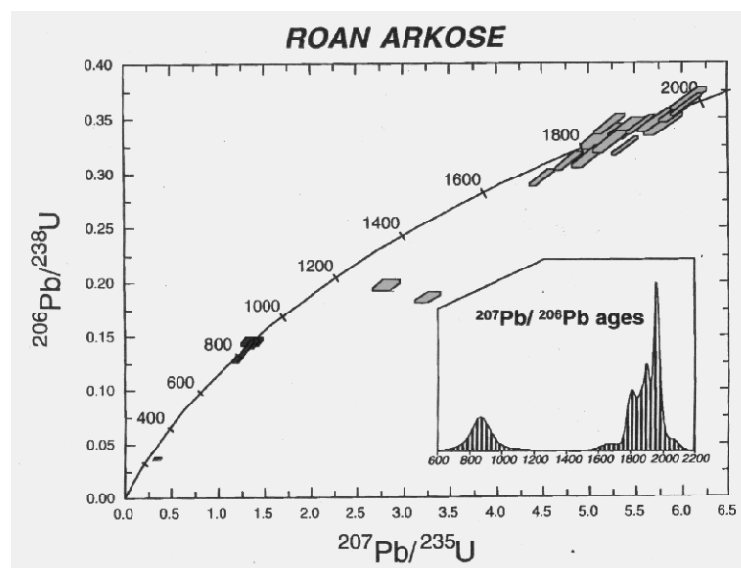


Figure 1: U-Pb concordia diagram showing the ages of detrital zircons from lower Roan Group arkose, 10 m above the contact with the Nchanga granite, Borehole P322, Nchanga Mine, Zambia.

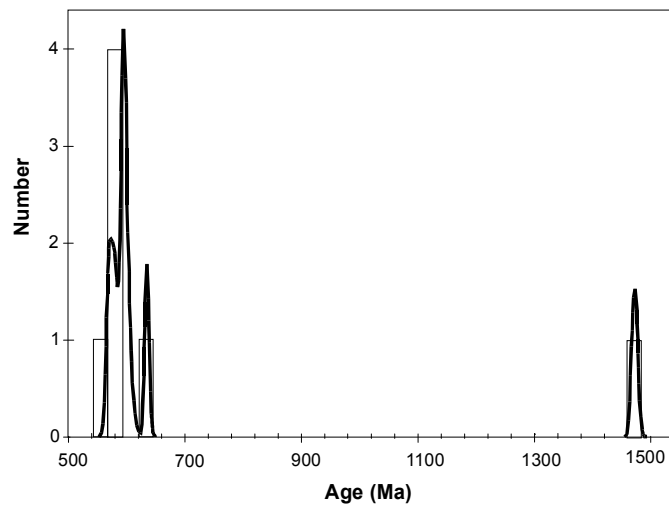


Figure 2: Histogram showing $^{40}\text{Ar}/^{39}\text{Ar}$ ages on individual detrital muscovite grains from a red siltstone of the Plateau Group, Kundelungu Plateau National Park, D. R. Congo

CONTRIBUTIONS TO THE GEOLOGY AND MINERALISATION OF THE CENTRAL AFRICAN COPPERBELT: III - NATURE OF METAMORPHIC AND EPIGENETIC FLUIDS

L.N. GREYLING, Y. YAO, L.J. ROBB and S. MASTER

Economic Geology Research Institute – Hugh Allsopp Laboratory,
School of Geosciences, University of the Witwatersrand, South Africa,
e-mail: greylin@science.pg.wits.ac.za

SYNOPSIS

Preliminary fluid inclusion results indicate the presence of aqueous-carbonic fluid species in pre-deformation fluids, and aqueous fluid species in syn-tectonic, and post-deformational fluids. Fluid inclusion microthermometry and Raman spectrometry of quartz veins in the Chambishi open pit indicate the presence of $\text{H}_2\text{O}-\text{NaCl}-\text{CO}_2\pm\text{CH}_4$ fluids, with $\text{Th} = 130-160^\circ\text{C}$, and salinities at 23 wt.% NaCl equiv. Syn-tectonic fluids from the Nchanga open pit show $\text{H}_2\text{O}-\text{NaCl}$ compositions. Two end-member fluids are present in post-deformational veins in the Nkana deposit, namely (a) a low-salinity (8-14 wt.% NaCl equiv.) and high Th of 300-400°C; and (b) high salinity (14-23 wt.% NaCl equiv.) and low Th of 100-150°C.

INTRODUCTION

Theories on the origin and primary mineralisation mechanism of the Neoproterozoic stratiform Cu-Co ores in the Central African Copperbelt range from syngenetic-diagenetic (Schneiderhöhn, 1931, Garlick, 1961, Sweeney & Binda, 1994) to epigenetic (Jackson, 1932). In an attempt, therefore, to quantify the role of various mineralising mechanisms, late fluid characteristics are compared to earlier diagenetic/connate fluid species associated with stratiform mineralisation. A detailed fluid inclusion study will document of the regional fluid characteristics (P-T-X-V) and aid in the modelling of the regional fluid evolution and relevance to post sedimentation mineralising events. This study focuses on the fluids trapped in vein quartz from the Nchanga, Nkana, Chambishi, Konkola, and Mufulira deposits, with the initial emphasis on late stage veins associated epigenetic (remobilised?) mineralisation. This paper is a summary of preliminary results of fluid inclusion microthermometry in vein quartz from various geological settings.

GEOLOGICAL SETTING

Stratiform Cu-Co ores are hosted in the Neoproterozoic Katangan Sequence on the border between the Democratic Republic of the Congo and Zambia (Fig. 1). The ores occur mostly in the Ore Shale, but are also found in overlying feldspathic quartzites, and wackes. The Katangan Sequence is divided in Zambia into the Roan Supergroup, Lower Kundelungu, and Upper Kundelungu Supergroups (Fig. 2). The sediments of the Katangan Sequence were metamorphosed and deformed to greenschist and amphibolite facies during the Lufilian orogeny at ca. 600 - 500 Ma (John et al., 2002).

PREVIOUS FLUID INCLUSION STUDIES

Pirmolin (1970) described the presence of several solid phases in fluid inclusions from a unmineralised cherty dolomite layer of the Mines Group of the Roan Supergroup in the Democratic Republic of Congo, and concluded that mineralising solutions reached temperatures of $\sim 200^\circ\text{C}$ at salinities of ~ 40 wt.% NaCl equiv.

Fluid inclusions, hosted in crosscutting vein quartz through the Ore Shale from Konkola Mine, showed post-trapping alteration features (e.g. leakage and annealing), which lead Sweeney (1987) to conclude that these veins had undergone at least one post-formational tectono-thermal event. He found that inclusions of the same vein system showed varying fluid chemistry at different stratigraphic horizons, and identified the presence of hydrocarbon inclusions in several samples.

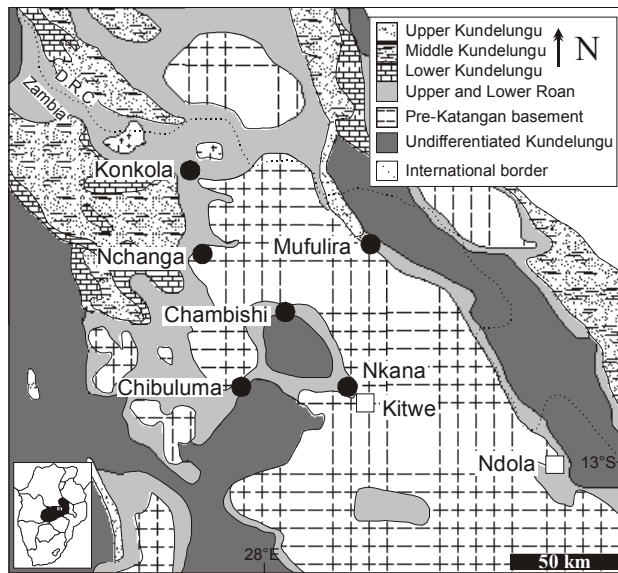


Fig. 1. Geological map of the Copperbelt in the Democratic Republic of Congo and Zambia.

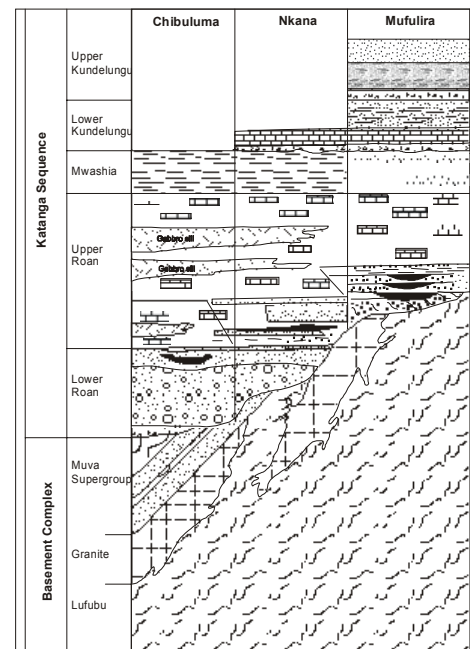


Fig. 2. Generalised stratigraphic profile of the Chibuluma, Nkana, and Mufulira deposits (after Fleischer et al., 1976).

This author also related the varying fluid chemistry to corresponding diagenetic changes in the different lithologies during basin evolution, and concluded that the veins formed by lateral migration of fluids during late diagenetic dewatering at temperatures of $\sim 120^{\circ}\text{C}$.

Richards et al. (1988) indicated the presence of a halite-saturated fluid at temperatures of $\sim 397^{\circ}\text{C}$ in veins from the Musoshi copper deposit (D.R.C.), where late hydrothermal veining caused extensive footwall- and ore shale- alteration. Fluids were composed of approximately 39 wt.% NaCl, 15 wt.% KCl, and minor amounts of CO₂. It is concluded that the hydrothermal alteration event post-dated the stratiform copper mineralisation, causing modification of existing sulphide textures. The event may have been linked to compressional deformation and metamorphism during the Lufulian orogeny (Richards et al., 1987).

Epithermal mineralisation at the Kansashi Copper Mine (Solwezi area, northwestern Zambia) was studied by Speiser et al. (1995), where vein mineralisation is related to hydrothermal alteration of the host rocks. Six fluid inclusion types were documented from the copper-quartz veins, and showed that epigenetic mineralisation precipitated from Na-Ca-Cl-H₂O-CO₂-(CH₄) brines. Ore formation pressures and temperatures correspond to 1.2 – 2.5 kbar and 230 – 310 °C respectively. Copper mineralisation post-dated host rock metamorphism, with crustal extension leading to increased heat flow and related hydrothermal fluid activity.

FLUID INCLUSIONS

Non-mineralised and mineralised (chalcocite-bornite-chalcopyrite-carrollite-malachite) quartz veins from the Chambishi, Nkana, Nchanga, Konkola, and Mufulira deposits in the Zambian Copperbelt are both discordant and bedding parallel and are representative of successive tectonic episodes during basin evolution. Samples in the Chambishi open pit were taken from quartz veins occurring bedding parallel to the Ore Shale (Fig. 3). Lateral secretion of mineralisation into the veins was noted with a refracted cleavage running through the quartz veins, indicating the emplacement of the quartz veins *prior to deformation and folding* of the mineralised sediments. Fluids in these samples show primary and secondary inclusions of H₂O-NaCl-CO₂±CH₄ compositions (Fig. 4), with a salinity of 23 wt.% NaCl equiv.

Quartz veins, occurring along the mineralised cupriferous vermiculite schist décollement plane in the Nchanga open pit, are representative of *syn-tectonic* fluids, and indicate the

presence of H₂O-NaCl fluids in primary fluid inclusions. These NaCl-saturated solutions were heterogeneously trapped, as shown by the varying liquid-vapour-solid ratios.

Post-tectonic fluids were sampled from drill core through the Nkana synclinorium, from mineralised K-feldspar-quartz-biotite-anhydrite assemblage veins crosscutting host sediments. Primary and secondary inclusions from these veins show compositions of aqueous solutions (H₂O-NaCl) (Fig. 5). Initial microthermometric results show two possible end-member fluids: (A) low-salinity (8-14 wt.% NaCl equiv.) and high Th (300-400°C), and (B) high salinity (14-23 wt.% NaCl equiv.) and low Th (100-150°C) (Fig. 6).

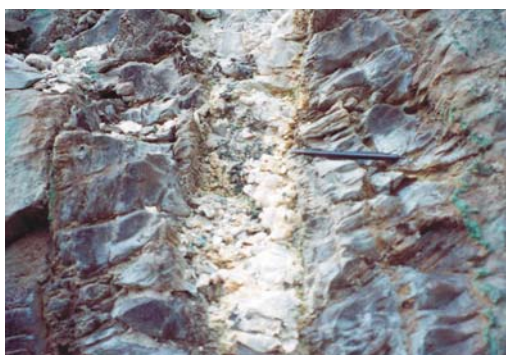


Fig. 3. Lateral secretion vein in Ore Shale.

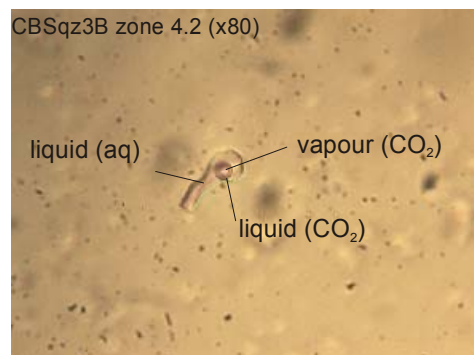


Fig. 4. Primary aqueous-carbonic fluid inclusion.



Fig. 5. Primary aqueous cluster inclusions.

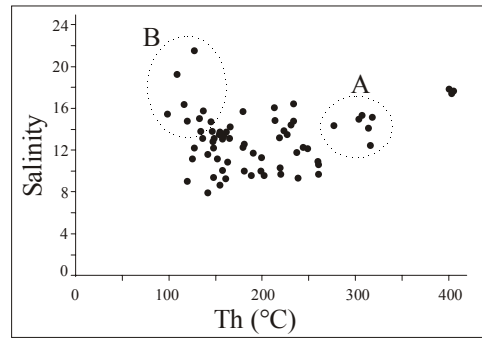


Fig. 6. Salinity (wt.% NaCl equiv.) vs. Th showing two end-member fluids.

DISCUSSION AND CONCLUSION

Initial studies of fluid inclusions, representative of various tectonic settings (pre-deformational, syn-tectonic, post-deformational), indicate the dominance of aqueous fluid species. Low temperature – high salinity fluids may be characteristic of basinal brines, which may correspond to early diagenetic stratiform mineralisation. High temperature – low salinity fluids are possibly derived from later regional metamorphic events, which are related to later stage remobilisation of mineralisation. It is suggested that stratiform Cu-Co mineralisation in the Zambian Copperbelt is resultant of multiple mineralisation events, involving diagenetic, metamorphic, and epigenetic processes.

ACKNOWLEDGEMENTS

Funding for this project is provided by the Economic Geology Research Institute, the University of the Witwatersrand and the National Research Foundation of South Africa. Anglo American (KCM), AVMIN, Non-Ferrous Metals Plc and First Quantum are thanked for providing access to the deposits.

REFERENCES

- Fleischer V.D., Garlick W.G., Haldane R., (1976) Geology of the Zambian Copperbelt. In: K.H. Wolf (ed.) Handbook of strata-bound and stratiform ore deposits. II – Regional studies and specific deposits. Vol. 6, Cu, Zn, Pb, and Ag deposits. Elsevier, Amsterdam. p. 223-351.

John T., Schenk V., Scherer E., Mezger K., Haase K., Tembo F. (2002) Subduction and continental collision in the Lufulian Arc-Zambezi Belt orogen (Zambia): implications to the Gondwana assembly. Abstract Volume: 19th colloquium of African Geology, El Jadida, Morocco, 19-22 March 2002, p.188.

Pirmolin J., (1970) Inclusions fluids dans la dolomite du Gisement stratiforme de Kamoto (Katanga Occidental). Annales de la Société Géologique de Belgique, T. 93, p.397-406.

Richards J.P., Krogh T.E., Spooner E.T.C., (1988) Fluid inclusion characteristics and U-Pb Rutile age of late hydrothermal alteration and veining at the Musoshi stratiform copper deposit, Central African Copper Belt, Zaire. Economic Geology, vol. 83, p.118-139.

Speiser A., Hein U.F., Porada H., (1995) The Kansanshi Copper Mine (Solwezi area, northwestern Zambia): Geology, wall-rock alteration and fluid inclusions. Mineral Deposits. Pasava, Kribek & Zak (eds), p. 389-392.

Sweeney M., (1987) The use of fluid inclusion geochemistry in determining the origin of veins, examples from the Zambian Copperbelt. Zambian Journal of Applied Earth Sciences, vol.1, p.18-28.

CONTRIBUTIONS TO THE GEOLOGY AND MINERALIZATION OF THE CENTRAL AFRICAN COPPERBELT: IV. MONAZITE U-Pb DATING AND ^{40}Ar - ^{39}Ar THERMOCHRONOLOGY OF METAMORPHIC EVENTS DURING THE LUFILIAN OROGENY.

C. RAINAUD¹, S. MASTER¹, R. A. ARMSTRONG², D. PHILLIPS^{2,3}
AND L. J. ROBB¹

¹Economic Geology Research Institute, School of Geosciences,
University of the Witwatersrand, P. Bag 3, WITS 2050, South Africa
²PRISE, Research School of Earth Sciences, Australian National University,
Canberra, Australia
³Present Address: University of Melbourne, Melbourne, Victoria, Australia

SYNOPSIS

We present new SHRIMP U-Pb age data on metamorphic monazite, as well as step-heating ^{40}Ar / ^{39}Ar plateau ages on metamorphic biotites and K-feldspar, from Katangan metasedimentary rocks from the Central African Copperbelt, which were deformed and metamorphosed during the Pan-African Lufilian Orogeny. Three samples of metamorphic monazites from the Chambishi structural basin give ages of 592 ± 22 Ma, 531 ± 12 Ma and 512 ± 17 Ma, which correspond respectively to the ages of eclogite facies metamorphism, talc-kyanite whiteschist metamorphism, and of a regional metamorphic/mineralization pulse elsewhere within the Lufilian orogen. A biotite from Luanshya gives a ^{40}Ar / ^{39}Ar plateau age of 585.8 ± 0.8 Ma, while several samples from the Chambishi basin give ^{40}Ar / ^{39}Ar biotite ages in the range of 493 to 485 Ma, and are a manifestation of regional uplift and cooling that affected the whole Katangan basin. The youngest age obtained is a ^{40}Ar / ^{39}Ar K-feldspar age of 448.5 ± 0.7 Ma from Musoshi, coinciding with a period of late syenite intrusion.

INTRODUCTION

The Katanga Supergroup is the host of the major stratiform sediment-hosted Cu-Co deposits, as well as numerous other deposits of Cu, Pb, Zn, U, Au, Fe etc., which constitute the Central African Copperbelt in Zambia and the Democratic Republic of Congo. The Katanga Supergroup of Central Africa is a Neoproterozoic metasedimentary sequence which consists of the Roan and Mwashya Groups, the Guba Group (formerly Lower and Upper Kundelungu Groups, Wendorff (2001)), and the Fungurume and Plateau Groups. The lowermost Roan Group was deposited after c. 880 Ma, the Mwashya group was deposited around 765 Ma; the lower part of the Guba Group was deposited between 765 and 735 Ma and the upper part before c. 602 Ma, and the Fungurume and Plateau Groups were deposited syntectonically in a foreland basin during the Lufilian orogeny, after c. 570 Ma. The Katanga Supergroup was deformed and metamorphosed during the Pan-African Zambezi and Lufilian orogenies (Porada & Berhorst, 2000), at between c. 600 to 480 Ma. A large number of older U-Pb, Rb-Sr and K-Ar age data from the Lufilian arc and Zambezi belt, spanning the time period 500 ± 100 Ma are summarised by Cahen et al. (1984).

MONAZITE SHRIMP U-Pb DATING

Metamorphic monazite grains for U-Pb SHRIMP dating were extracted from samples collected from boreholes RCB1 and RCB2 which are from the Chambishi structural basin in the Zambian Copperbelt. Sample RCB2/72 is from an altered tuff (biotite retrograded to chlorite, quartz, carbonate) interbedded with iron formation within the Mwashya Group, at a depth of 497 m in borehole RCB2. Euhedral monazite intergrown with biotite or chlorite from this sample give a SHRIMP U-Pb age of 592 ± 22 Ma (Figure 1). Sample RCB1/36 is a quartz-chlorite schist from a depth of 1283 m in borehole RCB1. Monazites from this sample give a SHRIMP U-Pb age of 531 ± 12 Ma (Figure 2). Sample RCB2/112 is a marly dolomitic

argillite, from a depth of 528 m in borehole RCB2. Monazites from this sample give a SHRIMP U-Pb age of 512 ± 17 Ma (Figure 3).

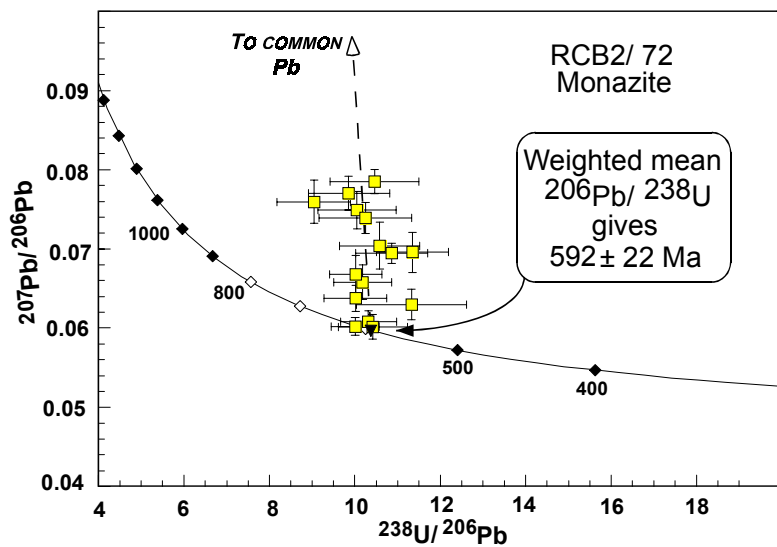


Figure 1: SHRIMP U-Pb age data on metamorphic monazite from RCB2/72 (Chambishi Basin, Zambian Copperbelt)

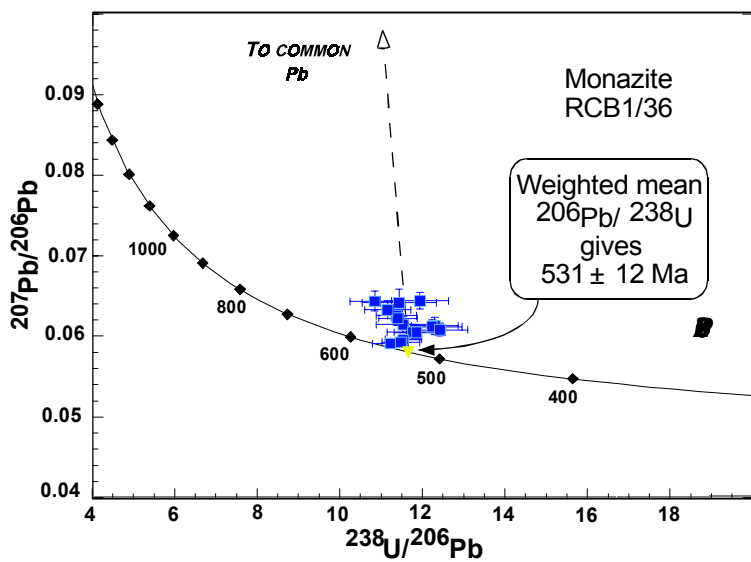
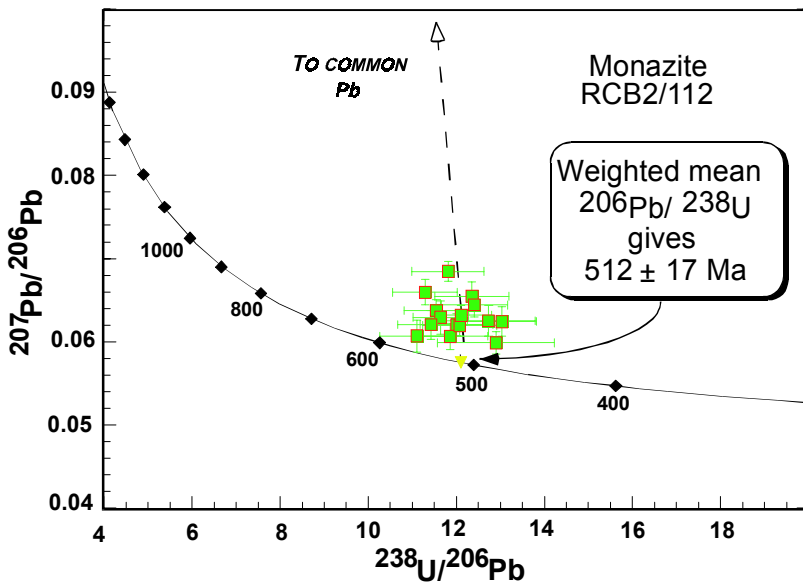


Figure 2: SHRIMP U-Pb age data on metamorphic monazite from RCB1/36 (Chambishi Basin, Zambian Copperbelt)



S

Figure 3: SHRIMP U-Pb age data on metamorphic monazite from RCB2/112 (Chambishi Basin, Zambian Copperbelt)

^{40}Ar - ^{39}Ar THERMOCHRONOLOGY

Metamorphic biotites were extracted from a number of samples ranging stratigraphically from the Lower and Upper Roan and Mwashya groups to the Grand Conglomerat at the base of the Guba (Kundelungu) Group, and were dated using the step-heating ^{40}Ar - ^{39}Ar dating technique. In addition, K-feldspar from one sample was dated using the same technique. The results are given in Table 1. Samples RCB2/112, RCB2/4, NN75/9 and MJZC9/25 are from boreholes drilled in the Chambishi Basin (Zambia); sample BH89/3 is from Luanshya (Zambia), and MUS1 is from Musoshi Mine (D.R. Congo).

Table 1: ^{40}Ar - ^{39}Ar plateau ages of biotites and K-feldspar in metamorphic rocks from the Katanga Supergroup, Central African Copperbelt

Sample	mineral dated	^{40}Ar - ^{39}Ar plateau age	Rock type	Stratigraphic position
BH89/3	biotite	585.8 ± 0.8 Ma	biotite-trem sch.	Lower Roan Gp
RCB2/112	biotite	492.6 ± 0.5 Ma	dolomitic marl	Mwashya Gp
NN75/9	biotite	487.3 ± 0.4 Ma	Rippled dolomite	Upper Roan Gp
RCB2/4	biotite	486.7 ± 0.6 Ma	Conglomerate	Lower Roan Gp
MJZC9/25	biotite	485.4 ± 0.9 Ma	Lam.grey shale	Grand Conglomerat Fm
MUS1	K-feldspar	448.5 ± 0.7 Ma	Arkose	Lower Roan Gp

DISCUSSION

In sample RCB2/72 the monazite U-Pb age of 592 ± 22 Ma is the oldest metamorphic age that we have found. This age is indistinguishable from the 595 ± 10 Ma Sm-Nd isochron age of eclogite facies metamorphism recorded from MORB-like metagabbroic eclogites from the Lufilian Arc of central Zambia (John et al., 2002). It is also similar to the 585.8 ± 0.8 Ma ^{40}Ar - ^{39}Ar age of biotite from a biotite-tremolite schist from Luanshya (sample BH89/3). A similar Rb-Sr model age of 582 ± 40 Ma was recorded from the Kafue rhyolites in the Zambezi Belt (Cahen et al., 1984). Interestingly, no K-Ar or Rb-Sr ages of c. 600-570 Ma have been found in the Domes Area, where older biotite K-Ar ages in the range of 708 ± 7 to 628 ± 7 Ma have been recorded in the Lolwa area, northwestern Kabombo Dome, and one Rb-Sr muscovite age of 744 ± 8 Ma was recorded from the Malundwe area, Mwombezhi Dome (Cosi et al., 1992).

Monazites from sample RCB1/36 have a U-Pb age of 531 ± 12 Ma. This age is indistinguishable from monazite U-Pb ages of c. 530 ± 2 Ma recorded from four talc-kyanite whiteschist localities distributed throughout the whole Lufilian Arc and Zambezi Belt (John et al., 2002). A similar biotite K-Ar age of 525 ± 5 Ma is recorded in a biotite schist from the Mutanda Bridge between the Solwezi and Mwombezhi Domes (Cosi et al., 1992).

Two distinct periods of mineralized vein emplacement at Kansanshi Mine have been dated at 512 and 502 Ma, using Re-Os dating of molybdenite, and SHRIMP U-Pb dating of monazite (Torrealday et al., 2000). These discrete episodes of mineralization have been related to post-tectonic pulses of metamorphic fluids, which appear to be recorded basinwide in the Katangan. Thus, the 512 Ma age has also been reported for late uraninite and rutile veining at Musoshi Mine (Richards et al., 1988a,b), and for uraninite mineralization at Nkana Mine (Darnley et al., 1961). In the Mwombezhi Dome, a muscovite Rb-Sr age of 512 ± 6 Ma and biotite K-Ar ages of 510 ± 6 and 518 ± 6 Ma have been obtained from the Chantete area in the NE extremity, while a biotite K-Ar age of 507 ± 6 Ma has been obtained from the centrally located Malundwe area (Cosi et al., 1992). A sample from the Kafue rhyolites in the Zambezi belt has a Rb-Sr model age age of 512 ± 35 Ma (Cahen et al., 1984). Hence the age of 512 ± 17 Ma for monazite from the Chambishi Basin (RCB2/112) is a further manifestation of the regional basinwide metamorphic event at c. 512 Ma.

The younger biotite ^{40}Ar - ^{39}Ar ages of 493 to 485 Ma reflect closure of the K-Ar system in biotite upon cooling to below 345-285°C (Harrison et al., 1985), and are a manifestation of regional uplift and cooling that affected the whole Katangan basin, since similar ages are widely recorded in the Domes Area of NW Zambia (Cosi et al., 1992), as well as in other parts of the Lufilian Arc (Cahen & Snelling, 1971). Our youngest ^{40}Ar - ^{39}Ar age of 449 ± 1 Ma on K-feldspar from Musoshi Mine (reflecting cooling below c. 300-150° C) is similar to a muscovite Rb-Sr age of 450 ± 9 Ma age from Malundwe in the Mwombezhi Dome (Cosi et al., 1992). This young metamorphic event corresponds to the age (458-427 Ma) of the late nepheline-syenite Mukumbi intrusion north of the Mwombezhi Dome (Cosi et al., 1992).

REFERENCES

- Cahen, L. & Snelling, N.J. (1971). Données radiométriques nouvelles par la méthode K-Ar. Existence d'une importante élévation de température post-tectonique dans les couches katangiennes du sud du Katanga et de la Zambia. Annales Soc. Géol. Belg., 94, 199-209.
- Cahen, L., Snelling, N.J., Delhal, J., Vail, J.R., Bonhomme, M. & Ledent, D. (1984). Geochronology and Evolution of Africa. Clarendon, Oxford, 512 pp.
- Cosi, M., De Bonis, A., Goso, G., Hunziker, J., Martinotti, G., Moratto, S., Robert, J.P. & Ruhlman, F. (1992). Late Proterozoic thrust tectonics, high pressure metamorphism and uranium mineralization in the Domes Area, Lufilian Arc, northwestern Zambia. Precambrian Res., 58, 215-240.
- Darnley, A.G., Horne, J.E.T., Smith, G.H., Chandler, T.R.D., Dance, D.F. & Preece, E.R. (1961). Ages of some uranium and thorium minerals from East and Central Africa. Mineral. Mag., 32, 716-724.
- Harrison, T.M., Duncan, I. & McDougall, I. (1985). Diffusion of ^{40}Ar in biotite: temperature, pressure and compositional effects. Geochim. Cosmochim. Acta, 49, 2461-2468.
- John, T., Schenk, V., Scherer, E., Mezger, K., Haase, K. & Tembo, F. (2002). Subduction and continental collision in the Lufilian Arc-Zambesi Belt orogen (Zambia): implications to the Gondwana assembly. Abstract, 19th Colloquium of African Geology, El Jadida, Morocco, 19-22 March 2002, p. 188.
- Porada, H. & Berhorst, V. (2000). Towards a new understanding of the Neoproterozoic-Early Palaeozoic Lufilian and northern Zambezi Belts in Zambia and the Democratic Republic of Congo. J. Afr. Earth Sci., 30, 727-771.

Richards, J.P., Krogh, T.E. & Spooner, E.T.C. (1988a). Fluid inclusion characteristics and U-Pb rutile age of late hydrothermal alteration and veining at the Musoshi stratiform copper deposit, Central African Copper Belt, Zaire. *Econ. Geol.*, 83, 118-139.

Richards, J.P., Cumming, G.L., Krstic, D., Wagner, P.A. & Spooner, E.T.C. (1988b). Pb isotope constraints on the age of sulfide ore deposition and U-Pb age of late uraninite veining at the Musoshi stratiform copper deposit, Central African Copper Belt, Zaire. *Econ. Geol.*, 83, 724-741.

Torrealday, H.I., Hitzman, M.W., Stein, H.J., Markey, R.J., Armstrong, R. & Broughton, D. (2000). Re-Os and U-Pb dating of the vein-hosted mineralization at the Kansanshi copper deposit, northern Zambia. *Economic Geology*, 95, 1165-1170.

Wendorff, M. (2001). New exploration criteria for 'megabreccia'-hosted Cu-Co deposits in the Katangan belt, central Africa. In: Piestrzynski, A. et al. (Eds.), *Mineral Deposits at the Beginning of the 21st Century*. Swets & Zeitlinger Publishers, Lisse, Netherlands, 19-22.

CONTRIBUTIONS TO THE GEOLOGY AND MINERALIZATION OF THE CENTRAL AFRICAN COPPERBELT: V. SPECULATIONS REGARDING THE ‘SNOWBALL EARTH’ AND REDOX CONTROLS ON STRATABOUND Cu-Co AND Pb-Zn MINERALIZATION

L. J. ROBB, S. MASTER, L. N. GREYLING,
Y. YAO and C. L. RAINAUD

Economic Geology Research Institute - Hugh Allsopp Laboratory,
School of Geosciences, University of the Witwatersrand, WITS 2050,
Johannesburg, South Africa.

SYNOPSIS

The major sediment-hosted Fe and Mn deposits of the world have formed by oxidative precipitation from ocean waters that are stratified in terms of redox state. There is mounting evidence that both Palaeoproterozoic Superior-type banded iron-formations and Neoproterozoic Rapitan-type iron ores formed in environments where fluctuations in redox states were influenced by global ice ages. Recent constraints on the age of the Katangan sequence in the Central African Copperbelt links much of its depositional history to the Cryogenian Period (850 to 650 Ma), during which time the Neoproterozoic ‘Snowball Earth’ occurred. This raises the question as to whether certain styles of stratiform sediment hosted copper (SSC) mineralization might also be genetically linked to the near-surface redox fluctuations that are associated with periods of global glaciation. Stratiform Cu-Co mineralization in the Copperbelt is early-to-late diagenetic in its timing and is suggested to be a product of the mixing of two fluids, one a pregnant oxidized solution and the other a reduced barren one. A source of reduced fluid might be compaction and diagenesis of sediments deposited during the global anoxia that accompanied the Sturtian/Chuos/Kaigas ice age at around 750 Ma. Fluids derived from such reduced sediments may also have been responsible for the formation of epigenetic Pb-Zn deposits hosted by cap carbonates. Our initial fluid inclusion studies indicate more than a single fluid population, although the relationship between fluids and the paragenetic sequence remains to be determined. Such a link needs to be tested by accurate age determinations of the stratabound mineralization events.

INTRODUCTION

The major sediment-hosted Fe and Mn deposits of the world have formed by oxidative precipitation from sea water that was stratified with respect to its redox state. Neoproterozoic Rapitan-type iron-formations formed in environments where fluctuations in near-surface redox states were influenced by two or more near-global ice ages, popularly referred to as the ‘Snowball Earth’ events (Hofmann & Schrag, 2000). There is mounting evidence that Palaeoproterozoic Superior-type banded iron-formations, as well as related bedded Mn ores, might also be related to a period of extensive low-latitude glaciation (Kirschvink et al., 2000). It is also intriguing to note that the Duitschland Formation of the Palaeoproterozoic Transvaal Supergroup is characterized by minor stratiform Cu deposits (Martini, 1979) hosted in limestones associated with diamictite units that are correlatable with the same low-latitude glaciogenic Makganyene diamictite with which the huge Fe and Mn ores of Griqualand West are linked (Bekker et al., 2001). Given that the solubilities of Cu, Co, Pb and Zn complexes in aqueous solution are redox sensitive, the question of environmental/climatic controls on the oxidative state of the near surface are perhaps also likely to be relevant to ore genetic considerations for the stratiform ores of the Central African Copperbelt. This is particularly so given the new constraints on the age of the Katangan sequence, a significant component of which was deposited during the Cryogenian Period (850 to 650 Ma).

RELEVANT GEOCHRONOLOGICAL CONSTRAINTS

We have recently provided U-Pb zircon geochronological constraints indicating that the Roan Group was deposited between 880 Ma (the age of the Nchanga granite and detrital zircons in the lower Roan sediments) and 760 Ma (a volcanic unit just below the Grand Conglomerat at the base of the Guba or Lower Kundelungu Supergroup; Key et al., 2001). A maximum age of the Upper Kundelungu (Plateau Group) sediments is provided by Ar-Ar ages of detrital muscovite of 565 Ma. The Katangan sequence was, therefore, deposited episodically over an extended period (>300 million years) of geological time. The two glacial diamictite units in the Katangan sequence, the Grand Conglomerat (GC) and Petit Conglomerat (PC) at the respective bases of the Lower and Upper Kundelungu Supergroups (now included in the Guba Group, Wendorff, 2001), are bracketed between 760 Ma and 580 Ma and are, therefore, possible correlatives of the Sturtian/Chuos/Kaigas (at circa 750 Ma) and the Marinoan/ Varangian/Numeens (at circa 600 Ma) glaciogenic deposits that define the Snowball Earth freeze-over. The two glaciogenic horizons are characterized by cap carbonate units immediately overlying them. Magnetite- and haematite-rich BIF units (with minor Mn) below the GC in the Mwashya are correlated with similar iron formations in the Rapitan, Urucum, Damara and other sequences worldwide, which are a reflection of globally stratified oceans during the Cryogenian period. Evidence that the Mwashya sediments were deposited during the global ice ages comes from preliminary carbon isotope data, which show a negative excursion in $\delta^{13}\text{C}$ in the Mwashya, going to a minimum of -5 permil PDB in the Grand Conglomerat, and recovering to more positive values in the Kakontwe cap carbonates. The C isotope data permit a chemostratigraphic correlation between the Mwashya and Guba Groups, and other Neoproterozoic successions deposited during the Sturtian/Chuos glaciation.

There are few if any accurate age data constraining the timing of stratiform Cu-Co mineralization in the Copperbelt. A K-Ar age of 870 ± 42 Ma (Cahen et al., 1984) for a microcline vein cutting stratiform ore is widely quoted, as is the range between 790 Ma and 750 Ma provided by Pb-Pb model ages for Pb-Zn mineralization from several deposits in the region (Kampunzu et al., 1999). However, Kamona et al. (1999) rejected the 3-stage "shale-curve" Pb-evolution model used by Kampunzu et al. (1999), and got ages of 680 Ma for Kabwe mineralization, and 456 ± 18 Ma for Kipushi mineralization. Richards et al. (1988) provided a Pb-Pb model age of 645 ± 15 Ma for Cu-Fe sulphides from the Musoshi Mine, a date interpreted as reflecting either primary ore deposition or Pb re-homogenization. Walraven and Chabu (1991) obtained a Pb model age of 823 Ma for Kinsenda copper sulphide mineralization. Given the long-lived depositional history of the Katangan sequences, it is clear that the concept of diagenetic mineralization is likely to be grossly diachronous and could itself have extended over an extended period of geological time. Diagenesis and related fluid flow in the lower Roan sediments were probably separated by more than 100 million years of time from those in the upper Mwashya and lower Kundelungu sequences.

NATURE OF STRATABOUND Cu-Co MINERALIZATION

Mineralization consists of disseminated copper and cobalt sulphide minerals (chalcocite, bornite, chalcopyrite, carrolite) occurring as dispersed grains, fracture fillings, near massive lenses and replacements of diagenetic pyrite, Fe-Ti detrital minerals and micaceous silicates. The sedimentary host rocks mainly form part of the lower Roan Supergroup and comprise a wide range of lithotypes, including basal continental clastics and aeolianites, shales and siltstones, evaporitic carbonates, dolomitic shales and stromatolitic bioherms. Much of the mineralization is linked to the 'Ore Shale', that was formed in a restricted marine or lacustrine environment, although many other sediment types are also mineralized. In at least one situation at Shituru Mine, stratiform mineralization is hosted by reduced volcaniclastic rocks in the Mwashya Group (Lefebvre, 1974). Unrug (1988) has emphasized the fact that stratiform Cu-Co mineralization is distributed throughout the Roan Supergroup but does not occur above the GC, into the Kundelungu sequences. Different scales of mineral zonation are evident in the district and, in general, there is metal segregation into Cu, Cu-Co and Pb-Zn rich zones.

NATURE OF Pb-Zn MINERALIZATION

Pb-Zn mineralization in the Katangan is epigenetic, and occurs in transgressive orebodies hosted in two different stratigraphic units. At Kabwe, Zambia, Pb-Zn-(V-Ga-Ge-Cd-Ag) mineralization in pipe-like bodies is hosted by carbonate rocks correlated with the Upper Roan Group. Highly saline (c. 30 wt.% eNaCl) fluid inclusions from Kabwe show homogenisation temperatures of 60 to 390°C (Kamona, 1993). At Kipushi, Kengere and Lombe in D. R. Congo, transgressive Zn-Pb-(Cu-Ga-Ge-Mo-As-Ag) mineralization occurring along faults and in breccia fill is hosted by the Kakontwe cap carbonate above the Grand Conglomerat. Kipushi fluids were reducing, since hydrocarbons ("shungite") are associated with the mineralization (Francotte & Jedwab, 1963), which was deposited at c. 300°C (T_h on fluid inclusions, Kapenda, unpubl. data, in Kampunzu et al., 1998).

REDOX BEHAVIOUR OF Cu, Co, Pb AND Zn

There is abundant geological evidence (e.g. replacement textures, reduction spheroids etc) to indicate that the formation of stratiform ores in the Copperbelt has been influenced by redox reactions involving electron transfer in an aqueous medium. The contrasting redox behaviour of metals such as Cu-Co, as well as Pb-Zn, can explain their segregation in such an environment and the development of metal zonation at a variety of scales. The higher the standard reduction potential (Eh_o) of a metal the more susceptible the species is to being reduced.

$Cu \leftrightarrow Cu^{2+} + 2e^-$	$Eh_o = +0.34V$
$Pb \leftrightarrow Pb^{2+} + 2e^-$	$Eh_o = -0.13V$
$Co \leftrightarrow Co^{2+} + 2e^-$	$Eh_o = -0.28V$
$Zn \leftrightarrow Zn^{2+} + 2e^-$	$Eh_o = -0.76V$

The contrasting characteristics of Cu and Co are illustrated in the redox reactions above and also illustrated in Figure 1. It is clear that progressive reduction will first result in the precipitation of Cu from an aqueous solution, followed under more reducing conditions by Co. Superposition of oxic and anoxic fluid fields on the Eh-pH diagram in Figure 1 shows that Cu and Co complexes are relatively soluble under oxic conditions but are less stable under reducing conditions.

The effects of mixing an oxidized, metal-charged fluid with a more reducing liquid such as an oilfield brine have been modelled by Metcalfe et al. (1994) who showed that addition of even a small proportion of the latter will, after only 5% mixing, dramatically change the redox state and promote the sequential precipitation of, first Cu, and then Pb and Zn (once all the Cu had effectively been stripped from solution Figure 2). Although data is not available for Co, the sequence is consistent with the paragenetic characteristics of SSC deposits in general.

GLOBAL ANOXIA AND THE FORMATION OF COPPERBELT STRATIFORM ORES?

Stratiform Cu-Co mineralization in the Copperbelt is generally regarded as being early-to-late diagenetic in its timing. Widely accepted models for the formation of SSC ores (Unrug, 1988; Jowett, 1986) envisage circulation of oxidized brines through porous continental (often aeolian) arenites that are themselves enriched in detritus from a metal fertile provenance. These fluids scavenge metals that have high solubilities in saline, oxidized and near neutral solutions (such as Cu, Co, U, Ni etc), with precipitation of metals occurring as they encounter environments where redox reactions take place (i.e. in the presence of diagenetic sulphides, organic rich sediments etc). Two scenarios exist, that are not mutually exclusive; (i) scavenging of metals by a *single oxidized fluid* passing through permeable strata with lateral precipitation of ores in the proximity of more reduced facies (Bechtel et al., 2002); or (ii) the mingling of *two fluids* in a single aquifer, one a pregnant oxidized solution and the other a reduced barren one (e.g., Bartholomé et al., 1972). Our initial fluid inclusion work suggests that the earliest fluids recorded (e.g. from Chambishi Mine) are characterized by low homogenization temperatures ($T_h = 130$ to 160°C) and constant high salinity (23 wt.% eNaCl; $H_2O-NaCl-CO_2\pm CH_4$) fluid compositions that are potentially diagenetic in origin. Later syn- to post-orogenic fluids (e.g. Nchanga and Nkana Mines) are more diverse in composition and typically have higher homogenization temperatures.

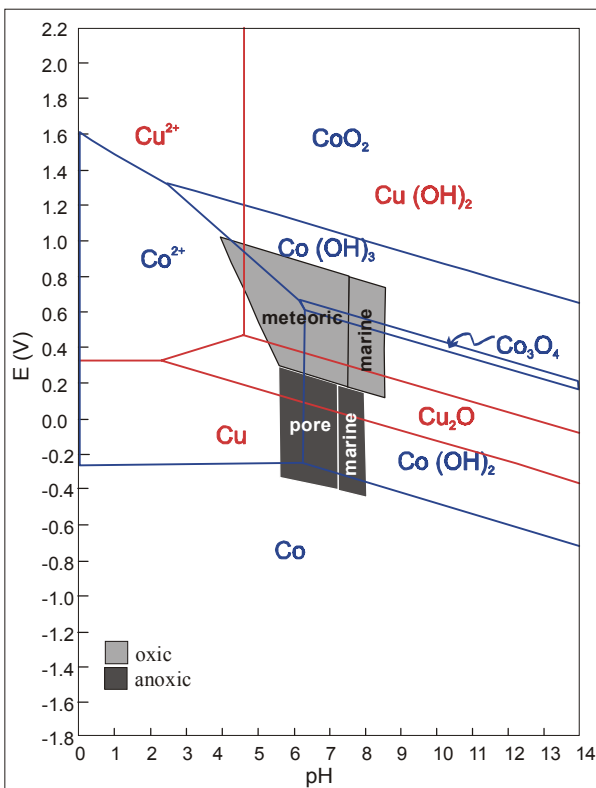


Figure 1: Potential - pH diagram for Cu and Co in the system Cu-Co-H₂O at 25°C (after de Zoubov et al., 1980, and Deltombe, 1980).

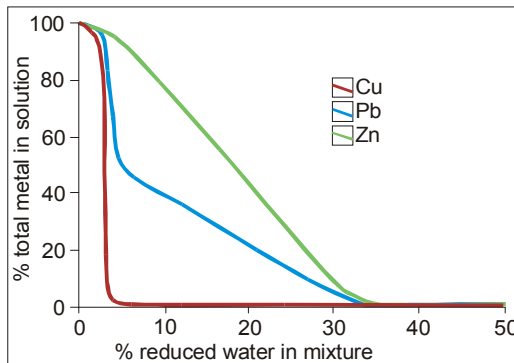


Figure 2: Fluid-rock equilibrium model showing the effect on Cu, Pb, and Zn solubility of mixing a reduced connate fluid with an oxidized metal-laden, diagenetic pore fluid (after Metcalfe et al., 1994).

In the ore genetic scenario involving the mixing of two fluids, the oxidised, metal-bearing fluid is generally thought to be a saline basin brine which became oxidising and chloride and sulphate enriched through reaction with red beds and evaporites. The reduced fluid is generally thought to be expelled into aquifers from the compaction of reduced organic-rich sediments. In the Katangan basin, oxidised brines could have evolved through reaction with the abundant evaporites in the

upper Roan Group. We suggest that the reduced fluids responsible for Pb-Zn mineralization, and for some of the Cu-Co mineralization in the two-fluid mixing model (e.g. at Shituru), could have been derived from the abundant black shales in the Mwashya Group, which were deposited during global anoxia coinciding with Snowball Earth conditions.

CONCLUSIONS

Although the conceptual notions regarding fluid mixing and metal deposition in SSC deposit environments are not new, they receive added credibility with respect to the Central African Copperbelt in the light of the new Cryogenian age constraints for Katangan deposition and preliminary fluid inclusion characteristics of ore bearing fluids. Confirmation of such a link with respect to the stratiform Cu-Co ores will need to be rigorously tested by obtaining accurate age determinations for the mineralization events.

REFERENCES

- Bartholomé, P., Evrard, P., Katekesha, F., Lopez-Ruiz, J. & Ngongo, M. (1972) Diagenetic ore-forming processes at Kamoto, Katanga, Republic of the Congo. In: Amstutz, G. C. & Bernard, A. J. (Eds.), Ores in sediments. Springer, Berlin, 21-41.
- Bechtel, A., Gratzer, R., Püttmann, W. & Oszczepalski, S. (2002). Geochemical characteristics across the oxic/anoxic interface (Rote Fäule front) within the Kupferschiefer of the Lubin-Sieroszowice mining district (SW Poland). *Chemical Geology*, 185, 9-31.
- Bekker, A., Kaufman, A. J., Karhu, J. A., Beukes, N. J., Swart, Q. D., Coetzee, L. L. & Eriksson, K. A. (2001). Chemostratigraphy of the Palaeoproterozoic Duitschland Formation, South Africa: Implications for coupled climate change and carbon cycling. *American Journal of Science*, 301, 261-285.
- De Zoubov, N., Vanleugenhanghe C., & Pourbaix M. (1980). Copper, Section 14.1. In: Pourbaix M. (Ed.), Atlas of electrochemical equilibria in aqueous solutions. National Association of Corrosion Engineers, Houston, Texas, U.S.A. CEBELCOR (ed.) Brussels. p. 384-392.
- Deltombe E. & Pourbaix M. (1980). Cobalt, Section 12.2. In: Pourbaix M. (Ed.), Atlas of electrochemical equilibria in aqueous solutions. National Association of Corrosion Engineers, Houston, Texas, U.S.A. CEBELCOR (Ed.) Brussels. p. 322-329.
- Cahen, L., Snelling., N. J., Delhal, J., Vail, J. R., Bonhomme, M. & Ledent, D. (1984). The Geochronology and Evolution of Africa. Clarendon, Oxford, 512 pp.
- Francotte, J. & Jedwab, J. (1963). Traces d'organites (?) dans la Shungite de Kipushi. *Bull. Soc. géol. Belg.*, 72, 393-400.
- Hofmann, P. F. & Schrag, D. P. (2000). Snowball Earth. *Scientific American*, 282(1), January, 50-57.
- Jowett, E. C. (1986). Genesis of Kupferschiefer Cu-Ag deposits by convective flow of Rotliegendes brines during Triassic rifting. *Economic Geology*, 81, 1823-1837.
- Kamona, F. (1993). The carbonate-hosted Kabwe Pb-Zn deposit, Central Zambia. Ph.D. thesis, TU Aachen, Germany, Mitteilungen zur Mineralogie und Lagerstättenlehre, 44, 207 pp.
- Kamona, F., Leveque, J., Friedrich, G. & Haack, U. (1999). Pb isotopes of the carbonate-hosted Kabwe, Tsumeb, and Kipushi Pb-Zn-Cu sulphide deposits in relation to Pan African orogenesis in the Damara-Lufilian Fold Belt of Central Africa. *Mineralium Deposita*, 34, 273 - 283.

- Kampunzu, A. B. & Cailteux, J. (1999). Tectonic evolution of the Lufilian Arc during the Pan-African orogenesis. *Gondwana Research*, 2(3), 401-421.
- Kampunzu, A. B., Wendorff, M., Kruger, F. J. & Intiomale, M. M. (1998). Pb isotopic ages of sediment-hosted Zn-Pb mineralisation in the Neoproterozoic Copperbelt of Zambia and Democratic Republic of Congo (ex-Zaire): re-evaluation and implications. *Chronique de la Recherche Minière*, No. 530, 55-61.
- Key, R. M., Liyungu, A. K., Njam, F. M., Somwe, V., Banda, J., Mosley, P. N. & Armstrong, R. A. (2001). The Western arm of the Lufilian Arc, NW Zambia and its potential for copper mineralization. *J. Afr. Earth Sci.*, 33 (3-4), 503-528.
- Kirschvink, J. L., Gaidos, E. J., Bertani, L. E., Beukes, N. J., Gutzmer, J., Maepa, L. N. & Steinberger, R. E. (2000). The Paleoproterozoic Snowball Earth: extreme climatic and geochemical global change and its biological consequences. *Proc. National Acad. Sci.*, 97, 1400-1405.
- Lefebvre, J. J. (1974). Mineralisations cupro-cobaltifères associées aux horizons pyroclastiques situés dans le faisceau supérieur de la Serie de Roan, à Shituru, Shaba, Zaire. In: Bartholomé, P. et al. (Eds.), *Gisements stratiformes et provinces cuprifères*. Soc. Géol. Belgique, Liège, 103-122.
- Martini, J. E. J. (1979). A copper-bearing bed in the Pretoria Group in northeastern Transvaal. *Geokongress '77: Geol. Soc. S. Afr. Spec. Publ.* 6, 65-72.
- Metcalfe, R., Rochelle, C. A., Savage, D. & Higgo, J. W. (1994). Fluid-rock interactions during continental red bed diagenesis: implications for theoretical models of mineralization in sedimentary basins. In: Parnell, J. (Ed.), *Geofluids: Origin, Migration and Evolution of Fluids in Sedimentary Basins*, Geological Society Special Publication No. 78, 301-324.
- Richards, J. P., Cumming, G. L., Krstic, D., Wagner, P. A. & Spooner, E. T. C. (1988). Pb isotope constraints on the age of sulfide ore deposition and U-Pb age of late uraninite veining at the Musoshi stratiform copper deposit, Central African Copper Belt, Zaire. *Econ. Geol.*, 83, 724-741.
- Unrug, R. (1988). Mineralization controls and source metals in the Lufilian Fold Belt, Shaba (Zaire), Zambia, and Angola. *Economic Geology*, 83, 1247-1258.
- Walraven, F. & Chabu, M. (1991). Pb-isotope geochemistry of the Kipushi Zn-Pb-Cu ore deposit, southeastern Zaire. Abstr., 1st Int. Symp. Geology and Mineral Resources of the Central and Southern African Subcontinent, 15-25 August 1991, Geol. Dept., Univ. Lubumbashi, Zaire, 42-45.
- Wendorff, M. (2001). New exploration criteria for 'megabreccia'-hosted Cu-Co deposits in the Katangan belt, central Africa. In: Pieczynski, A. et al. (Eds.), *Mineral Deposits at the Beginning of the 21st Century*. Swets & Zeitlinger Publishers, Lisse, Netherlands, 19-22.

3. PGE-BEARING LAYERED INTRUSIONS - CHINA

PGE-BEARING LAYERED INTRUSIONS IN THE SOUTHWEST SICHUAN PROVINCE, PEOPLE'S REPUBLIC OF CHINA

Y. Yao¹, M. J. Viljoen¹, R. P. Viljoen¹, A. H. Wilson², H. Zhong¹, B. G. Liu³, H. L. Ying³, G. Z. Tu³ and Y. N. Luo⁴

1: University of the Witwatersrand, Johannesburg, South Africa; 2: University of Natal, Durban, South Africa; 3: Chinese Academy of Sciences, Beijing, P.R. China; 4: Geological Exploration Bureau of Sichuan province, Chengdu, P.R. China

SYNOPSIS

PGE-bearing layered intrusions in the Pan-Xi and Danba areas of the southwestern Sichuan Province of China, occur in a 40-200 km belt, extending for 500 km in a north-south direction. The belt is located on the western margin of the Yangtze Platform. The basement to the east consists of Proterozoic metamorphic rocks, unconformably overlain by Phanerozoic sedimentary sequences. The mafic intrusions (400-250 Ma) were emplaced mainly during the Hercynian-Indosinian orogenies. Igneous layering, comprising mainly peridotite, pyroxenite and gabbro, is well developed in some of the intrusions. Two major types of PGE mineralization are present: (1) magmatic, layered Cu-Ni-PGE, and (2) late or post-magmatic, marginal, hydrothermal Cu-Ni-PGE. The latter type is characterized by silicification, serpentinization and carbonatization. Ore minerals mainly comprise chalcopyrite, pyrrhotite and pyrite. The PGM's are dominated by sperrylite (PtAs_2), merenskyite-moncheite ($(\text{Pd}, \text{Pt})\text{Te}_2$) and native platinum (Pt).

INTRODUCTION

Current production of Pt (<0.5 million ounces) in China cannot satisfy the market requirements (> 1.2 million ounces for 2001). Consequently, it is government strategy to locate and exploit new PGE deposits in China. PGE geochemical anomalies have recently been found in the Pan-Xi Layered Complex and this has initiated geological research and regional exploration for PGE deposits in the PanXi-Danba belt. As the foremost producer of PGE metals from the world's largest layered ultramafic-mafic intrusion, the Bushveld Complex (c. 2060 Ma), South Africa has developed outstanding expertise in both PGE research and in exploration and mining. A joint project to investigate PGE-bearing intrusions in both countries was consequently initiated. This paper presents a brief summary of the regional geology and intrusion-related PGE mineralization in the Pan-Xi and Danba areas of SW China.

GEOLOGICAL SETTING

PGE-bearing ultramafic-mafic intrusions lie close to the contact zone between the Yangtze Platform and the Qinghai-Xizang-West Yunnan fold belt in the west (Fig. 1). The Danba intrusions are located on the eastern margin of the fold belt, whereas the Panzhihua-Xichang (Pan-Xi) intrusions occur in the western portion of the Yangtze Platform (Fig. 1). The latter area is characterized by Precambrian basement overlain by a thick (>10000 m), sedimentary cover sequence. The geotectonic units of the Danba area forms part of the Indosinian (280-230 Ma) Songpan-Garze orogenic belt and they form part of the forefront of the Panzhihua-Xichang intracontinental rift belt. Regional deep-seated faults and fracture zones strike NS and NE-NNE, and control the distribution of regional intrusions and volcanic rocks. The igneous bodies were emplaced during the Hercynian-Indosinian orogenies (400-210 Ma, GMGR, 1998).

GEOLOGY OF THE PAN-XI AND DANBA AREAS

The basement of the Pan-Xi rift comprises Precambrian granulite, gneiss, schist, volcanics and sediments (1185-907 Ma, CMCJ, 1988), unconformably overlain by marine and continental sediments of Sinian-Tertiary age. The arcuate Hercynian-Indosinian deep-seated fault zones constitutes the western boundary of the Kangdian Palaeozoic uplift and controlled the eruption of the regionally

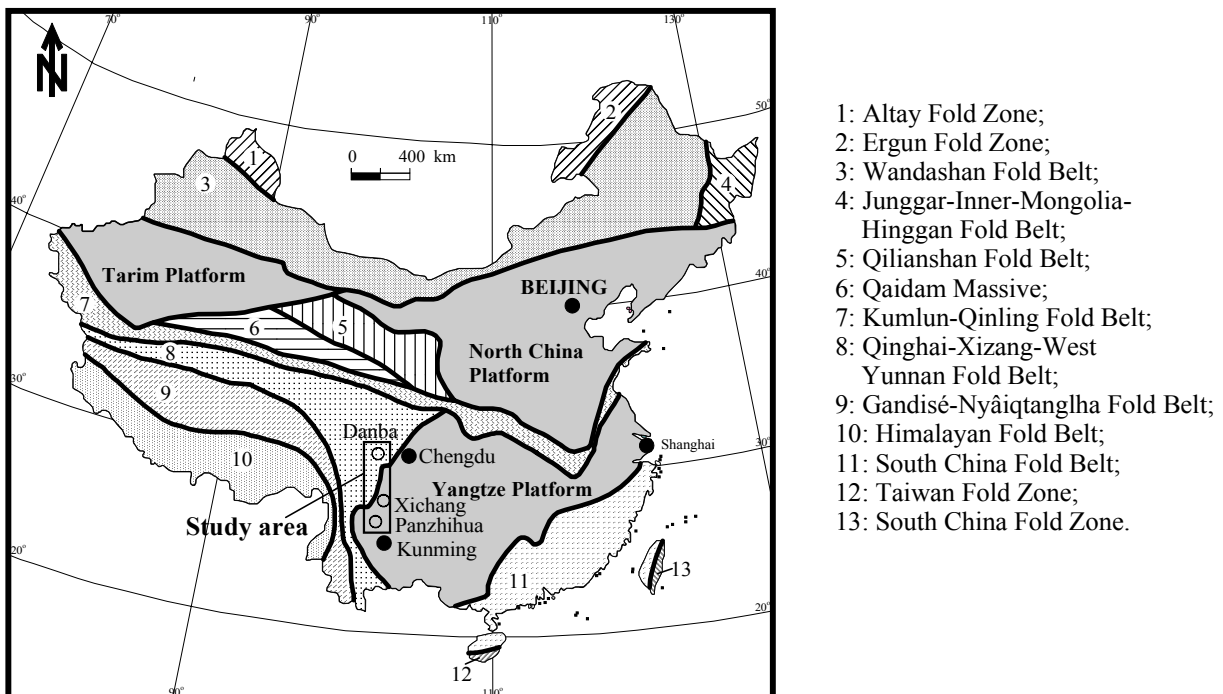


Figure 1: Geotectonic sketch map of China (modified after Ma et al., 1996), showing the position of the Panzhihua-Xichang (Pan-Xi) and Danba study areas.

extensive Upper Permian, Emeishan basalts and sedimentation of the Triassic basin (CMCJ, 1988). Most of the Ultramafic-mafic intrusions are comagmatic with syenite, alkaline granites and basalts (Fig. 2). In the Danba area, basement domains are composed of Precambrian metamorphic rocks overlain by Palaeozoic-Mesozoic marine sediments and meta-volcanic rocks (Li et al., 2000). Shear zones are well developed in the area. Regional faults trend mainly NW-SE and N-S and displace sedimentary units. Precambrian (847-916 Ma, Li et al., 2000) igneous intrusions and volcanic rocks outcrop as domains which are strongly migmatized. By contrast, the Palaeozoic ultramafic-mafic intrusions have been metamorphosed to amphibolite, uralitite and serpentinite in the late Hercynian orogeny (Li et al., 2000). In the Pan-Xi area, most of the Hercynian-Indosinian layered ultramafic-mafic intrusions, hosting giant V-Ti-magnetite ore deposits, have now been found to also contain PGE mineralization.

PGE-BEARING ULTRAMAFIC-MAFIC INTRUSIONS

A number layers within ultramafic-mafic intrusions as well as contact zones between wall rock and intrusion have been found to contain significant PGE mineralization. The Panzhihua mafic intrusion (Fig 2; 210-288 Ma, Fu, 2001) intruded Sinian limestone and is overlain by Emeishan basalt. It is composed mainly of gabbro, with minor peridotite and anorthosite towards the top. Layering within the intrusion is well developed (Fig. 3a). Ore bodies occur as layers in the gabbro with ore minerals being dominated by V-Ti-bearing magnetite, pyrrhotite, pyrite and chalcopyrite. PGE-bearing minerals include mainly sperrylite (PtAs_2), osmiridium (IrOs) and native platinum (Pt). PGE contents vary between 6.2 and 19.8 ppm and are concentrated in Co-Ni sulphides (Liang et al., 1998).

The Xinjie intrusion (Fig. 2; 258 Ma, Fu, 2001) is characterized by igneous layers forming three cumulate cycles of mainly coarse-grained peridotite, pyroxenite and gabbro (Fig. 3b). Hanging wall and footwall rocks are composed of Emeishan basalts. PGE-enriched layers (5-8m thick) occur in pyroxenite and peridotite at the base of Cycle I and are associated with sulphides. The PGE contents of the ores vary from 0.30 to 1.804 ppm. The PGMs in sulphides include sperrylite (PtAs_2), merenskyite-moncheite ($(\text{Pd}, \text{Pt})\text{Te}_2$), erlichmanite ($(\text{U}, \text{Os})\text{S}_2$), laurite-erlichmanite ($(\text{Ru}, \text{Os})\text{S}_2$) and native platinum (Pt).

The Yangliuping deposit at Danba has PGE metal reserves of more than 30 t. The intrusions were emplaced into Carboniferous schist, slate, marble and quartzite and comprise peridotite,

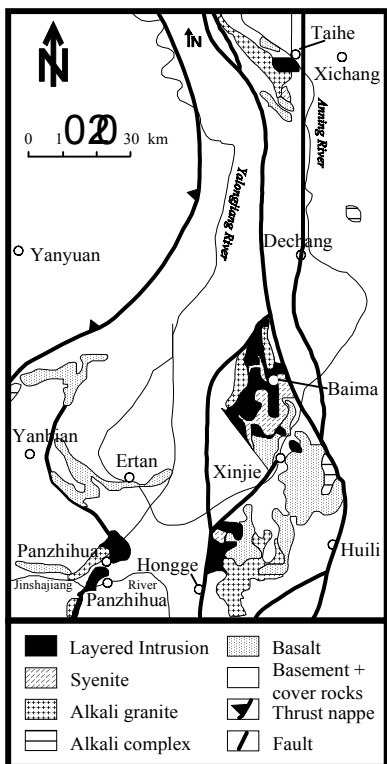


Figure 2: Simplified geological map of the Pan-Xi area showing the layered intrusions, alkalic to granitic plutons and basalt (after Liu et al., 1985).

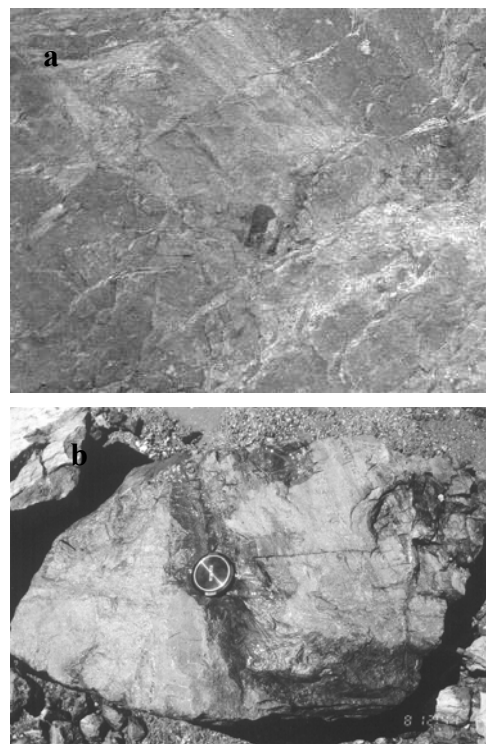


Figure 3: Photographs of (a) gabbro-anorthosite layers of the Panzhihua intrusion looking to the northwest and (b) massive pyrrhotite-chalcopyrite ores in calc-silicate from the Yanliuping mine.

Iherzolite, pyroxenite, gabbro (Fig. 3a) and diorite, from the base upwards. The ultramafic rocks were serpentinized, uralitized and steatized, while mafic rocks were saussuritized, sericitized and uralitized. PGE-bearing ore bodies occur in the altered lower part of various sequences as lenses or seams. In addition, detached Cu-Ni-PGE mineralization is also found within limestone (Fig. 3b). Ore minerals mainly include pyrrhotite, pentlandite, chalcopyrite, and pyrite. Major PGE minerals are sperrylite ($PtAs_2$) and borovskite ($PdSbTe$). PGE concentrations from massive sulphide ores average 5.184 ppm (Liang et al., 1998).

DISCUSSION AND CONCLUSIONS

The mineralised intrusions in the region were emplaced into a late Palaeozoic rift setting at c. 400-250 Ma. The intrusions comprise peridotite, pyroxenite and gabbro and show igneous layering. PGE mineralization is enriched at the base of intrusions and is also found in the lower marginal contact zone between wall rocks and intrusions. This latter type of mineralization is structurally controlled and related to late or post-magmatic processes, remobilising PGE originally hosted in the intrusions. The PGE-bearing intrusions at Danba were subjected to extensive alteration. It is concluded that the intrusion-related PGE mineralization in the Pan-Xi and Danba areas resulted from magmatic and late or post-magmatic hydrothermal processes. The known intrusion-related PGE ore deposits and prospects indicate that the areas have considerable potential of PGE exploration.

ACKNOWLEDGEMENTS

Field work was supported by the Bureau of Geology and Mineral Resources of the Sichuan Province and the Geological Department of the Panzhihua Mine. Financial support for the project was forthcoming from the National Research Foundation of South Africa and the Ministry of Science and Technology, People's Republic of China, who are gratefully acknowledged.

REFERENCES

- Bureau of Geology and Mineral Resources Exploration and Exploitation of Sichuan Province, Ministry of Geology and Mineral Resources, P. R. China) (GMGR, 1998). Atlas of geological resources and environment of Sichuan Province (in Chinese with English abstract). Chengdu Cartographic Publishing House, 102 p.
- Chinese Members of Co-operative Geological Group of China and Japan in the Pan-Xi Region (CMCJ, 1988). Petrotectonics of Panzhihua-Xichang region, Sichuan Province, China (in English). China Ocean Press, Beijing, 158 p.
- Fu, S. F. (2001). *Petrologic geochemistry of the Hongge and Xinjie layered intrusion in the Pan-Xi area*. Ph.D. dissertation (in Chinese with English abstract). Beijijing Institute of Geology and Geophysics, Chinese Academy of Sciences. 73 p.
- Li, Y. Q., Lai, X. Y., Hu, X. H., Zheng, Y. Z., Yang, X. J. and Xai D. Q. (2000). Isotopic geochronology of mesozone metamorphic rocks and noble metal mineralization in the Danba area (in Chinese). Institute of Geology and Mineral Resources, Bureau of Geology and Mineral Resoruces Exploration and Exploitation of Sichuan Province, 122 p.
- Liang Y. B., Liu, T. Y., Song, G. R. and Jin, Z. M. (1998). Platinum group element deposits in China (in Chinese). Metallurgical Industry Press, Beijing, 185 p.
- Liu D., Shen F. K., Zhang G. Z. (1985) Layered intrusions of the Panxi area, Sichuan province. In: Zhang Y. X. (ed.) Corpus of the Panxi paleorift studies in China (in Chinese). Geological Press, Beijing, p. 85-118.
- Ma, L. F., Ding, X. Z. and Fan, B. X. (1996). Explanation for the geological map of China. Geological Publishing House, Beijing. 1 sheet.

XINJIE LAYERED INTRUSION IN THE SICHUAN PROVINCE, SW CHINA: A GEOCHEMICAL, PETROLOGICAL AND PGE MINERALIZATION STUDY

Y. YAO¹, H. ZHONG¹, S. A. PREVEC¹, M. J. VILJOEN¹, R. P. VILJOEN¹, A. H. WILSON², B. G. LIU³, H. L. YING³ and Y. N. LUO⁴

1: University of the Witwatersrand, Johannesburg, South Africa;

2: University of Natal, Durban, South Africa;

3: Chinese Academy of Sciences, Beijing, P.R. China;

4: Geological Exploration Bureau of Sichuan province, Chengdu, P.R. China

SYNOPSIS

The Xinjie layered intrusion (ca. 258 Ma) is located in the SE portion of Sichuan Province, southwestern China, and is one of the major mafic bodies containing PGE layers in the region. The intrusion consists of three cumulate cycles, comprising mainly peridotite, pyroxenite and gabbro upwards. TiO_2 and P_2O_5 increase, while $Mg^{\#}$ ratios, Ni and Cu decrease towards the top of individual cycles. Initial $^{87}Sr/^{86}Sr$ ratios and $\varepsilon_{Nd}(t)$ values of rocks range from 0.7048 to 0.7080 and from -3.0 to +3.0, respectively. PGE mineralization is associated with Cu-Ni sulphides (chalcopyrite, pyrrhotite) in pyroxenite and peridotite at the bottom of cycle I. The PGMs are sperrylite, erlichmanite, $(Ru,Os)S_2$ and native Pt. The intrusion was formed by multi-cycle differentiation and mixing of magmas, derived from depleted mantle, and the PGE mineralization is a result of magmatic sulphidization at early stage of its evolution.

INTRODUCTION

The Pan-Xi area of Sichuan Province of southwestern China lies close to the contact between the Yangtze Platform and the Qinghai-Xizang-West Yunnan Fold Belt, and consists of Precambrian basement and Phanerozoic cover sequences. The Hercynian-Indosinian (400-250 Ma) Orogeny formed regionally widespread, mafic intrusions (Yao et al., 2002, this volume), which are well known to host numerous giant V-Ti-Fe and Cu-Ni-sulphide deposits (Fig. 1). In early 1980s, a number of the intrusions were found to contain PGE-enriched zones. However, there were no detailed studies of PGE mineralization until recent years, when the consumption of platinum in China increased rapidly to over one million ounces in 2001.

The Xinjie layered intrusion is one of the major mafic plutons hosting PGE mineralization in the area and is located about 8 km north of the city of Miyi. The intrusion, striking a NW-SE direction with dimensions of 7 by 1 km, intruded the Sinian dolomitic limestone and Precambrian basement (consisting of the Kangding Complex). Its footwall and hangingwall are the Permian Emeishan basalt and syenite, respectively (Fig.1). The intrusion has been dated at ca. 258 Ma by U-Pb zircon (Fu, 2001), supported by two, precise, slightly older Rb-Sr ages. This paper aims at documenting geochemistry, petrology and PGE mineralization of the intrusion and at discussing its petrogenesis, based on existing information and on new Rb-Sr and Sm-Nd isotopic data.

PETROGRAPHY

Igneous layering in the Xinjie intrusion is well developed and is composed of three cumulate cycles, comprising five lithological zones (Fu 2001). The main rock types are mainly coarse-grained cumulus melagabbros, pyroxenites and peridotites, in which PGE, copper and nickel mineralization has been recently recognized. At the contact between cycle I and the Permian basalts, the chilled border zone is composed of fine-grained gabbro, which is graduated upwards to pyroxenite and peridotite. The peridotite occurs mainly at the bottom of each cycle and contains a minor amount of Ti-Fe-bearing oxides. The pyroxenite occurs above the peridotite and also bears minor Ti-Fe oxides. The gabbro comprises a major portion of the intrusion and is present at the top of individual cycles (Fig. 2). Rock-forming minerals consist mainly of plagioclase, clinopyroxene, olivine and Ti-Fe bearing oxides. The V-Ti-magnetite ores occur mainly at the top of cycles I and II (Fig. 2).

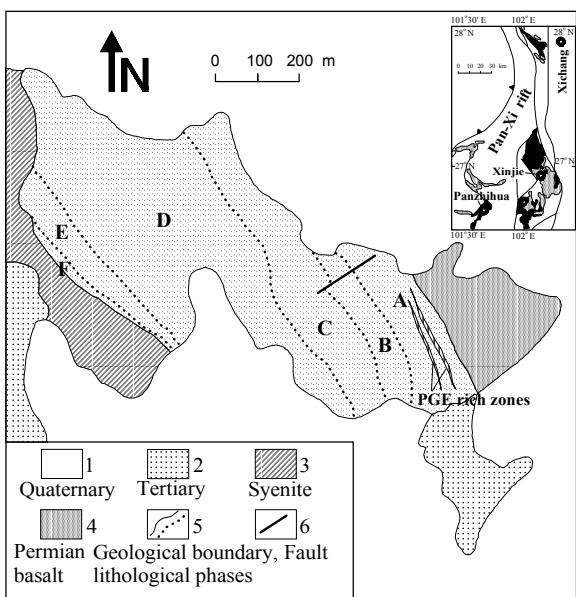


Figure 1. Geological map showing the NW portion of the Xinjie intrusion (modified after Zhang et al., 1997). Inset: Black: mafic intrusion+syenite+granitoid; White: Precambrian

	Depth (m)	Cycle	Zone	Lithology	Mineral.
Syenite	0			Amphibole-quartz syenite	
III	0-200	F	Gabbro	Gabbro	
	200-400		Gabbro	Gabbro, plagioclase pyroxenite	
	400-600	E	Pyroxenite	Pyroxenite, peridotite, plagioclase-bearing peridotite, plagioclase pyroxenite	
	600-800		Pyroxenite	Pyroxenite, plagioclase pyroxenite, olivine pyroxenite	Ti-poor Fe V-Ti-poor Fe
	800-1000	D	Olivine pyro.	Diabase gabbro	Major Ti-poor Fe
	1000-1200		Oli./Pl. pyro., Pl. peri.	Oli./Pl. pyro., Pl. peri.	
I	0-200	C	Gab.	Gab., Pl. pyro.	Ti poor
	200-400		Oli. gab/pyro., Oli. anor.	Oli. gab/pyro., Oli. anor.	V-Ti-Fe
	400-600	B	Pl. pyroxenite	Pl. pyroxenite	
	600-800		Pl. peridotite	Pl. peridotite	
	800-1000	A	Pl. pyro./peri.	Pl. pyro./peri.	
	1000-1200		Peridotite, Oli. peridotite, Pl. pyroxenite	Peridotite, Oli. peridotite, Pl. pyroxenite	PGE rich zones
	1200		Upper Permian Omeishan basalt	Upper Permian Omeishan basalt	Weak Cu

Figure 2. Petrographic and mineralization features of the Xinjie intrusion (modified after Hu, 2001). Gab.=gabbro, mineral.=mineralization, Oli.=olivine, peri.=peridotite, Pl.=plagioclase, pyro.=pyroxenite.

GEOCHEMISTRY

The major element geochemical variation broadly corresponds to the modal lithological within-cycle zones. As a whole, SiO_2 and P_2O_5 increase, while $\text{Mg}^{\#}$ ratios decrease toward cycle III (Fig. 3); Ni, Cu and PGE are enriched at the bottom of cycle I and decrease upwards (Fig. 4). Reversal trends also occur in each cycle and at transitional zones of individual cycles (Figs. 3-4). The transition elements (Ti, V, Cr, Mn, Fe, Co, Ni, Cu) are similar in primitive mantle-normalized patterns, and are characterized by significant depletion of Cr and Ni in each cycle. REE concentrations are between 110 and 180 ppm, showing progressively higher abundance from cycle I to III. The chondrite-normalized REE

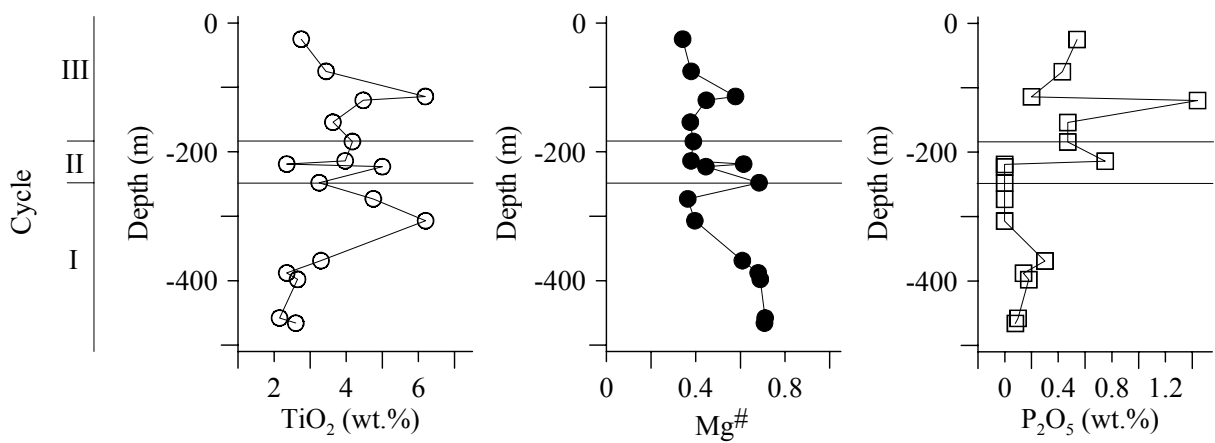


Figure 3. Vertical trends of TiO_2 and P_2O_5 contents and $\text{Mg}^{\#}$ ratios in the three cycles of the Xinjie intrusion (modified from Luo, 1981).

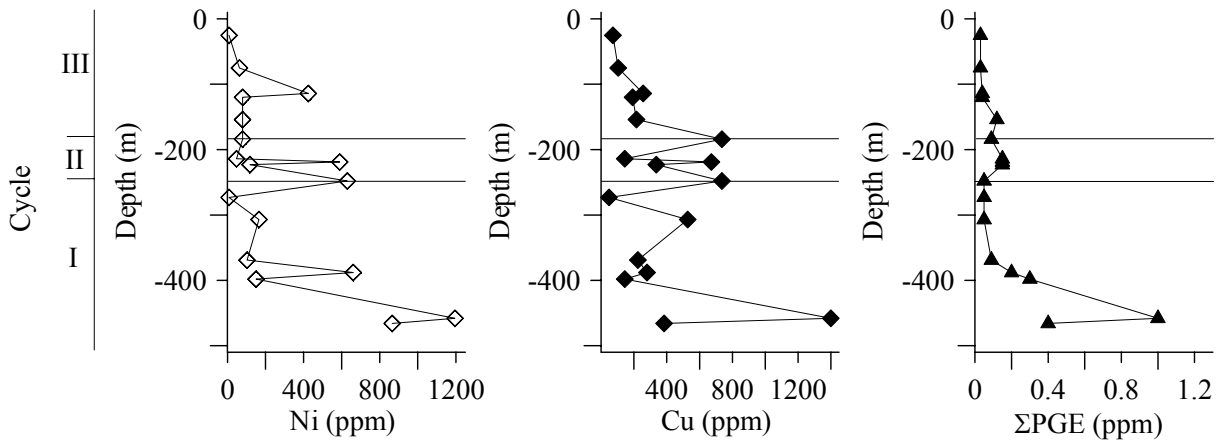


Figure 4. Vertical trends of Ni, Cu and total PGE (Σ PGE) contents in the three cycles of the Xinjie intrusion (modified from Luo, 1981).

patterns are broadly similar, but are enriched in LREE upwards, with $(La/Sm)_N$ and $(Ce/Yb)_N$ values of 1.1-7.9 and 3.1-28.8, with no significant Eu anomalies (Fu, 2001; Zhong, 2001).

Initial $^{87}\text{Sr}/^{86}\text{Sr}$ ratios of various rocks in the three cycles are between 0.7048 and 0.7066 ($n=15$, Fu, 2001), and between 0.7050 and 0.7080 in cycle I ($n=20$, this study). The $(^{87}\text{Sr}/^{86}\text{Sr})_i$ ratios decrease from the bottom to the top of cycle I and increase in cycle II-III. Within individual cycles, slight variations of $(^{87}\text{Sr}/^{86}\text{Sr})_i$ ratios are observed, and abrupt reversals are shown at the transitional zones of each new cycle. Nd isotopes show a corresponding decrease in cycle I from $\varepsilon_{\text{Nd}}(t)$ of around -3 at the base to +3 near the top of the cycle. Both Sr and Nd show evidence of crustal contamination in the marginal zone immediately adjacent to the footwall, and progressively decreasing amounts of crustal contamination upwards through cycle I. Significant isotopes in basal cycle 1 cannot be attributed to crustal contamination, requiring an alternative reservoir or a secondary enrichment mechanism.

PGE MINERALIZATION

The PGE mineralization is mainly concentrated in plagioclase-bearing pyroxenite and peridotite at the bottom of Cycle I (Fig. 4), and is associated with Cu-Ni sulphides (chalcopyrite and pyrrhotite). The PGE-bearing V-Ti-magnetite layers consist mainly of ilmenite, high-Fe chromite and Ti-bearing high-Fe chromite and minor Cu, Ni, Co sulphides at the top of cycles I-II. The 5-8m thick, PGE-enriched zones at the bottom of cycle I have PGE contents falling from 0.30 to 1.80 ppm, constituting two independent PGE ore bodies (Fig. 1). By contrast, PGE concentrations at the base of cycle II range from 0.20-0.42 ppm. The PGMs in the sulphides are dominated by sperrylite, erlichmanite, $(\text{Ru}, \text{Os})\text{S}_2$ and native Pt (Liang et al., 1998).

DISCUSSION AND CONCLUSIONS

A combination of primitive and evolved mantle-derived magmas has been suggested to explain the repetitive cumulate cycles, the resultant classic sawtooth geochemical, and the abrupt trend reversals at the transition zones between individual cycles (Fu, 2001; Zhong, 2001; Zhong et al., 2002, this volume). The PGE mineralization is related to sulphides at the bottom of cycle I, reflecting magmatic sulphidization at an early stage of fractionation. The transition elements and the Sr-Nd isotopic signatures of the intrusion suggest that the source of magmas for the intrusion is similar to that of the Emeishan basalts, derived from depleted mantle wedge by partial melting (Fu, 2001). It is therefore suggested that the Xinjie layered intrusion was formed by multi-cycle magmatic plumes and differentiation and that the PGE mineralization is a result of early-stage sulphidization of magma.

ACKNOWLEDGEMENTS

Field work was supported by the Bureau of Geology and Mineral Resources of Sichuan Province. Financial support from the National Research Foundation of South Africa and the Ministry of Science and Technology, People's Republic of China was gratefully acknowledged.

REFERENCES

- Fu, S. F. (2001) Petrologic geochemistry of the Hongge and Xinjie layered intrusion in the Pan-Xi area. Ph.D. dissertation (in Chinese with English abstract). Beijing Institute of Geology and Geophysics, Chinese Academy of Sciences. 73p.
- H. Zhong, H., Yao, Y., Zhou, X. H., Liu, B. G., Sun, M., Zhou, M. F., Viljoen, M. J. and Viljoen, R. P. (2002) Trace element geochemistry of the Hongge layered intrusion in the Pan-Xi area, Southwestern China. (Extended abstract to the Geoconference2002, Namibia, 22-26 July 2002).
- Liang Y. B., Liu, T. Y., Song, G. R. and Jin, Z. M. (1998) Platinum Group Element Deposits in China (in Chinese). Metallurgical Industry Press, Beijing, 185p.
- Luo Y N (1981) The characteristics of Ti-chromite mineralization in Xinjie layered ultramafic-mafic intrusion in Panzhihua area, China (in Chinese). *Geochimica* 10: 66-73.
- Yao, Y., Viljoen, M. J., Viljoen, R. P., Wilson, A. H., Zhong, H., Liu, B. G., Ying, H. L., Tu, G. Z. and Luo, Y. N. (2002) PGE-bearing layered intrusions in southwest Sichuan Province, People's Republic of China. (Extended abstract to the Geoconference2002, Namibia, 22-26 July 2002).
- Zhang, C. J., Wang, Y. L., Wang, D. Y., Li, X. L., Xie, K. H. and Fan, C. Y. (1997) Geochemistry of superlarge Cu-Ni (PGE) sulphide deposits associated with ultramafic-mafic intrusions (in Chinese). Special Report, Chengdu Institute of Science and Technology, 126p.
- Zhong, H. (2001) Platinum-group-element geochemistry and magma evolution of the Hongge and Xinjie layered intrusions in the Pan-Xi area. Post-doctoral report (in Chinese with English abstract). Beijing Institute of Geology and Geophysics, Chinese Academy of Sciences. 66p.

TRACE ELEMENT GEOCHEMISTRY OF THE HONGGE LAYERED INTRUSION IN THE PAN-XI AREA, SOUTHWESTERN CHINA

H. ZHONG^{1, 2}, Y. YAO¹, X. H. ZHOU², B. G. LIU², M. SUN³, M. F. ZHOU³,
M. J. VILJOEN¹, and R. P. VILJOEN¹

1. University of the Witwatersrand, Johannesburg, South Africa;

2. Chinese Academy of Sciences, Beijing 100029, China;

3. University of Hong Kong, Pokfulam Road, Hong Kong, China.

SYNOPSIS

The Hongge layered intrusion is one of several major ultramafic-mafic plutonic bodies hosting giant Fe-V-Ti deposits and PGE mineralization in the Pan-Xi area of the Sichuan Province of S.W. China. The layered intrusion is comprised of three zones, namely, the olivine clinopyroxenite, clinopyroxenite and gabbro zones, from the base up. The intrusion is spatially and temporally related to the regionally extensive Late Permian, Emeishan flood basalts. The Mg[#] ratios decrease cyclically and Zr and Nb contents increase upwards within individual units. The Cr/Sc and Cr/V ratios decrease and Zr/Y ratios increase upwards, whereas Zr/Rb ratios are very variable from the bottom to the top. Abrupt reversals of the above trace element contents and ratios occur at the boundary of individual units, supporting a mixing model of magmas in that a new, more primitive liquid, was mixed with a residual, more evolved liquid.

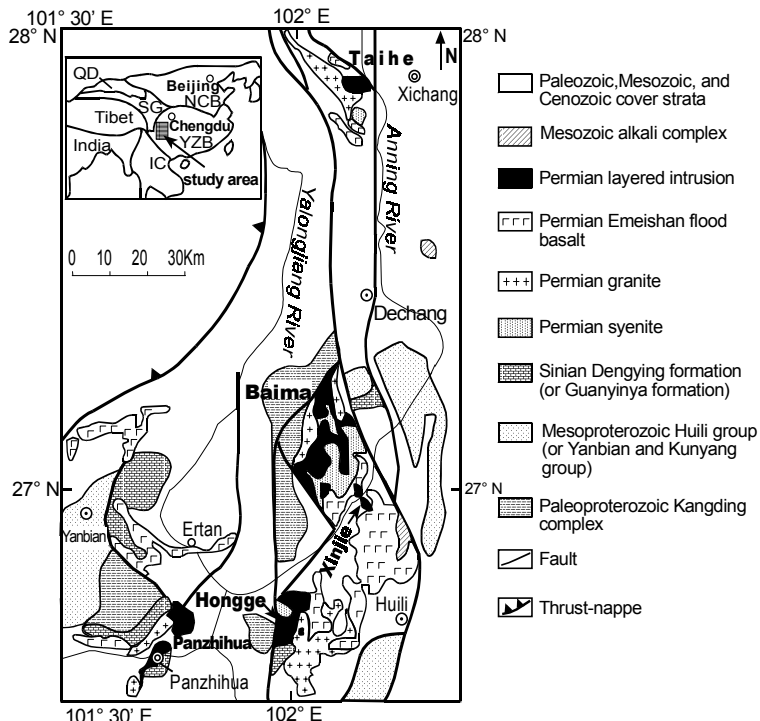
INTRODUCTION

Ultramafic-mafic layered intrusions in the Pan-Xi area of the southwestern Sichuan Province of China, which is located on the western margin of the Yangtze Craton in the eastern portion of the Tibetan Plateau, host numerous giant Fe-V-Ti and Cu-Ni-sulfide deposits such as the Panzhihua, Hongge, Xinjie, Baima and Taihe deposits (Fig.1), which have recently been found to contain PGE mineralization. The basement of the Craton comprises Precambrian, granulite-amphibolite facies, metamorphic rocks, termed the Kangding Complex. The Craton was subjected to multiple-stage geotectonic movements, of which the late Variscan-Indosinian (280-230 Ma) rifting is the most significant one (Cong, 1988). The event resulted in extensive emplacement of N-S trending, fault-controlled, mineralized mafic intrusions and the eruption of the Emeishan basalts which are 1,500-2,700 m thick and > 2.5 × 10⁵ km² in outcrop area (Chung and Jahn, 1995).

The Hongge layered intrusion is a typical example of a layered complex from the region (Fig. 1), in which PGE mineralization has been reported in the lower part (Luo, 1981). A mixing model of magmas to explain PGE enrichment has recently been proposed by Zhong et al. (2002), on the basis of geochemical characteristics of PGE and chalcophile elements (Cu, Ni). Trace elements provide evidence for the role of interstitial liquid and postcumulus processes in the evolution of crystal mushes (Cawthorn, 1983; Wilson et al., 1999). This paper documents trace element geochemistry in the vertical profile and tests the hypothesis of multiple injections of magmas for the Hongge intrusion.

GEOLOGY AND PETROGRAPHY

The Hongge layered intrusion outcrops in an area of about 60 km² and intrudes the Sinian Dengying Formation (dolomitic limestone) and granitic genisses of the Kangding Complex. The Dengying Formation was metamorphosed to marble in places adjacent to the intrusion.



Zone	Cyclic unit	Thickness (m)	Rock assemblage	Mineralization
Upper, Gabbro Zone (UGZ)	Cycle 4	>545	light-colored flow gabbro clinopyroxenite, olivine clinopyroxenite, lherzolite	MH
		220	dark-colored flow gabbro banded gabbro plagioclase-bearing clinopyroxenite clinopyroxenite, lherzolite pegmatitic clinopyroxenite dark-colored flow gabbro, anorthosite plagioclase-bearing clinopyroxenite	MH
Middle, Clinopyroxenite Zone (MCZ)	Cycle 3	87	clinopyroxenite	MH
	Cycle 2	63	olivine clinopyroxenite medium-grained equigranular diopside pyroxenite clinopyroxenite olivine clinopyroxenite, lherzolite, dunite	MH
Lower, Olivine Clinopyroxenite Zone (LOZ)	Cycle 1	165	heterogranoular clinopyroxenite plagioclase-bearing olivine clinopyroxenite, clinopyroxenite clinopyroxenite, hornblende olivine clinopyroxenite	PGEI
		177	plagioclase-bearing hornblende olivine clinopyroxenite coarse-grained hornblende olivine clinopyroxenite	PGEI

Figure 1. Geological map of the Pan-Xi area showing the distribution of layered intrusions (compiled after Liu et al., 1985; Chung and Jahn, 1995). IC-Indochina; NCB-North China Craton; QD-Qaidam; YZB-Yangtze Craton; SG-Songpan-Ganze accretionary complex

Figure 2. Stratigraphic column of the Hongge layered intrusion showing main rock types and location of main magnetite horizons (MH), and PGE-enriched layers (PGEI) (modified after Luo, 1981).

The Emeishan basalts are present to the northeast of the Hongge intrusion and together with the later body were intruded by Permian granites and syenites (Fig.1). Igneous layers of the intrusion are well developed and consist of three zones, namely, a lower olivine clinopyroxenite zone (LOZ), a middle clinopyroxenite zone (MCZ), and an upper gabbro zone (UGZ). The LOZ and UGZ are characterized by single compositional cyclic units but the MCZ is dominated by two compositional cyclic units (Fig. 2). The MCZ and UGZ contain thick layers hosting disseminated V- and Ti-rich magnetite. PGE-enriched layers occur in the lower parts of the LOZ and the MCZ and are marked by Cu-and Ni-rich sulfide minerals (Fig. 2, Zhong et al., 2002).

TRACE ELEMENT GEOCHEMISTRY

Samples for this study were taken from five drill holes in an area where abundant magnetite is present. Major and trace elements were determined on pressed powder pellets using a Phillips PW 2400 X-ray fluorescence spectrometer at the University of Hong Kong. The analytical precision is better than 5 wt.%.

Various elemental concentrations and ratios have been plotted against stratigraphic height within the LOZ and MCZ (Figs. 3 and 4). Across individual units, Mg[#] ratios decrease while Zr and Nb contents increase upwards. At the transition zone of individual new units, Mg[#] ratios clearly increase. As shown in figures 3 and 4, the curves show a classic saw tooth pattern with abrupt reversals at the beginning

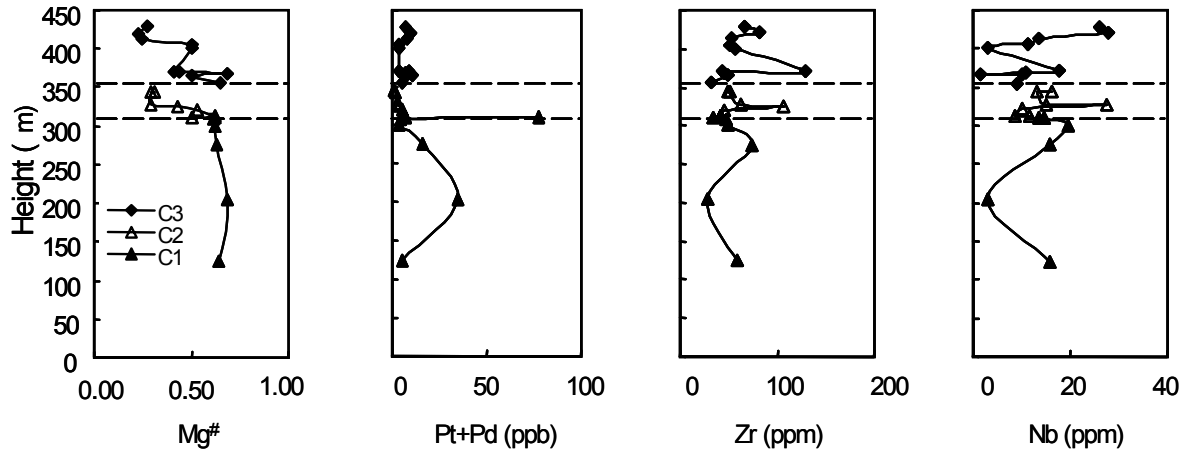


Figure 3. Vertical variations of Mg[#], Pt+Pd, Zr and Nb contents within the three cyclic units in the Hongge intrusion. C1: cycle 1; C2: cycle 2; C3: cycle 3. Pt+Pd contents are from Zhong et al. (2002).

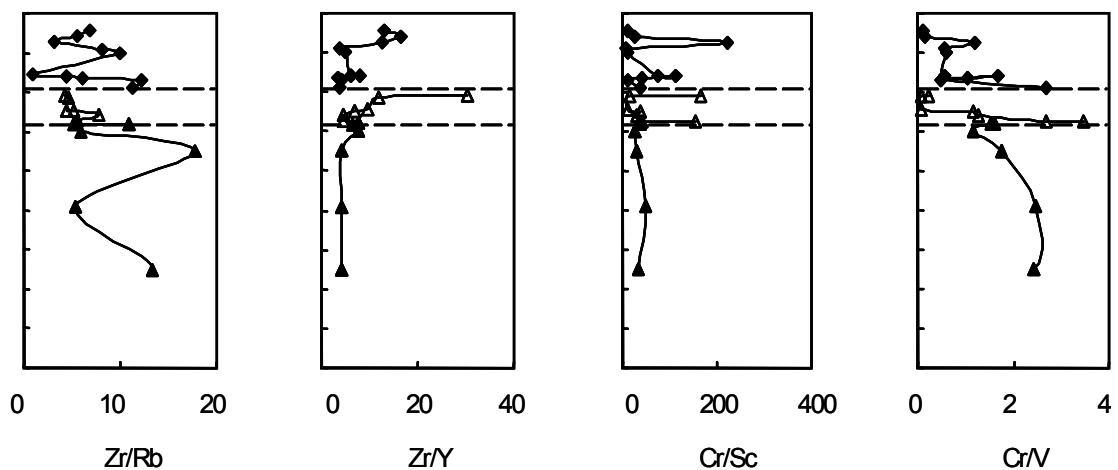


Figure 4. Vertical variations of Zr/Rb, Zr/Y, Cr/Sc and Cr/V ratios within the three cyclic units in the Hongge intrusion. Legends as in Fig. 3.

of each cycle. In addition, Cr/Sc and Cr/V ratios decrease while Zr/Y ratios increase upwards within each cyclic unit, whereas Zr/Rb ratios are quite variable. It is noted that compositional terminations related to the different element ratios are also present within the cyclic units due to the lack of samples analyzed.

DISCUSSION

Zhong et al. (2002) argued that the cyclic units of the Hongge layered intrusion may have resulted from crystal fractionation and mixing between a primitive and evolved magma based on the geochemical characteristics of PGE and chalcophile elements. The trace element data provide more detailed geochemical constraints on the mixing model of magmas.

The Mg[#], Cr/Sc and Cr/V ratios consistently decrease upwards within the three cyclic units and show an abrupt increase between the transition zones of the units. The former is consistent with fractional crystallization of magmas. The vertical increase of Zr and Nb contents and Zr/Y ratios show incompatible behaviour, which can also be related to the fractional crystallization of the magmas. Simple fractional crystallization cannot however explain the abrupt increase of Mg[#], Cr/Sc and Cr/V ratios across the boundary of individual units and the geochemical trends of Zr and Nb contents, and Zr/Rb and Zr/Y ratios, shown in the profile. The saw tooth pattern of the trace elements and their ratios throughout the intrusion is possibly related to a mixing model, in which rocks with primitive chemical signatures at the base of the units were abruptly overlapped by more evolved rocks at the top of previous cycles. As shown in Figure 3, the contents of Pt+Pd are high in the transition zone between the cycle 1 and cycle 2, where the olivine clinopyroxenites are relatively enriched in sulfides (e.g. pyrrhotite, chalcopyrite).

The incompatible element ratios avoid the uncertainty of random variations in the proportion of trapped liquids (Cawthorn, 1983). The abrupt change of the Zr/Y and Zr/Nb ratio across the transition zone of individual cycles strongly supports the addition of a new magma to the remaining liquid. It appears that the new magma has different ratios of trace elements from the evolved magma.

CONCLUSIONS

Each of the three cyclic units in the Hongge layered intrusion represents addition of a new magma to an already evolved one. A more primitive liquid was periodically added to and blended with a more evolved liquid resting on the crystal pile. The two magmas have different contents of the compatible and incompatible trace elements which resulted in a saw tooth pattern of the trace element distribution and their ratios. The PGE enrichment in the olivine clinopyroxenite is related to fractional crystallization and sulfur saturation in the magma.

ACKNOWLEDGMENTS

The Geology Team 106 of Sichuan Province are thanked for their hospitality during field work. This study was financially supported by the A25 Project of the State Climbing Program of China and a HKU Outstanding Young Researcher Award to Min Sun.

REFERENCES

- Cawthorn R. G. (1983) Magma addition and possible decoupling of major- and trace-element behaviour in the Bushveld Complex, South Africa. *Chem. Geol.* 39: 335-345.
- Chung S. L. and Jahn B. M. (1995) Plume-lithosphere interaction in generation of the Emeishan flood basalts at the Permian-Triassic boundary. *Geology* 23: 889-892.
- Cong B. L. (1988) Formation and evolution of the Pan-Xi paleorift (in Chinese). Science Press, Beijing, 424 p.
- Liu D., Shen F. K. and Zhang G. Z. (1985) Layered intrusions of the Panxi area, Sichuan province. In: Zhang Y. X. (ed.) Corpus of the Panxi paleorift studies in China (in Chinese). Geological Press, Beijing, p. 85-118.
- Luo Y. N. (1981) The characteristics of Ti-chromite mineralization in Xinjie layered ultramafic-mafic intrusion in Panzhihua area, China (in Chinese). *Geochimica* 10: 66-73.
- Wilson A. H., Lee C. A. and Brown R. T. (1999) Geochemistry of the Merensky reef, Rustenburg Section, Bushveld Complex: controls on the silicate framework and distribution of trace elements. *Mineral*

Deposita 34: 657-672.

Zhong H., Zhou X. H., Zhou M. F., Sun M. and Liu B. G. (2002) Platinum-group element geochemistry of the Hongge Fe-V-Ti deposit in the Pan-Xi area, southwestern China. *Mineral Deposita* 37: 226-239.

4. BUSHVELD COMPLEX AND OTHER INTRUSIONS

A RE-EVALUATION OF THE LINK BETWEEN CHROMITITE FORMATION AND PGE ENRICHMENT IN THE BUSHVELD COMPLEX

JUDITH A. KINNAIRD¹, F. JOHAN KRUGER¹, PAUL A.M. NEX²
and R. GRANT CAWTHORN²

Economic Geology Research Institute – Hugh Allsopp Laboratory, School of Geosciences, University of the Witwatersrand, WITS 2050, South Africa.

email: 065jak@cosmos.wits.ac.za

SYNOPSIS

The mafic layered suite of the Bushveld Complex hosts a number of substantial PGE-bearing chromitite layers. $^{87}\text{Sr}/^{86}\text{Sr}$ isotope variations on interstitial plagioclase from chromitites and different silicate host rocks show that the magma from which the chromitites formed ($\text{Sr}_i < 0.7099$) usually differed radically from the resident liquid from which the immediate footwall rocks crystallised (Sr_i c. 0.7060 - 0.7064). These high Sr-isotope ratios can only have been produced by sudden and extensive contamination from an extremely radiogenic component, the only viable source for which is the felsitic roof rocks. Contamination occurred when a new magma influx penetrated the residual liquid and interacted with the overlying roof-rock as well as mixing with the resident liquid. Chromite cascaded to the floor, together with a small amount of magma adherent to the chromite or entrained within the slurry to produce interstitial silicates with enriched isotopic ratios. The close correspondence of chromitite and PGE enrichment strongly suggests that the processes that resulted in chromite formation also triggered precipitation of the PGE's. The major PGM and chromitite ore deposits of the Bushveld Complex are therefore unconformity related, and are associated with mixing of new magma, coupled to simultaneous contamination by roof-rock melt.

INTRODUCTION

The mafic layered suite of the 2.05 Ga old Bushveld Complex hosts a number of substantial PGE-bearing chromitite layers, within the Critical Zone. Although it has been the Merensky Reef of the Bushveld Complex that has produced the bulk of South Africa's platinum, the first recorded occurrence of PGE is from a chromitite (Hall and Humphrey 1908). Initially these discoveries did not flourish due to metallurgical constraints, and the discovery in 1924 of the pipe-like bodies (Onverwacht, Mooihoek and Driekop) with payable Pt-Fe alloys, and then the S-enriched chromite bearing Merensky Reef both of which were more straightforward to process. Interest in chromitite as a source of PGE was suppressed until the late 1970's and 1980's when metallurgical breakthroughs and increased demand led to mining of UG2 chromitite ore (Cawthorn, 1999).

Three groups of chromitites occur (Cousins and Feringa, 1964): a Lower Group (LG) of up to seven major layers in feldspathic pyroxenite, a Middle Group (MG) with four layers hosted by feldspathic pyroxenite or norite, and an Upper Group (UG) usually of two chromitite packages, hosted in pyroxenite, norite or anorthosite. Two to four thin chromitite layers (each 1-20 mm) define the top and bottom of the main mineralisation of the Merensky Reef. There is a systematic chemical variation from bottom to top chromitite layers, in terms of Cr:Fe ratios and the abundance and proportion of PGE's (Fig. 1). Although all chromitites are enriched in PGE's relative to the host rocks, the UG2 layer shows the highest concentrations of PGE's in the various chromitite layers and grades may locally exceed 10 g/t.

In the 1980's the model of Naldrett and coworkers.(e.g. Naldrett, 1989), in which a very high ratio of magma to an immiscible sulphide liquid (R-factor) associated with magma influx and mixing gained favour, due to the presence of sulfide in the Merensky Reef. However, the Bushveld Complex as a whole is a relatively sulphide-poor system with <500 ppm S in 99% of the 7-9 km thick layered sequence (Maier and Barnes 1999; Maier et al. 2002). PGE enrichment in chromitite layers led to the suggestion of a relationship between the two, although a direct link was questioned because of the lack of good grade in UG1 and UG3 chromitites, the high grade of PGE's in the Merensky Reef – which has only thin

associated chromitites, and the paucity of chromite in the Platreef (Cawthorn, 1999). However, it is the process of chromitite formation that is a key to understanding PGE enrichment, not the absolute amount of chromitite that formed.

Irvine showed that chromite crystallization can be induced by felsic (silica) contamination (Irvine, 1975) or by mixing of “parental” magma and more evolved residua (Irvine, 1977). Recently, Schoenberg *et al.* (1999) showed that chromitite layers have exotic enriched Sr-isotope systematics which are completely different from those of the host silicate rocks, and which imply sudden and major contamination by a ‘granitic’ crustal component. Furthermore, this contamination was only active while the chromitite was forming and ceased once the chromitite stopped forming. Current studies have confirmed and extended these observations.

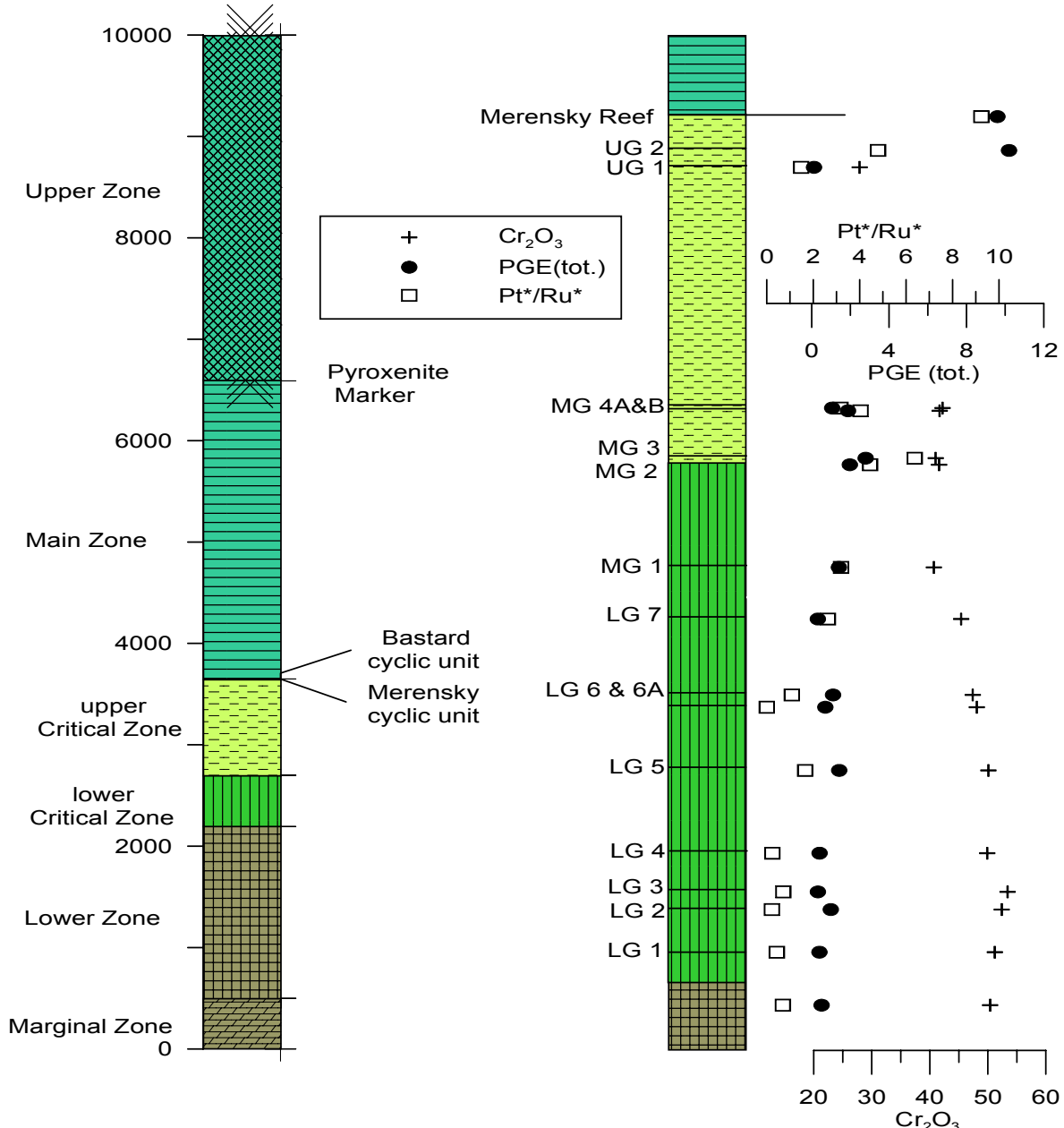


Fig. 1 Stratigraphy showing the generalised thickness of the zones within the mafic layered Suite, Bushveld Complex. The column on the right shows the position of the major chromitite layers within the Critical Zone. The percentage of Cr_2O_3 in chromite is shown together with PGE compositional data for each of the chromitite layers based on Scoon and Teigler (1994). $\text{Pt}^* = \text{Pt} + \text{Pd} + \text{Rh}$; $\text{Ru}^* = \text{Ru} + \text{Ir} + \text{Os}$.

Sr-ISOTOPE STUDIES

Three cores from different parts of the Bushveld Complex have been studied to include lithologies from below the LG5 chromitite to those above the UG2 layer. More than 80 plagioclase samples were selected at regular intervals through apparently homogeneous lithologies, close to lithological boundaries, from the immediate footwall and hanging wall to the chromitite layers, as well as from the base, middle and top of the chromitite layers when possible.

Detailed studies of $^{87}\text{Sr}/^{86}\text{Sr}$ isotope variations on plagioclase from chromitites and different silicate host rocks (e.g. Fig. 2) show that the magma from which the chromitites formed (interstitial plagioclase $\text{Sr}_i < 0.7099$) usually differed radically from the resident liquid from which the immediate footwall rocks crystallised (Sr_i c. 0.7060 - 0.7064). High initial strontium ratios also occur in silicate lithologies with a significant proportion of streaky chromite stringers. There is a rapid return to ‘normal’ isotopic compositions in the silicates above the chromitites, and in some cases within the upper portions of the chromitites themselves. The only viable source for this component *in the chamber* is the felsitic roof-rock melt that later crystallised to form granophyre.

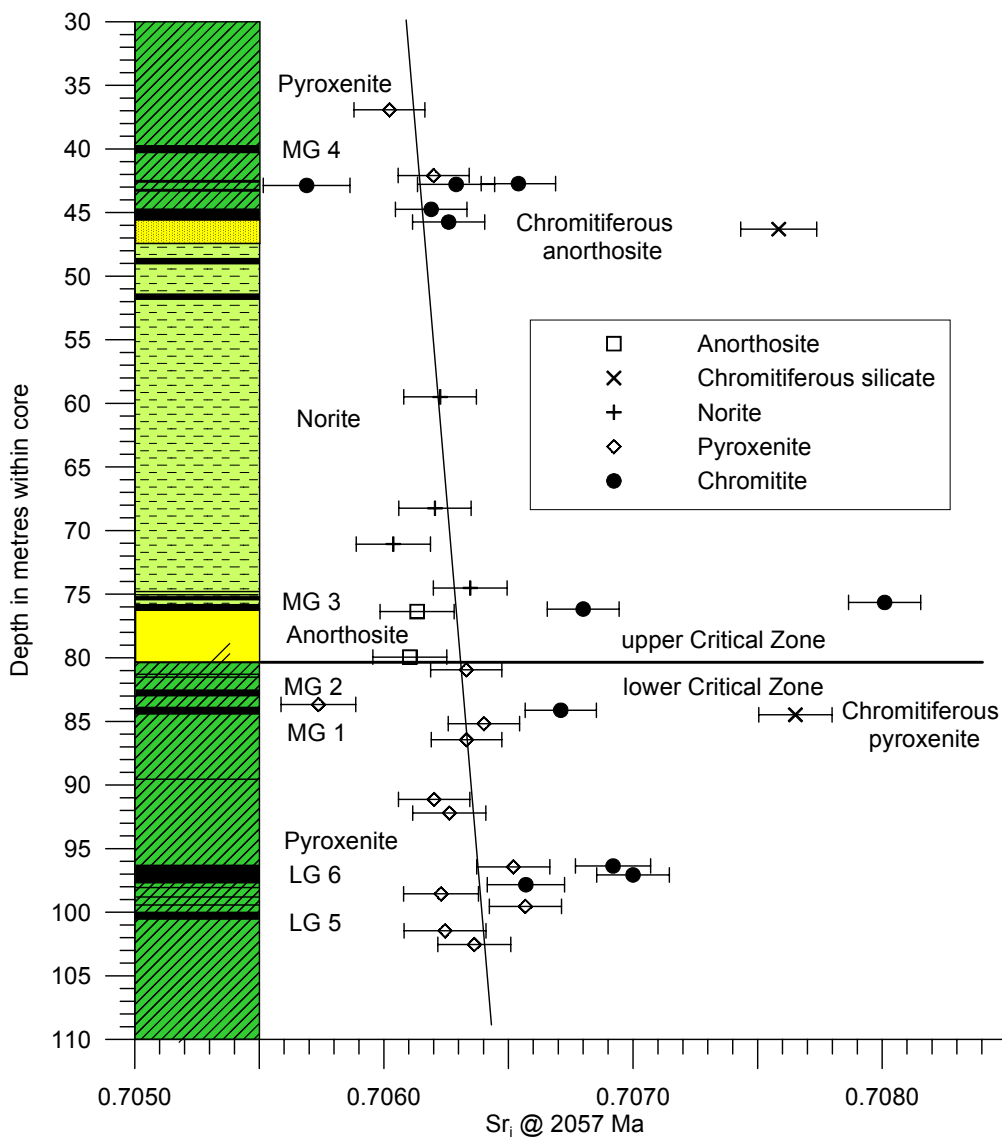


Fig 2. Initial strontium isotope ratio profile in lower-upper Critical Zone silicates and chromitites, demonstrating higher Sr_i ratios in the plagioclase from chromitites. Horizontal bars indicate 2-sigma error for Sr values. Data from AM38 core, south of the Steelpoort. The MG chromitites straddle the boundary between the lower Critical Zone and the Upper Critical Zone and by convention, MG1 and MG2 lie below the first anorthosite package, and MG3 and MG4 are

above. The isotopic trend line illustrates the slight upward decrease in initial Sr ratio of the silicate rocks from the lower Critical Zone to the upper Critical Zone. (Data from Kinnaird et al. in press)

A MODEL FOR CHROMITE FORMATION

It is envisaged that repeated influxes of new magma erupted into the Bushveld magma chamber as fountains along zones of weakness in the crust beneath the chamber (Fig. 3). When initial momentum was high these curtains (or line fountains) of magma penetrated the entire thickness of the resident magma and 'hit the roof' incorporating a component of melted roof as well as interacting with the resident liquid. This process contaminated both the new magma and the resident entrained melt with a silica-rich component that induced crystallization of copious chromite. The chromite was carried to the floor of the chamber by the collapsing fountain and spread out as a turbiditic flow to form chromitite layers. The flow would have been energised by continued crystallisation of chromitite close to source, with fluidity promoted by the rounded form of the chromite crystals. Chromite only crystallized while there was roof-melt interaction or there was sufficient compositional contrast to force the mixture into the chromite phase field. The contamination process stopped when the head of the fountain ceased to impinge on the felsic roof-rock melt and any further magma influx was uncontaminated by the roof-rock melt and only entrained, and mixed with, the resident magma, the influx flowing out beneath the resident magma.

The high Sr initial ratios at the base of some chromitites represent a phase of contamination by felsic roof material during the initial fountain surge with later chromitite showing lower Sr initial ratios originating by a magma mixing process. Chromitites, which do not show elevated initial Sr ratios e.g., UG3, formed from magma mixing without significant contamination. This proposed model implies repeated magma influxes in the C_LZ and C_UZ with each of the chromitites representing the product of a magma mixing process. Since the base of each major chromitite layer represents a point at which the magma chamber expanded vertically and laterally and there was some deformation and erosion of the footwall rocks, the base of the major chromitite layers (and the Merensky Reef) represent para-unconformities within the magmatic stratigraphy. Supportive evidence for crustal contamination during chromitite, and Merensky Reef development, is provided by chemical and isotopic evidence. Osmium isotope data from the majority of chromitite and Merensky Reef show that there was significant addition of ¹⁸⁷O to the chromitites, and therefore a significant crustal input, from the Middle Group upwards (Schoenberg et al. 1999).

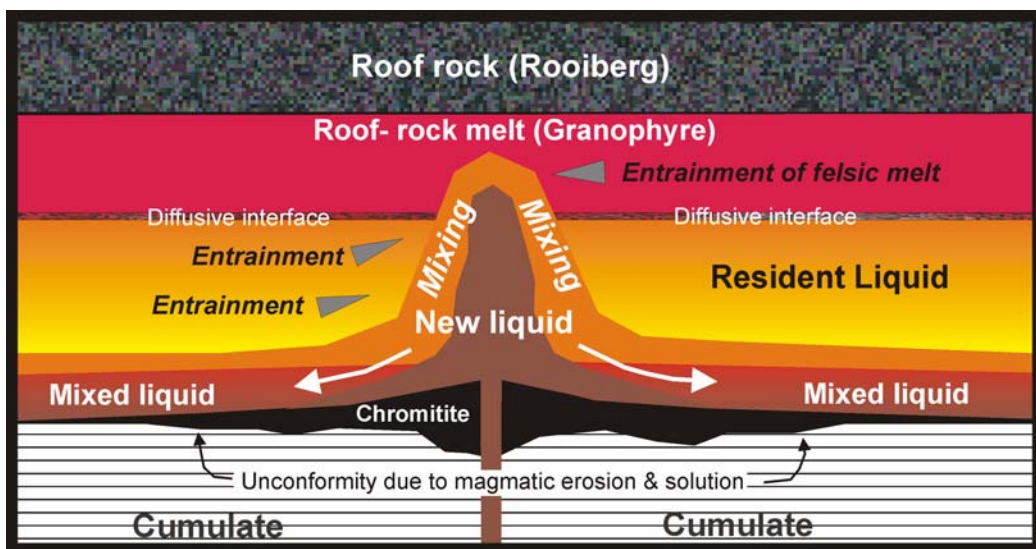


Fig. 3 Schematic diagram of the envisaged magma intrusion and mixing process. Introduction of a new magma ($Ro = 0.705 - 0.706$) as an active fountain resulted in entrainment of the resident mafic liquid and if there was sufficient upward momentum roof-rock melt ($Ro > 0.72$) was also entrained. This resulted in contamination by a silica-rich component with the resulting forced crystallisation of chromite and PGM's. The mixed liquids are out of equilibrium with the floor cumulates and react and erode to form an unconformity onto which the chromite/PGM ore is deposited (Kinnaird et al, in press)

THE LINK BETWEEN CHROMITE FORMATION AND PGE ENRICHMENT

Mungall (2002) suggested that the silicate magmas that crystallised chromite were close to PGE saturation and could be perturbed into precipitating alloys by small reductions in their oxidation states. The $\text{Fe}^{3+}/\text{Fe}^{2+}$ ratio in chromite always exceeds that of the melt (Mungall, 2002) and Cr^{3+} is preferentially incorporated relative to Cr^{2+} (Roeder and Reynolds, 1991), resulting in a reduced boundary layer, in which micronuggets of alloy formed (see Mungall, 2002). During hiatuses in chromite growth the alloys reacted with melt to form laurite, which was incorporated into chromites as growth resumed in response to random fluctuations during turbulent magma mixing (Mungall, 2002).

PGM formation therefore was triggered as the physics and chemistry of the magma changed during contamination by felsic roof melts, mixing with resident magma and precipitation of chromite. The small PGM crystals were collected and incorporated by the more abundant chromite grains as suggested by Hiemstra (1979). All chromitites are enriched in PGE relative to source rocks and host rocks. Although PGE abundance may be less in some layers, e.g. UG1 and UG3, the relative enrichment of both chromite and PGE is of the same order of magnitude relative to associated rocks (Kruger et al., 2002). The magma that initiated the Merensky Reef was of a fundamentally different composition relative to previous intrusions as shown by a marked increase in initial strontium ratio. Nevertheless, the processes of contamination and magma mixing still produced PGE mineralisation and chromite, even though the amount of chromite is small, so it is the processes that are important not the composition of the intruding magma, nor the amount of chromite that formed. There is abundant petrological and isotopic evidence that fluids have played a role in re-distributing PGE's (Campbell et al., 1983) but we would argue that this occurred after the primary precipitation of PGE's as a result of contamination and magma mixing.

CONCLUSIONS

The abundance of chromitite layers indicates frequent replenishment of the chamber with new magma. Introduction of this magma ($\text{Ro} = 0.705 - 0.706$) as an active fountain resulted in mixing of the resident mafic liquid and if there was sufficient upward momentum, roof-rock melt ($\text{Ro} > 0.72$) was also entrained. This resulted in contamination by a silica-rich component with the resulting forced crystallisation of chromite. Chromite crystals cascaded onto the floor of the chamber and spread laterally for significant distances as a turbidite flow. The mixed liquids were out of equilibrium with the floor cumulates and may have eroded the footwall to form an unconformity onto which the chromite ore was deposited. Contamination of new magma influxes, and mixing with resident magma not only caused chromitite formation but also triggered PGM crystallization as micronuggets of alloy which were then incorporated in the chromite slurry. It is an important economic implication in this model that PGE concentrations should also be high in chromitite footwall where high Sr initial ratios are associated with wisps of chromite. Each of the chromitites therefore represents the product of a magma mixing process. There is therefore a complex interplay between repeated magma influxes, possibly from different sources, roof contamination, fractionation and potential floor contamination.

REFERENCES

- Campbell, I., Naldrett, A.J. & Barnes S.J. (1983). A model for the origin of the platinum-rich sulfide horizons in the Bushveld and Stillwater Complexes. *Journal of Petrology* **24**, 133-165
- Cawthorn, R.G. (1999). The discovery of the platiniferous Merensky Reef in 1924. *S. Afr. J. Geol.* **103**, 178-183
- Cousins, C.A. and Feringa, G. 1964. The chromite deposits of the western belt of the Bushveld Complex. In: The geology of some ore deposits in southern Africa. Ed: S.H. Haughton. *Spec. Pub. Geol. Soc. S. Afr.* **2**, 183-202.
- Hall, A.L. and Humphrey, W.A. 1908. On the occurrence of chromite along the southern and eastern margins of the Bushveld plutonic complex. *Trans. Geol. Soc. S. Afr.* **11**, 69-77.
- Hiemstra, S.A. (1979). The role of collectors in the formation of the platinum deposits in the Bushveld Complex. *Canad. Mineral.* **17**, 469-482.
- Irvine, T.N. (1975). Crystallization sequences in the Muskox intrusion and other layered intrusions- II. Origin of chromitite layers and similar deposits of other magmatic ores. *Geochim. Cosmochim. Acta* **39** 991-1020.
- Irvine, T.N. (1977). Origin of chromitite layers in the Muskox intrusion and other stratiform intrusions: a new interpretation. *Geology* **5**, 273-277.
- Kinnaird, J.A. Kruger, F.J., Nex, P.A.M. and Cawthorn, R.G. In press. Chromitite formation – a key to understanding processes of platinum enrichment. *Trans. Inst. Min. Metall Section B*.
- Kruger, F.J., Kinnaird, J.A. Nex, P.A.M. and Cawthorn, R.G. 2002. Chromite is the key to PGE. Abstr. 9th Internat. Platinum Symp. July, Stillwater, USA.

- Maier, W.D. and Barnes, S-J. 1999. Platinum-group elements in silicate rocks of the Lower, Critical and Main Zones at Union section, western Bushveld complex. *J.Petrol.* **40**, 1647-1671.
- Maier, W.D., Barnes, S-J. and Li, C. 2002. A re-evaluation of the role of crustal contamination in the formation of magmatic sulfides in the Bushveld Complex. 9th International Platinum Symposium, July 21-25, 2002, Billings, Montana, USA*
- Mungall, J. 2002. A model for co-precipitation of Platinum-Group minerals with chromite silicate melts. Abstract for 9th International Platinum Symposium, July 21-25, 2002, Billings, Montana, USA
- Naldrett, A.J. (1989). Stratiform PGE deposits in layered intrusions. *Rev. Econ. Geol.*, **4**, 135-166
- Roeder, P.L. and Reynolds, I. 1991. Crystallization of chromite and chromium solubility in basaltic melts. *J. Petrol.*, **32**, 909-934
- Schoenberg, R., Kruger, F.J., Nagler, T.F., Meisel, T. and Kramers, J.D. (1999). PGE enrichment in chromitite layers and the Merensky Reef of the western Bushveld Complex; a Re-Os and Rb-Sr isotope study. *Earth Planet. Sci. Lett.* **172**, 49-64.
- Scoon, R.G. and Teigler, B. (1994). Platinum Group element mineralisation in the Critical Zone of the western Bushveld Complex: 1. Sulphide-poor chromitites below the UG2. *Econ. Geol.*, **89**, 1094-1121

PLAGIOCLASE-RICH CYCLIC UNITS IN THE BUSHVELD COMPLEX

L. SPIES and R.G. CAWTHORN

Department of geology, University of the Witwatersrand, Johannesburg, South Africa
spiesl@science.pg.wits.ac.za

SYNOPSIS

We have made a very detailed study of modal proportions in cyclic units of the Bushveld Complex. Such information can be used to test hypotheses relating to the composition of added magmas, and accumulation processes. A quantitative determination of the mode is presented here. Most significant is the proportion of plagioclase. We note that the bulk proportion of plagioclase in the UG2 cyclic unit is 64%, i.e. close to the cotectic proportion. For the Merensky cyclic unit the proportion is 74%, well in excess of the cotectic. We suggest that these values are not expected if crystallization has taken place from an ultramafic magma. These successions contain non-cotectic proportions of minerals and we suggest that such gradual changes in modal proportion require some process of mineral sorting during accumulation. The source of the excess plagioclase must be sought in the new magma injected at the level of the Merensky Reef. We suggest that the magma was not primitive and ultramafic, but relatively evolved. Most basaltic magmas have plagioclase phenocrysts and plagioclase as liquidus mineral. Such a magma might be the source of the excess plagioclase in the Merensky and Bastard cyclic units.

INTRODUCTION

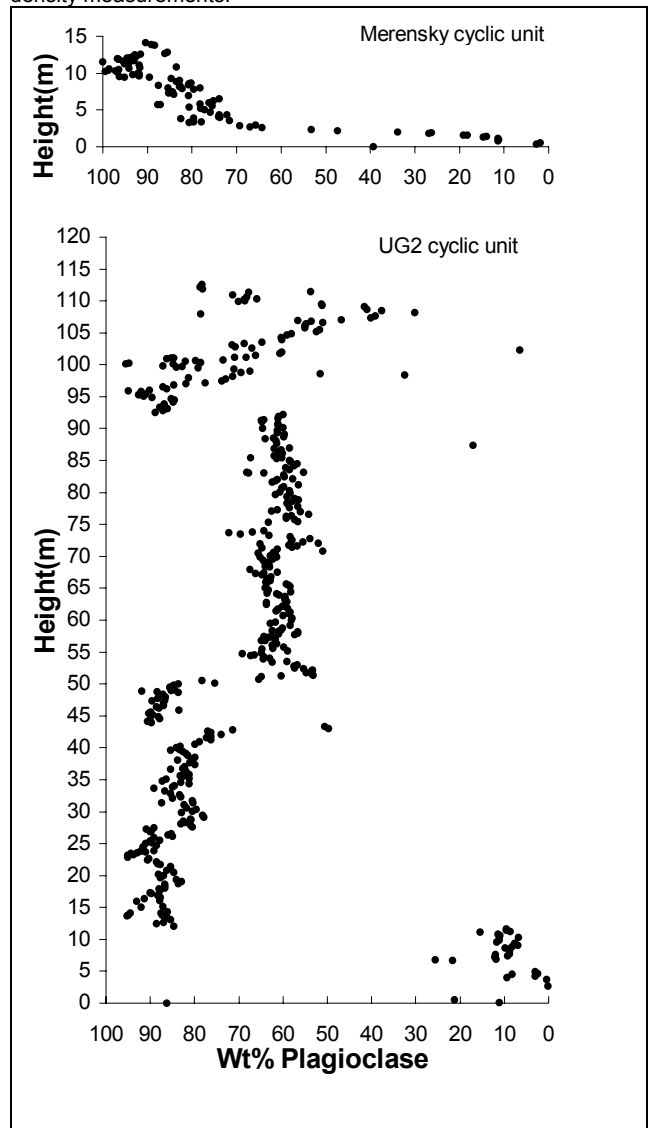
Layered intrusions are constructed from modally layered sequences of rocks, referred to as cyclic units. Such units are well developed in the Upper Critical Zone of the Bushveld Complex, South Africa, and comprise chromitite, pyroxenite, occasionally harzburgite, norite and anorthosite.

One hypothesis for the genesis of cyclic units involves the addition of ultrabasic magma that crystallizes orthopyroxene. Fractionation then leads to orthopyroxene and plagioclase crystallization. The genesis of the uppermost layer of anorthosite is problematical since an initially orthopyroxene-saturated magma cannot ultimately crystallize only plagioclase, and so a process of crystal settling needs to be invoked. To date, no rigorous attempt has been made to determine the bulk modal proportions of these cyclic units. Such information can be used to test hypotheses relating to the composition of added magmas, and accumulation processes. A quantitative determination of the mode is presented here.

The study is based on core through the UG2 and Merensky cyclic units, generously provided by Impala Platinum Mines Ltd, situated in the western limb of the Bushveld Complex.

DETERMINATION OF MODE FROM DENSITY
Rocks of the Upper Critical Zone consist almost entirely of plagioclase and orthopyroxene. Away from the chromitite layers only traces of chromite occur. Density can therefore be used as a measure of the plagioclase content, the advantage being that in a borecore section the

Figure 1: Plot of proportion of plagioclase (by weight) versus height for the UG2 and Merensky cyclic units, determined from density measurements.



density of every piece of core can be determined. Several samples, ranging from anorthosite to pyroxenite were analysed by XRF to provide a calibration between density and proportion of plagioclase.

Fig. 1 displays the resultant vertical variation in weight proportion of plagioclase through the studied interval. Most significant is the proportion of plagioclase, with a weighted average of 64 and 74% in the UG2 and Merensky cyclic units respectively.

COTECTIC PROPORTIONS IN NORITE

Eales *et al.* (1986) argued that there was little tendency in the Upper Critical Zone for cotectic norite compositions to be developed. In the UG2 cyclic unit there is 40m of norite from 50-90m. Ninety determinations of plagioclase content (from the density) within this section yielded an average of $63\% \pm 1$. Such a homogeneous section probably results from crystallization at the orthopyroxene-plagioclase cotectic. Hence, we suggest that cotectic norite can form but probably is under represented in most geochemical sampling exercises.

The second issue of interest is the evidence for modal sorting. The lower 90m of the UG2 cyclic unit shows a pyroxenite (12m) followed by an anorthosite (38m), followed by norite (40m). However, above that comes a sequence in which the proportion of plagioclase decreases from close to 100% to 32% over ± 15 m. A second and exactly opposite trend is observed for the Merensky cyclic unit, with the proportion of plagioclase increasing rapidly from 25% to 70% over 3m and then increasing more slowly with height to over 90% in the next 10m. These successions contain non-cotectic proportions of minerals and we suggest that such gradual changes in modal proportion require some process of mineral sorting during accumulation.

We further note that the bulk proportion of plagioclase in the UG2 cyclic unit is 64%, i.e. close to the cotectic proportion. For the Merensky cyclic unit the proportion is 74%, well in excess of the cotectic. We suggest that these values are not expected if crystallization has taken place from an ultramafic magma.

LATERAL VARIATION IN MODAL PROPORTIONS

Modelling magmatic processes in the Bushveld Complex may be limited by lateral variation (Maier and Eales, 1997). In the western limb the UG2 cyclic unit varies from 40-140m from northwest to southeast. They estimated that the proportion of plagioclase varied from 40-72% in the same direction, with 65% plagioclase at Impala Mine.

For the Merensky cyclic unit, at Rustenburg Platinum Mine, analyses by

Lee (1983) can be summed to give an average composition of 80% by weight of plagioclase. At Impala Mine, the data suggests 86% plagioclase. For other mines, the proportion ranges from 54% (Union) to 80%. The overlying Bastard cyclic unit has also been studied. Lithological sections and estimates of composition (Table 1) show the range in plagioclase content is from 78% (Union) to 85% (Rustenburg). The Bastard cyclic unit is therefore more plagioclase-rich than the Merensky cyclic unit and thus we have reservations about ultramafic magma being added.

ORIGIN OF EXCESS PLAGIOCLASE

Rounded plagioclase inclusions in cumulus pyroxene at the base of the UG1 and UG2 cyclic units were considered by Eales *et al.* (1986) to be grains suspended in the magma from the previous cycle. These partially dissolved as hotter, pyroxene-rich magma was injected and mixed, being enclosed in the resultant cumulus pyroxene grains. Hence, some plagioclase in cyclic units may have been inherited from previous cyclic units. If the magma produced a pyroxenite layer at the base of the next cyclic unit the mixed liquid couldn't change composition beyond the cotectic position otherwise it would not be able to crystallize a layer of pyroxenite. Therefore the liquid did not become plagioclase rich relative to the cotectic, and so could not produce an excess of plagioclase. Another reason for questioning whether the UG2 cyclic unit could be the source of the excess plagioclase is initial $^{87}\text{Sr}/^{86}\text{Sr}$, which increases dramatically immediately above the Merensky Reef and through the Bastard cyclic unit (Kruger, 1994). Any plagioclase grains derived from the UG2 cyclic unit and below would have had a ratio of 0.7063. The Merensky cyclic unit has an excess of plagioclase of about

Table 1: Thickness and calculated plagioclase contents of Merensky and Bastard cyclic units in the western Bushveld Complex

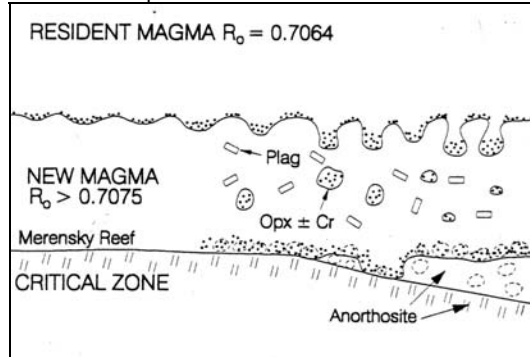
	Total thickness (m)	Wt% plagioclase
Bastard Cyclic Unit		
Amandelbuilt	60.50	78
Union	63.00	78
Rooderand	47.50	82
Impala	53.50	84
Rustenburg	63.00	85
Western	49.50	79
Merensky Cyclic Unit		
Amandelbuilt	17.50	65
Union	25.00	54
Impala	11.10	86
Impala	13.63	86
Rustenburg	10.20	80
Western (west)	10.30	76

10% and a range of initial ratios from 0.7073 – 0.708 and the Bastard cyclic unit has an even greater excess of plagioclase with a significantly higher initial ratio. If that excess of plagioclase had been derived from the UG2 cyclic unit it would have lowered the initial ratio relative to the Merensky cyclic unit. Because of this relationship of increasing initial ratio with increasing excess plagioclase from Merensky to Bastard cyclic units the concept that all the excess plagioclase is derived from footwall cyclic units must be questioned.

The source of the excess plagioclase must be sought in the new magma injected at the level of the Merensky Reef. As the new magma has fundamentally different Sr isotopic ratios, it is also shown by Kruger (1992) and Cawthorn (1996) that the magma was not primitive and ultramafic, but relatively evolved. Most basaltic magmas have plagioclase phenocrysts and plagioclase as liquidus mineral. Such a magma might be the source of the excess plagioclase in the Merensky and Bastard cyclic units.

The model proposed here (Fig. 2) for the different magmas involved in the formation of the Merensky and Bastard cyclic units, follows that suggested by Kruger (1994). The resident magma has an initial $^{87}\text{Sr}/^{86}\text{Sr}$ of 0.7064 and lies at the orthopyroxene-plagioclase cotectic. A relatively cool, evolved dense basaltic magma is injected below the residual magma. It has an isotopic ratio of about 0.709. Resident magma cooled by the underlying magma causes pyroxene and plagioclase to crystallize. Pyroxene accumulating at the two-liquid interface sinks, entraining some resident liquid and become enriched in pyroxene forming a layer – the Merensky pyroxenite. Since the interstitial liquid is derived mainly from the resident magma and partly from interaction with the new magma its initial ratio is dominated by the former at 0.707. Plagioclase nucleates from the lower magma while some pyroxene continues to sink from the upper, resident magma. The initial ratio steadily increases upwards in the Merensky Cyclic unit as more plagioclase from the new magma is incorporated into the accumulating succession. The process is repeated in forming the Bastard cyclic unit with whole-rock initial ratios closer to that of the new magma.

Figure 2: Schematic model for the formation of the Merensky cyclic unit, based largely on Kruger (1992). See text for explanation.



REFERENCES

- Cawthorn RG (1996). Re-evaluation of magma composition and processes in the uppermost Critical Zone of the Bushveld Complex. *Mineral. Mag.*, **60**, 128-135.
- Eales HV, Marsh JS, Mitchell AA, de Klerk WJ, Kruger FJ, and Field M (1986). Some geochemical constraints upon models for the crystallization of the Upper Critical Zone-Main Zone interval, northwestern Bushveld Complex. *Mineral. Mag.*, **50**, 567-582.
- Irvine TN (1970). Crystallization sequences in the Muskox intrusion and other layered intrusions. I. Olivine-pyroxene-plagioclase relations. *Geological Society of South Africa, Spec. Pub.*, **1**, 441-476.
- Kruger FJ (1992). The origin of the Merensky cyclic unit: Sr isotopic and mineralogical evidence for an alternative orthomagmatic model. *Austral. Journal Earth. Sci.*, **39**, 255-261.
- Kruger FJ (1994). The Sr-isotope stratigraphy of the western Bushveld Complex. *S. Afr. J. Geol.*, **97**, 393-398.
- Lee CA (1983). Trace and platinum-group element geochemistry and the development of the Merensky unit of the western Bushveld Complex. *Mineral. Deposita*, **18**, 173-190.
- Maier WD and Eales HV (1997). Correlation within the UG2-Merensky Reef interval of the western Bushveld Complex, based on geochemical, mineralogical and petrological data. *Geol. Surv. S. Afr. Bull.*, **120**, 56pp.

BIFURCATING CHROMITITES IN THE BUSHVELD COMPLEX, SOUTH AFRICA: MAGMATIC ANALOGUES OF SAND VOLCANOES

P.A. NEX

School of Geosciences, University of the Witwatersrand, Johannesburg,
South Africa
065nex@cosmos.wits.ac.za

SYNOPSIS

In the Bushveld Complex chromitite layers occur frequently within the Critical Zone and provide some spectacular exposures of layered rocks. In particular, Dwars River in the eastern Bushveld is well known for the unique intimate association of chromitite and anorthosite layers. A coherent explanation for bifurcating chromitite layers and other features of the UG1 and its footwall has been found. There is a correlation between domal structures and bifurcation direction of the chromitites. The unconsolidated footwall experienced liquefaction possibly due to major magma influx and associated seismicity. This resulted in structures analogous to those seen in sediments that undergo liquefaction including sand volcanoes or boils. Bifurcations in chromitite layers occur where the “background sedimentation” of chromitite occurs at the same time as periodic localized extrusion of plagioclase plus magma slurry at the magma-cumulate pile interface. These form “water lilies” of anorthosite, which build up on top of each other to form domes. At the same time accumulating chromitite forms multiple layers which vary in thickness from those formed from a single layer of chromitite grains to those over 0.5 m in thickness. Subsequent post-depositional structures suggest continued liquefaction in the footwall rocks and disruption of the already formed chromitite layers which was accentuated by the reversed density gradient between chromitite and anorthosite.

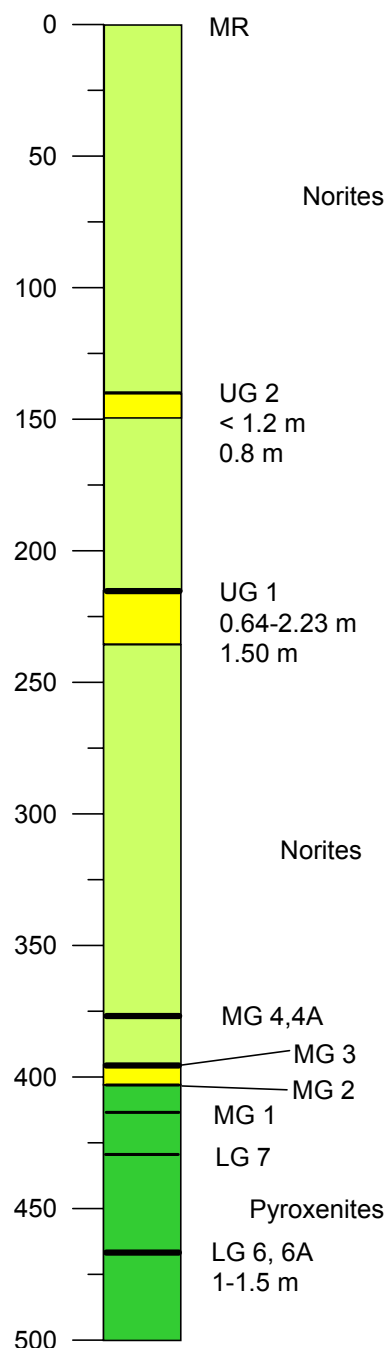
INTRODUCTION

The Bushveld Igneous Complex (BIC) in South Africa is the world's largest layered intrusion and is famed for its magmatic ore deposits of chrome, platinum and vanadium. The layered mafic rocks of the BIC have been divided into a number of zones; Marginal, Lower, Critical, Main and Upper in which the Critical Zone is made up of varying cycles of chromitite, pyroxenite, norite and anorthosite. Chromitite layers are confined to the Critical Zone which is sub-divided into upper and lower parts with the boundary between the two marked by the appearance of the first anorthosite layer of cumulus plagioclase. Chromitite layers within the Critical Zone have been divided into lower, middle and upper groups (Cousins and Feringa, 1964) each of which contain a number of individual chromitite layers. The focus of this study is the UG 1 chromitite layer which is the lowest of the Upper Group chromitites. It is also the first substantial chromitite layer within the upper Critical Zone and is underlain by a thicker anorthosite footwall than any other chromitite within the Critical Zone. This study is based on field and underground mapping and examination of the UG1 and its footwall and proposes a model for the formation of chromitite bifurcations and regards the disruption of chromitite-anorthosite layers as the culmination of multiple processes. Exposures of the UG1 have been examined in detail at Dwars River and underground in the western Bushveld.

FIELD CHARACTERISTICS

Exposures of the UG 1 at Dwars River are well known for the rare association of chromitite and anorthosite layers and are frequently figured in text books (e.g. Ashwal, 1993; Cawthorn et al., 1996). Outcrops at Dwars River show bifurcations of individual chromitite layers together with disruption and disturbance of chromitite-anorthosite layers and bifurcated chromitites. This disruption has been documented in part by Lee (1981) who broadly termed them “post-depositional structures” and considered them a consequence of a reversed density gradient between the > 1 m thick UG1 chromitite and its underlying anorthosite footwall sequence prior to complete consolidation.

Chromitite Layers in the Rustenburg Area,
data from Schürmann et al. (1998)



UG 1 Borehole intersection
from Brakspruit Shaft, RPM

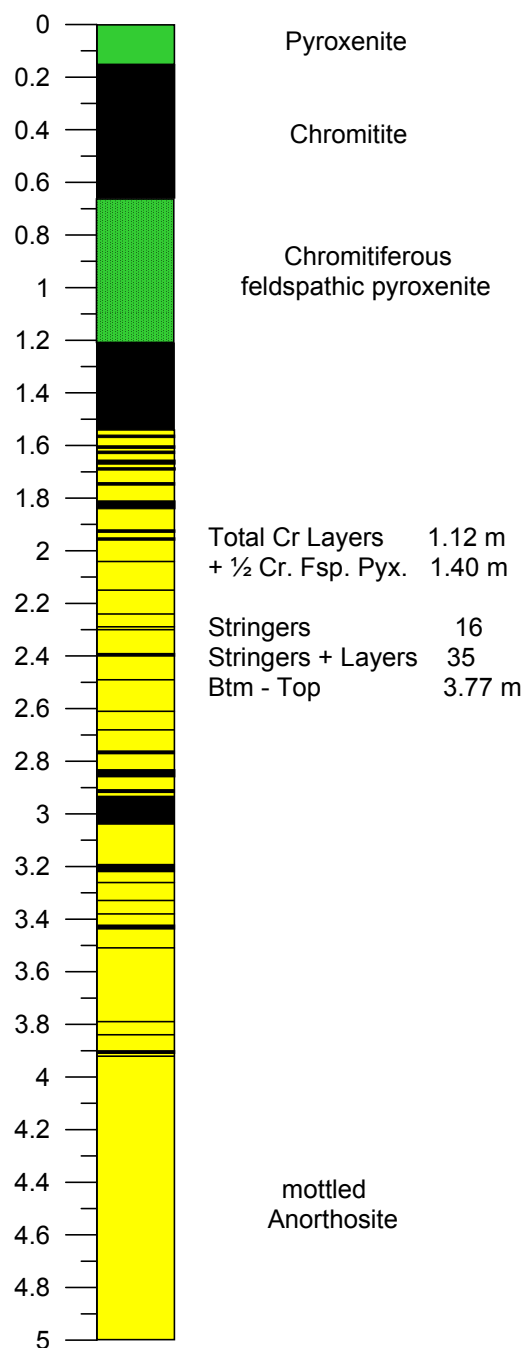


Fig. 1 Stratigraphy of the Critical Zone of the Bushveld Complex in the Rustenburg area together with a representative borehole core log of the UG1 from Brakspruit shaft. Depths are in metres on the left of each log.

The UG1 chromitite typically, but not always, consists of multiple chromitite layers within a footwall anorthosite and a hanging wall of feldspathic pyroxenite (Fig. 1). In some places it has been noted to consist of a single chromitite layer (de Klerk, 1982; Lea, 1996). The footwall mottled anorthosite grades downwards into layered anorthosite and norite and frequently shows mobilization and structures similar to those seen as a result of soft-sediment deformation. Chromitite layers of varying thickness (1-200 mm) occur within the footwall

anorthosite over a stratigraphic interval varying from 2 to 10 m. These generally have sharp planar contacts although there are exposures where gradational and / or irregular contacts are present and some anorthosites contain disseminated chromitite grains forming discontinuous layers. The thin chromitite layers within the footwall anorthosite bifurcate at a low angle (generally less than 25°) and the total thickness of the chromitite is maintained on outcrop scale from the unbifurcated chromitite to the combined thickness of multiple chromitite layers. Above the highest anorthosite-chromitite contact, the UG1 typically consists of two major chromitite layers each approximately 0.4 m thick with a chromitiferous feldspathic pyroxenite parting although this parting is not always present. The hanging wall to the UG1 chromitite is a relatively homogeneous pyroxenite that exhibits little variation. Features, which have been noted within the hanging wall, are sub-vertical anorthositic veins, which appear to emanate from the top of the UG1 chromitite. These have also been noted by Lee, (1981), and Viljoen et al., (1986). Disruption of the chromitite-anorthosite layers occurs frequently and includes fluid/magma-escape structures, discontinuous chromitites, folded chromitites, brecciated chromitites, and "intrusive" anorthosites (Fig. 2). These are frequently associated with mottled anorthosite that exhibits gradational and cross-cutting relationships with the host-lithology. These structures are demonstrably later than the formation of chromitite bifurcations.



Fig. 2. Disruption of chromitite-anorthosite layers by later anorthosite showing blocks of chromitite derived from overlying UG1 material. Scale is 100 mm in length.

A significant feature that has been revealed by detailed mapping is the presence of domal structures and a correlation between bifurcation direction and the core of domal structures. Bifurcations dominantly open-out towards the core of the domal structures and using an analogy from fold terminology could be said to "face outwards" from the domes. In haulages underground which are strike-parallel, continuous exposure of the UG1 and its footwall anorthosite are observed over distances of up to 800 m, although the restricted height of the haulages (3.5 m) results in only the top or bottom of the UG1 being exposed in any one section of the haulage. Domes are extremely well exposed in both sides of the haulage providing good three-dimensional sections. The domes are an extremely prominent feature

and exposures reveal a geometric relationship between the domes and chromitite bifurcations. Some features of the domes are:

1. Domes generally have an amplitude of 1-5 m and a wavelength of 10-40 m,
2. Bifurcations are symmetrically orientated with respect to the core of the dome,
3. Chromite layers split towards the dome centre, thus chromitite layers are more numerous in the centre of the dome. Within a single lens of anorthosite the number of discrete chromitite layers can increase from 0 to more than 30 in the centre over a horizontal distance of 5 m,
4. Some dome structures are cored by chromitite dykes which terminate downwards,
5. In one locality anorthosite forms a cross-cutting dyke body in the core of a dome which extrudes above the UG1 chromitite and locally forms the hanging wall to the UG1 chromitite,
6. Where a chromitite layer bifurcates the total chromitite thickness in the single layer totals the total chromitite thickness of the two bifurcations in the immediate locality.

Some of these features are summarised in a schematic diagram shown in Fig 3. Post-depositional structures are commonly associated with the domes and disrupt chromitite-anorthosite layers and the chromitite bifurcations. It is therefore fundamental that the formation of the bifurcations must predate the post-depositional structures.

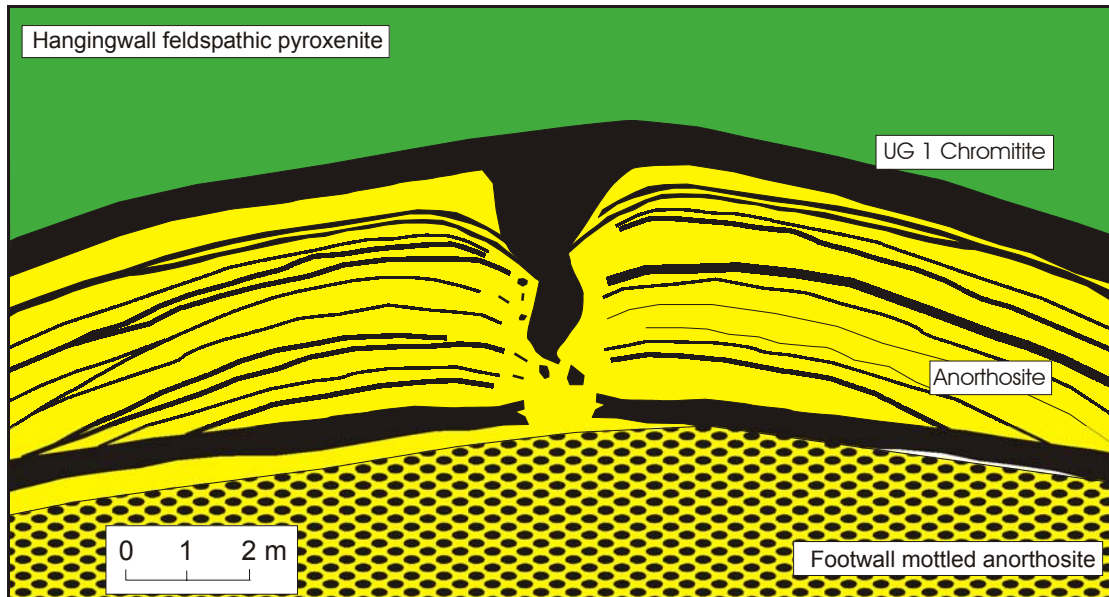


Fig. 3. Schematic diagram of domal structures associated with the UG1 showing the geometrical relationship between bifurcation directions and the dome cores.

MODEL

Any model to explain the chromitite bifurcations must account for the fundamental correlation between symmetry of bifurcations with respect to the domal structures. Previous workers have not fully addressed the question of the origin of bifurcations and the occurrence and significance of domes has been under-represented in the literature. It is also significant that disrupted chromitite / anorthosite layering shows either:

1. ductile deformation of chromitite or,
2. ductile deformation of chromitite and anorthosite together or,
3. brittle deformation of chromitite.

and in only one place has evidence been found for brittle deformation of anorthosite on its own which together with the evidence for ductile deformation of the footwall anorthosite is clear evidence for anorthositic melt migration which post-dates the formation of chromitite layers. Models must also explain the variation in the thickness of chromitite layers from those which are just a single grain of chromite thick to those greater than 0.5 m.

A model which achieves the demands above can be found by comparing the structures in the UG1 chromitite layer and footwall with structures found in sedimentary rocks as a result of fluidisation, particularly sand volcanoes and sand boils. Examination of cross-sections of both sand volcanoes and UG1 domes shows that the features in both have similar geometrical relationships (Fig. 4). It is envisaged that while the footwall anorthosite was still unconsolidated possibly to a depth in excess of 10 m, liquefaction of the footwall occurred and at a similar time chromitite commenced accumulating. Chromitite accumulation provided the 'background sedimentation' during which time periodic extrusion of anorthosite crystals plus magma occurred at the magma - cumulate-pile interface. The anorthosite crystals would have formed sub-circular lenses of anorthosite that punctuated background chromitite accumulation. The thickness of chromitite layers forming during periodic extrusion of anorthosite and magma would therefore depend on the presence or absence of anorthosite 'volcanoes' and the rates at which both anorthosite and chromitite crystals were accumulating. This mechanism explains the formation of dome structures, the geometrical relationship between bifurcations and domes, and the occurrence of chromitite layers on a variety of scales.

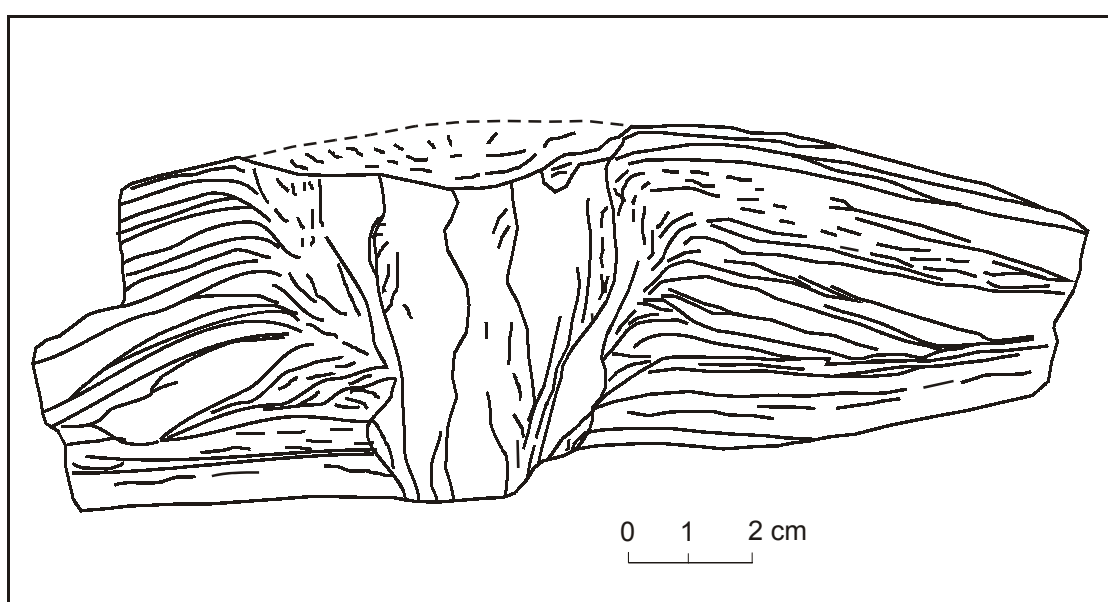


Fig. 4. Diagram of the internal structure of a sand volcano from the Carboniferous of Ireland, from Gill and Kuenen, (1958).

The formation of sand boils or volcanoes in sedimentary rocks has been noted from both preserved sedimentary structures in ancient rocks (Gill and Kuenen, 1958) and also forming in currently unconsolidated sediments (Holzer and Clark, 1993; Rastogi, 2001). They occur when a layer of unconsolidated sediment is fluidised and transport of fluid and suspended grains takes place through overlying sediment to the sediment-water interface. The slurry of fluid plus grains is then "erupted" at the sediment-water interface forming domal structures akin to volcanoes. In a similar fashion we envisage fluidisation of the UG1 footwall, for which there is abundant evidence, movement of material vertically and expulsion of an anorthosite slurry at the interface between magma and the cumulate pile.

This model can account for all the features of the domes indicated above and also other structures within the UG1 sequence. As in sedimentary rocks it is difficult to establish unequivocally a trigger for the fluidisation that results in the domes. In sedimentary rocks features like sand volcanoes are often used as an indicator of palaeoseismicity (Rossetti, 1999) although other workers have cautioned against their use as they can form from fluid movement not associated with earthquakes (Li et al, 1996).

CONCLUSIONS

The occurrence of bifurcations in the UG1 footwall can be explained by a process analogous to that which forms sand volcanoes in sedimentary environments. Further accumulation of chromitite resulted in a reversed density gradient between partially consolidated footwall and the UG1 chromitite. This in turn led to disruption and disturbance of the already formed chromitite-anorthosite layers analogous to structures of soft-sediment deformation seen in sedimentary rocks.

ACKNOWLEDGEMENTS

Thanks to those mining companies and geologists who facilitated access to UG1 chromitite exposures particularly Nico Denner, Frikke Fensham, Rob Ingram, Johan Marais, Anton Mauve and Alan Page. Thanks are also due to Grant Cawthorn, Judith Kinnaird and Johan "Moose" Kruger for animated and encouraging discussion.

REFERENCES

- Ashwal, L.D. 1993 *Anorthosites* Springer-Verlag, Berlin pp422.
- Cawthorn, R.G. 1996 *Layered Intrusions* Elsevier, Amsterdam pp531
- Cousins, C.A. and Feringa, G. 1964 The chromite deposits of the western belt of the Bushveld Complex In: Houghton, S.H. (Ed.) *The geology of some ore deposits in southern Africa*, Special Publication of the Geological Society of South Africa **2** 183-202.
- Gill, W.D. and Kuenen, P.H. 1958 Sand volcanoes on slumps in the Carboniferous of County Clare, Ireland. *Journal of the Geological Society* **113** 441-460.
- Holzer, T.L. and Clark, M.M. 1993 Sand boils without earthquakes. *Geology* **21** 873-876.
- De Klerk, W.J. 1982 The geology, geochemistry and silicate mineralogy of the upper Critical Zone of the north-western Bushveld Complex, at Rustenburg Platinum Mines, Union Section. Msc thesis, Rhodes University, Grahamstown, South Africa.
- Lea, S.D. 1996 The geology of the Upper Critical Zone, north-eastern Bushveld Complex. *South African Journal of Geology* **99** 263-283.
- Lee, C.A. 1981 Post-deposition structures in the Bushveld Complex mafic sequence. *Journal of the Geological Society* **138** 327-341.
- Li, Y., Craven, J., Schweig, E.S. and Obermeier, S.F. 1996 Sand boils induced by the 1993 Mississippi River flood: Could they one day be misinterpreted as earthquake-induced liquefaction. *Geology* **24** 171-174.
- Rastogi, B.K. 2001 Ground deformation study of the M_w 7.7 Bhuj eathquake of 2001. *Episodes* **24** 160-165.
- Rosetti, D. F. 1999 Soft-sediment deformation structures in late Albian to Cenomanian deposits, Sao Luis Basin, northern Brazil: evidence for palaeoseismicity. *Sedimentology* **46** 1065-1081.
- Schürmann, L.W., Grabe, P-J. and Steenkamp, C.J. 1998 Chromium In: Wilson, M.G.C. and Anhaeusser, C.R. (Eds.) *The Mineral Resources of South Africa Handbook*, Council for Geoscience, 16 90-105.
- Viljoen, M.J., de Klerk, W.J., Coetzer, P.M., Hatch, N.P., Kinloch, E. and Peyerl, W. 1986 The Union section of Rustenburg Platinum Mines Ltd with reference to the Merensky Reef. In: Anhaeusser, C.R. and Maske, S. (Eds.) *Mineral Deposits of Southern Africa* Geological Society of South Africa, Johannesburg 1061-1090.

THE MOCHILA LAYERED COMPLEX-VENEZUELA

A PGE EXPLORATION CASE STUDY

R.P. VILJOEN

Centre for Applied Mining and Exploration Geology

University of the Witwatersrand, Johannesburg.

e-mail: 065rich@cosmos.wits.ac.za

SYNOPSIS

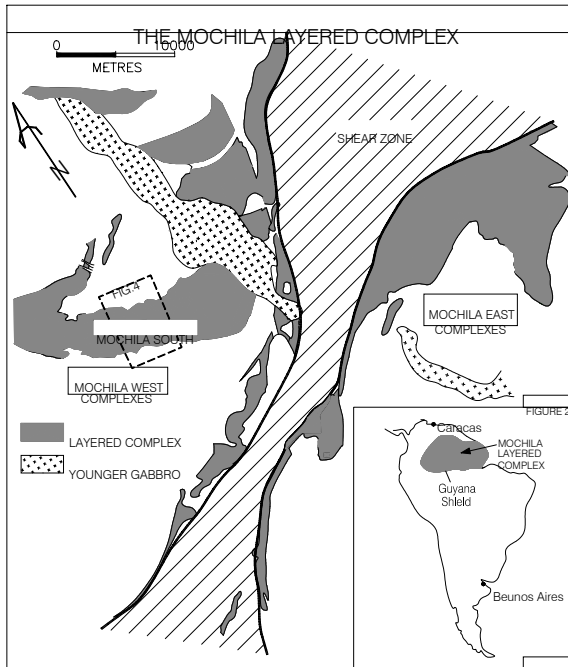
The Mochila layered ultramafic complex has been emplaced into the early Proterozoic Chicanan greenstone belt of the Guyana shield of S.E. Venezuela. The complex, in addition to being weathered to a depth of 35 meters, is covered by tropical rain forest and a variety of exploration techniques have been used in gaining an appreciation of its geology and economic potential.

Aeromagnetics was particularly useful when combined with soil geochemistry in defining 4 differentiation cycles within the complex which is steeply dipping and up to 2,400 meters wide. Two lower ultramafic cycles, comprised essentially of basal dunitic to peridotitic zones passing upwards into mainly clinopyroxenites, are present within the lower ultramafic unit. These cycles are separated from two similar upper cycles, constituting the upper ultramafic unit, by a distinctive gabbro unit.

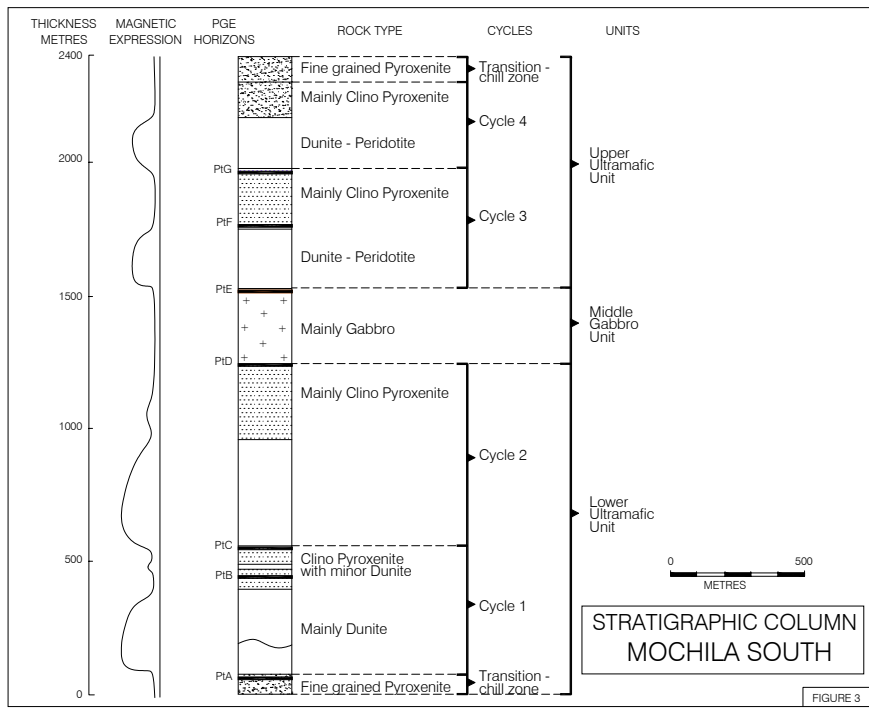
The use of Cu, Ni,Cr,Ti and V geochemistry helped significantly in defining these cycles and in establishing differentiation trends or way up criteria. Seven PGE horizons lying mainly at or close to lithological contacts have been identified within the complex and PGE enrichment has taken place in saprolite. Metallurgical tests on the extractability of the PGE's from saprolite are in progress and the establishment of an opencast operation is being investigated.

GEOLOGY

The Mochila complex has been emplaced into volcanics of the Chicanan greenstone belt, one of a number of early Proterozoic greenstone belts of the Guyana shield of eastern Venezuela (Fig. 1). The Complex has undergone a substantial amount of structural disturbance with 12 individual bodies (Fig. 2) thought to have constituted a once larger, more continuous layered complex of the type common in greenstone belts in many parts of the world (Viljoen, 2000). The Mochila South Complex (Fig. 2) one of the largest of the bodies and displays the most continuous, relatively undisturbed layering. It extends for some 20 kilometers in a west-northwest to east-south-east direction has an average width of 2.4 kms and has been subjected to the most comprehensive exploration programme (Viljoen, 2000).



The Complex can be divided into a Lower Ultramafic Unit and an Upper Ultramafic Unit, separated by a Middle Gabbro Unit (Fig. 3). It is comprised of four differentiation cycles, the first two of which occur in the Lower Ultramafic Unit while cycles 3 and 4, constitute the upper, somewhat less Ultramafic Unit. The Lower Ultramafic unit is some 1200 meters thick and is the most ultramafic component of the complex being divided into two dunite-peridotite to clino pyroxenite cycles. Zones of laterite and birbirite are mainly confined to the olivine-rich lithologies of the Lower Ultramafic Unit. The Middle Gabbro Unit constitutes an important, non-magnetic marker in the middle of the sequence and separates the lower and upper ultramafic units (Fig. 3). The Upper Ultramafic Unit is comprised of two magmatic cycles, both of which show differentiation sequences from dunite-peridotite to clinopyroxenite.



PGE MINERALIZATION

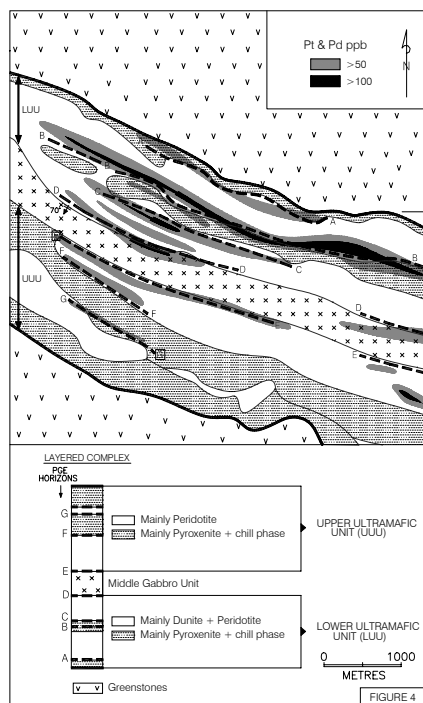
Seven linear zones of PGE enrichment have been identified within the Mochila south complex from soil geochemistry, auger drilling and diamond drilling. These zones are designated A to G on figure 4. The most important PGE anomalies and mineralized layers lie within the clino pyroxenite zone lying above the dunite peridotite of cycle 1 (Horizon B) and at the top of the pyroxenite zone of the Lower Ultramafic Unit in contact with the gabbro marker (Horizon D). Other PGE anomalies, which are largely untested, are shown on figure 4.

EXPLORATION

The Mochila Complex provides an informative case study of the use of a range of exploration methodologies in PGE exploration in tropical rain forest with very limited exposure and deep weathering. A range of new data were invaluable in establishing the regional setting of the complex and in compiling a new geological map on which the stratigraphy, structure and locality of the seven PGE -rich layers of the Mochila South Complex is based (Fig. 4, Viljoen, 2000).

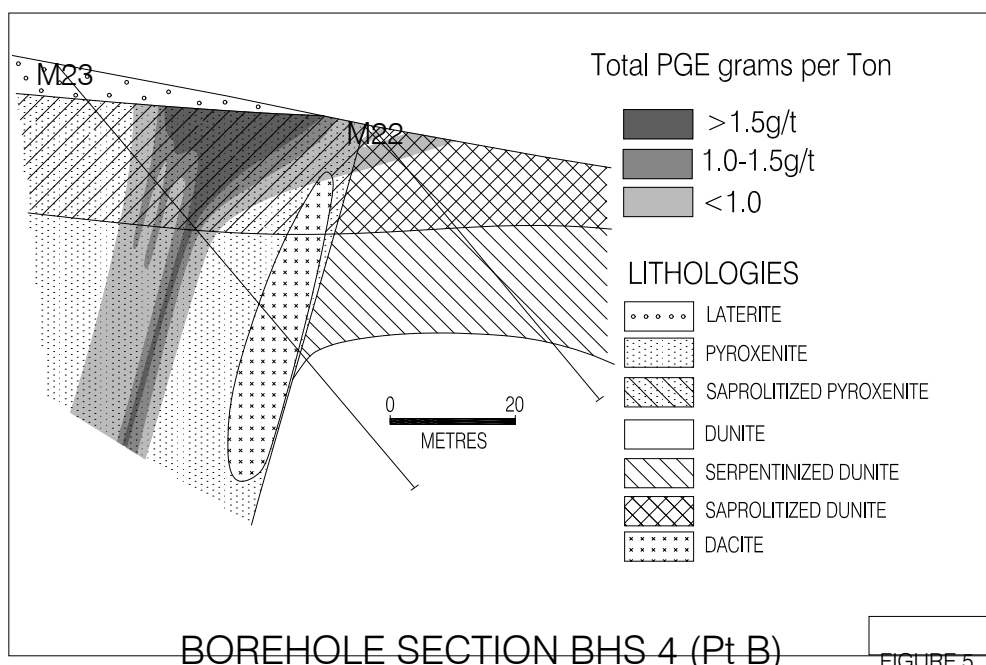
SPOT imagery was interpreted at a scale of 1:100 000 and provided important information on the position of artisanal workings and areas of laterite cover. Radar imagery interpretation complemented the satellite information and provided useful structural data.

Aeromagnetics provided the single most important set of data. The interpretation of the first vertical derivative product being used as the basis for the compilation of a new geological map. The magnetite-rich, serpentinized, olivine-bearing lithologies, as well as magnetite in surficial birbirite, generally demarcated the basal layers of the various cycles. This observation, coupled with sporadic field occurrences of gabbros, pyroxenites, harzburgites and dunites, provided the initial indication that the area was underlain by extensive tracts of differentiated rocks comprising part of a major layered intrusion (Viljoen, 2000).



Radiometrics also assisted in the construction of a new geological map. The total field data helped to distinguish various lithologies while the potassium channel is of particular use in indicating zones of alteration associated with gold mineralization which also occurs in the area.

Soil Geochemistry, interpreted in conjunction with aeromagnetics, proved to be vitally important in deriving the framework of igneous layering and younging direction present within the complex and in defining the seven PGE enriched zones. Elements analysed included PGEs (Pt and Pd) Au, Ni, Cu, Cr, Ti and V. The close correlation between aeromagnetics and various diagnostic elements and in particular between magnetic high and low contacts is a feature of this interpretation. Linear Cr and Ni anomalies are prominent in the Lower Ultramafic unit and help to define it, while linear V, Ti and Cu anomalies are diagnostic of the Upper Ultramafic Unit. Platinum and palladium anomalies in soil samples, together with subtle gold anomalies, defined the PGE rich target horizons.



EVALUATION

The PGEs have become enriched in the 35 metre deep-weathered or saprolite zone, particularly overlying the B and D PGE horizons, and mushroom-shaped areas of enrichment near the surface are apparent (Fig. 5). The average grade of the fresh rock material in the B horizon is in the order of 1g/t over 5 meters, whereas the enriched saprolite contains a 25m wide zone of greater than 1.5g/t which tapers towards the base of the saprolite zone (Fig. 5). Existing resources on the B and D horizons are being evaluated with a view to an opencast mining operation. Tests on the nature and extractability of the PGE's in the saprolite are being conducted and have been encouraging. The fresh rock PGE potential of the complex remains to be tested.

ACKNOWLEDGEMENTS

The author wishes to thank Mr. Peter Tinoco of the ODC company of Venezuela, the owners of the concessions, for granting permission to publish this paper. A considerable amount of effort by a number of Gold Fields geologists, including Dr Hannes Henckel, Mr Julian Misiewicz and Mr Gavin Conway, has been devoted to the study of the Mochila Complex, and their contributions to our understanding of the geology are gratefully acknowledged.

REFERENCES

Viljoen RP. (2000). A Review of the Geology and Economic Potential of the Mochila layered Complex, Venezuela. Unpublished ODC- GFL report.

THE FOY OFFSET DYKE, AN ORE-BEARING IMPACT GENERATED FRACTURE, SUBDURY STRUCTURE, ONTARIO, CANADA

M. G. TUCHSCHERER^{1*} and J. G. SPRAY²

¹Impact Cratering Research Group, School of Geosciences, University of the Witwatersrand, Private Bag 3, P.O. Wits 2050, South Africa.

^{*}(E-mail: tuchscm@science.pg.wits.ac.za)

²Planetary and Space Science Centre, University of New Brunswick, 2 Bailey Drive, Fredericton, N.B., E3B 5A3, Canada.

SYNOPSIS

The >35 km long Foy Offset Dyke is an igneous body associated with the 1.85 Ga Sudbury impact structure. It is proposed that the radial dykes at Sudbury are related to the modification stage of the cratering event. Catastrophic tensional radial fracturing of the crust upon rebound of the Sudbury transient cavity facilitated the downward intrusion of a primitive bulk impact melt breccia. Litho/geochemical variations with strike are a function of the uplifted Levack Gneiss Complex and downfaulted Huronian outliers, proximal and distal to the Sudbury Igneous Complex (SIC), respectively. End-member mass balance calculations indicate that the bulk impact melt can be modelled by mixing local target rocks, a 40-50% East Bull Lake anorthosite component with a 50-60% Cartier Granitoid mix. Gravitational capture of primary magmatic Ni-Cu-PGE massive sulfide bearing breccia ore is interpreted to have been rapid, simultaneous with the crystallization of the most primitive proximal Foy inclusion-rich groundmass.

INTRODUCTION

The Sudbury Structure, Ontario, Canada, hosts the world's largest source of magmatic Ni-Cu-PGE ore: 1648 Mt at 1.20% Ni and 1.03% Cu [1]. It was not until the discovery of shatter cones and their interpreted shock origin that the astrobleme hypothesis was suggested in 1964 [2]. Since then, controversy about the origin of the structure has reigned between traditional magmatic [3] and meteorite impact models [4]. With time, uncontested geological evidence has surfaced furthering the impact hypothesis, e.g. decorated planar deformation features [5], impact generated diamonds [6], extraterrestrial helium isotopic signatures in fullerenes [7], isotopic evidence for crustal melting [8], and a non-intrusive origin for the SIC imaged by vibroseis surveying [9]. Despite the phenomenal accumulation of scientific information, not much detailed work has been performed on North Range radial dykes, such as the Foy dyke, the topic of this investigation.

GEOLOGICAL SETTING:

The Foy Offset Dyke is one of five known radial dykes associated with the Sudbury impact structure. It is located in the North Range of the Sudbury region and strikes concentrically over 15 km west-northwest to north-northwest, 15 km north-northeast, and >5 km north. It connects to the SIC, a 2.5 km thick differentiated impact melt sheet, via a 450 m wide embayment that is host to the ore-bearing Sublayer. The dyke is heavily faulted by minor NW-SE trending faults, the northward-trending regional Onaping fault set, and by the concentric Hess Offset Dyke. The latter divides the dyke into the proximal and distal Foy at the 15 km mark. Host country rocks belong to the Abitibi Subprovince. They consist of the Levack Gneiss Complex (LGC), the Cartier Granitoid, metavolcanic rocks of the Benny Greenstone Belt (BGB), Huronian sedimentary outliers, and three diabasic intrusive pulses. The LGC has undergone upper amphibolite to lower granulite facies metamorphism during the Kenoran Orogeny at 2711 ± 7 Ma with peak metamorphism occurring at 2647 ± 2 Ma. The Cartier Granitoid has been dated at 2642 ± 1 Ma and belongs to the Algoma Domain, one of the largest felsic plutonic unit of the Canadian Superior Province. The BGB, concentrically situated northwest and northeast of the SIC, consists

of a succession of metasedimentary rocks interlayered with metavolcanics that have been metamorphosed to greenschist and amphibolite facies during the Kenoran Orogeny. Metasedimentary rocks of the Paleoproterozoic Huronian Supergroup from the Southern Province occur as minor outliers in the vicinity of the distal Foy and most likely provided a more extensive cover to the Archean basement. The diabase pulses have been dated at 2454 ± 2 Ma for the Matachewan, $2219 - 3.5 / +3.6$ Ma for the Nipissing sills and dykes, and 1238 ± 4 Ma for Sudbury diabase dykes.

PETROGRAPHY/GEOCHEMISTRY:

The Foy Offset Dyke represents a polymict impact melt breccia with variable inclusion and melt contents. It comprises three distinct geochemical environments, the embayment, the proximal Foy with an added 2.5 km of the distal Foy, and the distal Foy. These can be further broken down by the Foy's internal lithologies, inclusion-rich quartz diorite (IQD), and inclusion-poor quartz diorite (QD). It should be noted that quartz diorite is not representative of the Foy groundmass composition that is generally granodioritic to quartz-monadioritic (CIPW normative). Field observations reveal the QD occurs symmetrically along the dyke's margins. A variety of QD is also found in the embayment, distinct to that environment. Field observations also indicate the inclusion content diminishes with strike towards the distal Foy.

Geochemistry reveals the groundmass throughout the dyke has a near-uniform Mg # ($MgO/MgO + FeO$) of 0.35. Major elements plotted versus SiO_2 reveal constant assimilation trend lines for all lithologies. The embayment (Sublayer) rocks exhibit more basic compositions (52-57 wt.% SiO_2), followed by QD (57-60 wt.% SiO_2), IQD (60-63 wt.% SiO_2), and QD chilled margins (63-64 wt.% SiO_2), the latter being the best candidate for the bulk impact melt composition. Embayment lithologies, situated below the SIC, show the most compositional variation: FeO_{tot} , MgO , and CaO decrease, whereas Na_2O and K_2O increase with distance from the SIC. A slight geochemical shift is noted in SiO_2 , CaO , Na_2O , and K_2O at 22 km from the SIC, whereas alumina and TiO_2 are constant throughout the dyke at ~15 and ~0.7 wt.%, respectively.

Light Rare Earth Element (LREE) geochemistry indicates the dyke is intimately related to the averaged SIC after Lightfoot et al. [10]. Sm/La ratios are similar for all lithologies, embayment excluded. Heavy Rare Earth Element (HREE) ratios (Yb/Gd) increase with strike vectoring towards the averaged SIC value, as expected by the total and progressive assimilation of inclusions towards the distal Foy. A Yb/Gd versus Sm/La plot isolates the Proximal Foy IQD Groundmass (PFG) as the most primitive lithology, i.e. the impact melt that crystallized first after dyke emplacement. It is, therefore, the best indicator of post-emplacement secondary processes: assimilation, magmatic fractionation, and alteration. Averaged Ni and Cu values from the PFG, 115.4 ppm and 90.5 ppm, respectively, indicate these initial concentrations were sufficient to produce the massive Sudbury ore reserves after SIC differentiation. The Ni versus Cu ratio of whole rock samples averages at 1.3, with a R correlation factor for the regression of all data of 0.9686, indicating the Ni/Cu reservoir had been homogenized with dyke emplacement. End-member mass balance calculations between selected target rocks show the initial impact melt can be reasonably estimated with respect to the PFG (Fig. 1). This composition is best approximated by a mixture of 40-50% layered East Bull Lake type gabbronoritic anorthosite (megaclast composition from the Foy embayment) with a 50-60% Cartier Granitoid component [11].

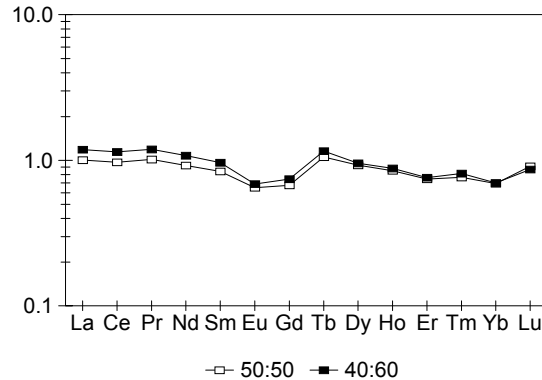


Figure 1: Rare earth element patterns for Proximal Foy Groundmass (PFG) modeled as an anorthosite and Cartier Granitoid mixture. Open squares indicate to a mixture of 50:50 anorthosite : Cartier, and black squares a 40:60 mixture.

EMPLACEMENT MECHANISM:

The upward catastrophic collapse of the Sudbury transient cavity during the modification stage of cratering can be called upon to explain the formation of radial dykes. The orientation of evenly distributed radial fractures, as seen in Sudbury [12] and lunar craters [13], is focussed towards ground zero and therefore should be a function of the central uplift. Dyke orientation is a function of the dominant stress field during emplacement. In the case of the Sudbury radial dykes, the collar of Levack Gneiss below the northern footwall contact of the SIC has been interpreted as an uplifted segment of the crust [14], in agreement with the present study. The LGC would have provided an important stress field upon its ascent. Massive rebound of mid- to deep-crustal lithologies must occur within seconds or minutes after impact [13]. The downward vacuum-induced capture of an early primitive bulk impact melt breccia must occur during this instant through rebound-assisted tensional fracturing. This should occur when the vertically oriented stress field overwhelms the confining lithostatic pressure. Radial fracturing should also be enhanced in central regions of large craters where the crust has just been thinned and considerably weakened, e.g. due to the pervasive presence of pseudotachylite veins and dykes [15].

REFERENCES:

- [1] Eckstrand, O.R., (1996) *Geol. of Can. Min. Ore Depo.*, 8, 583-614. [2] Dietz, R.S., (1964) *Journal of Geology*, 72, 412-434. [3] Naldrett, T., 1984, *OGS Spec. Vol.* 1, 533-569. [4] Grieve, R.A.F., 1994, *OGS Spec. Vol.* 5, 119-132. [5] Dressler, B.O., 1984, *OGS Spec. Vol.* 1, 97-136. [6] Masaitis, V.L. et al., 1999, *Geol. Soc. of Am. Spec. Pap.* 339, 317-321. [7] Becker, L. et al., 1996, *Science*, 272, 249-252. [8] Dickin, A.P., 1999, *Geol. Soc. of Am. Spec. Pap.* 339, 361-371. [9] Milkereit, B. et al., *Geology*, 20, 807-811. [10] Lightfoot, P. C. et al., 1997, *Economic Geology*, 92, 289-307. [11] Melrum, A., 1997, *Precambrian Research*, 82, 265-285. [12] Dressler, B.O., 1982-83, *OGS Comp. Map.* 2491. [13] Melosh, H.J., 1989, *Impact Cratering*, 1-245. [14] Card, K., 1994, *Cur. Res.* 1994-C; GSC, 269-278. [15] Fedorowich, J.S. et al., 1999, *Geol. Soc. of Am. Spec. Pap.* 339, 305-315.

5. WITWATERSRAND

SEDIMENTOLOGICAL MODEL AND RE-EVALUATION OF THE MAIN REEF LEADER, CENTRAL RAND GOLDFIELD

M.J. VILJOEN and R.P. VILJOEN

Centre for Applied Mining & Exploration Geology (CAMEG)
Dept. of Geology, University of the Witwatersrand
e-mail: 065mjvil@cosmos.wits.ac.za

SYNOPSIS

The Main Reef Leader contained the highest gold grades and was the most extensively mined of all of the Reefs of the Central Rand Goldfield, having produced nearly 5000 tons of gold. Mining ceased in the mid seventies at a vertical depth of just under 3 km. Underground sampling information from old mine plans and records was compiled and regularized into 50 x 50m block values, and these data have been interpreted and integrated to create an overall sedimentological model with related gold value distribution trends. Data sets interpreted include reef thickness, percentage internal quartzite, gold grade in g/t & gold content in cm g/t. Areas of thicker reef (>60 cm) correlate closely with areas of higher percentage internal quartzite, and define a number of major channels. Thinner areas adjoining the channels contained the highest gold values. The proximal part of a major distributary system with associated ore shoots is situated close to the old Village Main mine, with subsidiary distributary systems occurring at Simmer and Jack and at Consolidated Main Reef (Fig. 1). This distributary pattern is supported by an isopach map of the Main Bird Series which conforms to the distributary systems noted above. Down dip projections were made from the various interpretations with added information from 6 deep boreholes. A remaining deep level resource of about 30 million ounces has been calculated from this study. Isopleth maps for zircon & leucoxene show that the largest heavy mineral grains in the reef matrix occur at Robinson (Village main) Mine. Osmiridium content per million ounces of gold, together with lowest silver fineness, as well as an area of thickest Kimberley shale, all support the presence of a major entry point at this locality. A hitherto unrecognized or documented major entry point, in addition to the well-established ones on the West Rand and at ERPM, has been shown to exist for the Main Reef Leader in the middle of the Central Rand Goldfield.

INTRODUCTION

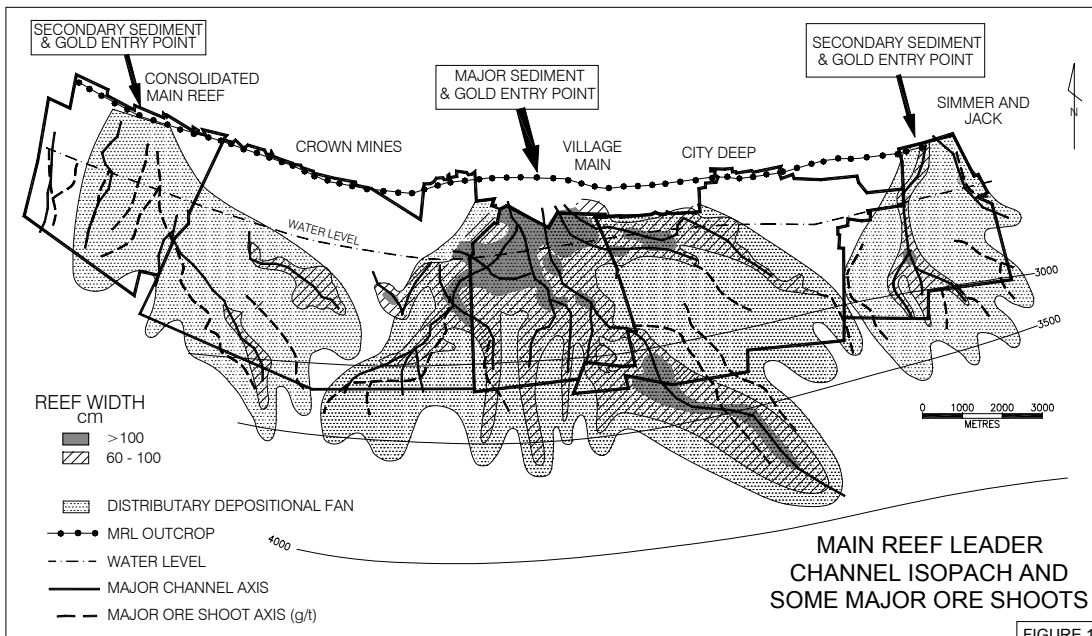
The Centre for Applied Mining and Exploration Geology (CAMEG), working with and on behalf of Innovative Property Developments (IPROP), have delineated a substantial gold resource south of Johannesburg in the area where the world's greatest gold-field was discovered in 1886 and where the mining of the auriferous conglomerates ceased in the mid-seventies. Regularized 50 x 50 block values calculated by Rand Mines for reef thickness in cm, together with percentage internal quartzite, gold values in g/t and gold content in cm g/t were used as the basis for reef modelling on a number of reef horizons.

MODELLING OF CHANNEL THICKNESS AND GOLD VALUES

From these data, the main channels that carried the gold and related sediment into the depositional basin (reflected by thicker reef areas) were modelled. Gold has been concentrated both within, and more particularly, on the edges of the channels to form higher-grade ore shoots, a feature recognized and documented by Reynecke in 1925. The contouring of gold values was aided considerably by utilizing the thicker high-energy channel axes, which also contain the highest percentage of internal quartzite, as a broad guide in creating a meaningful model on which the resource calculation could be based.

Three main entry points emerged from this modelling, and these fed sediment and gold into the Central Rand depositional basin to form large coalescing fans that now constitute the Main Reef Leader (Fig 1). A number of discrete channels with associated ore shoots have been defined with the most robust cluster emanating from an entry point feeder site on the north side of the Robinson Deep (now Village Main) mine, and extending to the southwest

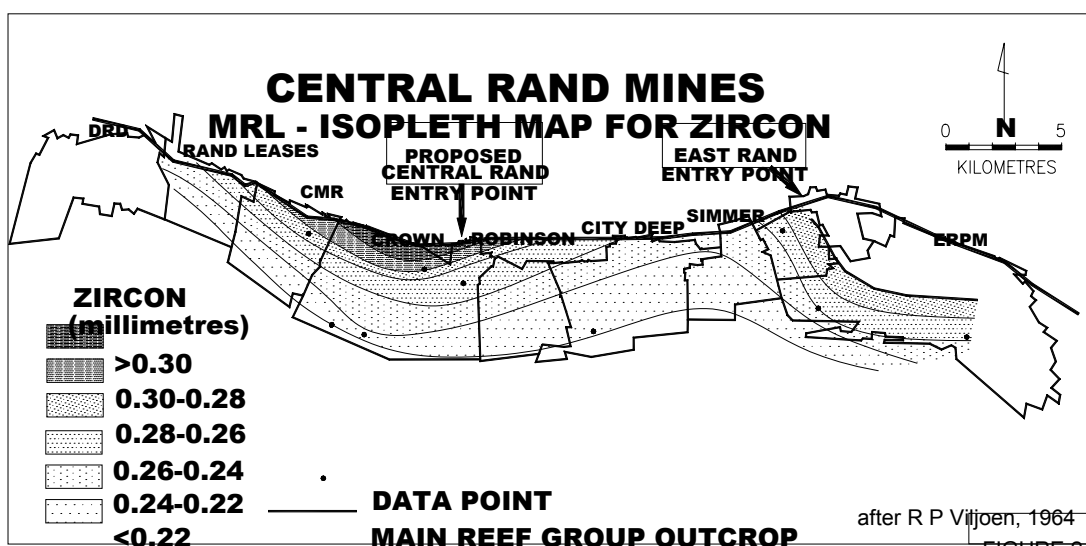
south and southeast. Less robust, but equally gold-rich sedimentary fans emanating from discrete entry points with several distributary channels exist at CMR and Simmer and Jack (Fig. 1). The most robust channel on the Main Reef Leader trends to the southeast of the major central entry point and is persistent for a considerable distance downdip, where it appears to be the main controlling distributary feature for the gold in the deep resource (Fig. 1).



The evaluation carried out by CAMEG has established the presence of a multimillion ounce gold resource on the Main Reef Leader, at depths varying between 2900 and 3200 meters below surface within the existing mine lease boundaries of the Central Rand. This resource represents a crucially important updip extension of, and is contiguous with, the multimillion-ounce Argonaut resource lying to the south, at depths of between 3200 and 3800 m.

MODELLING OF SEDIMENTOLOGICAL AND MINERALOGICAL DATA

Information on the thickness variation of the Kimberley shale was compiled by Pretorius (unpublished). A broad isopach map of the Kimberley shale based on these data was compiled, and this shows a thinning in the Robinson mine area corresponding to the position of the proposed main entry point.



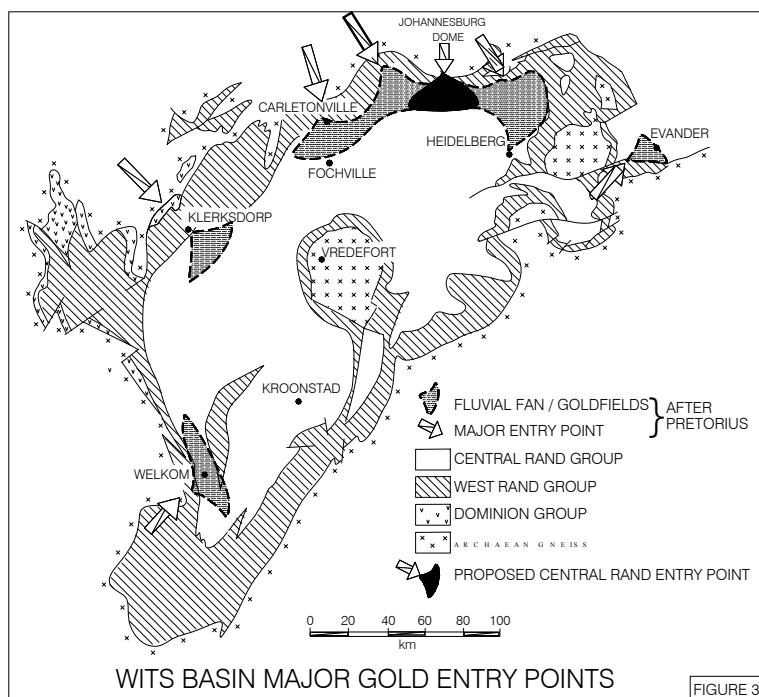
An isopach of the Main Bird Series compiled by Rand Mines shows an area of significant thickening of this sedimentary package at Robinson deep with major axes of thickened sediment trending to the SE and the SW & corresponding closely to the positions of the two main distributary channels constituting the Robinson mine central entry point. Areas of

thicker Main Bird sediment also occur on the west side of CMR & the east side of Simmer & Jack & correspond broadly with the postulated second order entry points in these areas. Viljoen (1963) showed that a systematic decrease in zircon size and degree of rounding, from a median of 0.312 mm grain size near the outcrop of the Main Reef, to 0.211 mm median grain size at 3000 m depth, exists. Contouring of the zircon size data showed an area of largest zircons centered on Crown Mines and Robinson mine close to the proposed major entry point (Fig. 2). An isopleth map of leucoxene showed essentially the same pattern with grain sizes, ranging from less than 0.4 mm near surface at Crown Mines / Robinson mine, to less than 0.24 mm at depth.

Contouring of osmiridium content per million ounces of gold from data compiled by Pretorius (unpublished) once again showed the same pattern with values ranging from > 400 ounces at surface near Crown mines / Robinson mine, to less than 200 ounces at depth. The silver content of bullion increased from < 7% at surface to greater than 11% at depth and shows a similar pattern.

All of the above, more broadly based interpretations, support and confirm the more precise interpretations of channels and are shoots derived from the detailed modelling discussed earlier.

It is concluded that in addition to the well defined West Rand and eastern (ERPM) entry points defined by Pretorius, (1987) another major entry point occurs between them in the middle of the Central Rand Goldfield as shown in figure 3.



The study, in line with the objectives of CAMEG, has contributed to the practical training of students, particularly in the fields of data synthesis and interpretation, resource modelling, and evaluation and environmental studies. At the same time, a potentially economic resource worth hundreds of millions of rands has been defined, modeled and evaluated in detail and will be promoted to the mining sector.

REFERENCES

- Pretorius, D.A. 1981: Gold and uranium in quartz pebble conglomerates. Economic Geology 75th anniversary vol., p. 117-138.
- Reinecke, L. 1927. The location of payable ore-bodies in the Gold –Bearing Reefs of the Witwatersrand, Trans. Geol. Soc. A. Afri., 30, 89-120.
- Viljoen, R.P. 1963. Petrographic and Mineragraphic Aspects of the Main Reef and Main Reef Leader of the Main Bird Series, Witwatersrand System unpubl. MSc thesis. Univ. of Witwatersrand. 193 pp.

MINERALIZATION ASSOCIATED WITH IMPACT STRUCTURES, WITH SPECIAL REFERENCE TO THE VREDEFORT-WITWATERSRAND SYSTEM

WOLF UWE REIMOLD

Impact Cratering Research Group, School of Geosciences, University of the Witwatersrand, Private Bag 3, P.O. Wits 2050, Johannesburg, RSA (E-mail: 065wur@cosmos.wits.ac.za)

SYNOPSIS

The terrestrial impact crater record comprises a large number of structures that contain economic ore deposits. Some examples are the iron ore deposits in Ternovka crater (Ukraine), the Ni and PGE deposits of the Sudbury Structure in Canada, and the hydrocarbon deposits around the Avak structure in Alaska. The annual production of hydrocarbons from North American impact craters is estimated at 5 billion \$. In general, progenetic, syngenetic, and epigenetic deposits in impact structures are distinguished. South Africa's Vredefort impact structure, the largest and oldest impact structure known on Earth, encompasses the entire Witwatersrand Basin with its outstanding gold and uranium deposits. The effects of the impact event on these deposits and whether they belong to the progenetic or epigenetic type will be investigated.

Thirty years after the peak of lunar research and as a direct consequence of the space exploration of the second half of the 20th Century, the importance of impact cratering for the evolution of the surfaces of all solid bodies in the Solar System has been generally accepted. The terrestrial impact crater record currently includes some 165 impact structures. It is skewed towards Precambrian terranes in North America, Australia, Scandinavia, Eurasia, and parts of Africa, and is certainly not yet comprehensive. Reasons for this are multifold and include factors such as particular attention to this planetary process in developed countries, accessibility of old strata, vegetation density, and various factors concerning accessibility of terrane for geological analysis. In recent decades, vast progress has been made in the understanding of impact cratering physics, the geology of impact structures, and the role that this fundamental process has played in planetary evolution (e.g., genesis of the Moon; early heavy bombardment of terrestrial planets) and throughout the terrestrial biostratigraphic record. Three basic types of impact structures are distinguished: simple bowl-shaped craters of generally < 4 km diameter, complex craters with central uplifts and complex rim structure, and very large, so-called multi-ring, impact basins.

In contrast to the surface of the Moon, only few truly gigantic impact structures of likely multi-ring basin structure are known on Earth: Chicxulub (Mexico, ca. 200 km diameter, 65 Ma old, and linked to the K/T boundary impact-triggered mass extinction), Sudbury (Canada, 200-250 km, 1850 Ma), and Vredefort (South Africa, 2020±5 Ma). In addition, a few 80-120 km diameter structures could also be multi-ring impact basins, which includes the Popigai structure in Siberia that was recently declared a World Heritage Area and because of its wealth of impact diamonds is known as Russia's Natural Treasury, and the Morokweng structure in North West Province, South Africa, which is 70-80 km in diameter and 145 Ma old (Jurassic/Cretaceous boundary, associated with a minor mass extinction).

A large number of impact structures are associated with large or, at least, significant ore deposits (e.g., Grieve and Masaitis, 1994; Reimold, 1996). It is noteworthy that outstanding deposits are not necessarily related to very large impact structures. For example, many of the relatively small structures in North America are prolific hydrocarbon sources. The three giants of terrestrial impact structures, however, are all associated with enormous ore reserves. Chicxulub was, in fact, discovered as a direct consequence of geophysical exploration for hydrocarbons in the Gulf of Mexico. The Nickel and associated PGE deposits of the Sudbury Structure are legendary, and so are the gold deposits of the Witwatersrand Basin in South Africa, from where at least 45% of

all gold produced in the world originates. The Vredefort impact structure is centered on the Vredefort dome located near the geographical center of the Witwatersrand Basin.

Generally, three types of ore deposits in impact structures are distinguished (Grieve and Masaitis, 1994): progenetic, syngenetic, and epigenetic deposits. Examples of progenetic deposits are the uranium occurrences in the Canadian Carswell structure, iron ore deposits in Ternovka (Krivoi Rog, Ukraine), and the gold and uranium resources in the Witwatersrand basin of South Africa (cf. below). Foremost amongst the syngenetic ore deposits in impact structures must be the resources of the Sudbury Structure that were generated as a direct consequence of the impact event. A prime example for an epigenetic deposit are the hydrothermal Pb-Zn mineralizations of the Boda District, Siljan impact structure, Sweden.

From an ore exploration point of view, are there any direct conclusions that can be drawn from the impact crater-ore deposit record? Clearly, several parameters – not unique to impact cratering but also to volcanic terranes and tectonically active areas – apply:

- ▶ Enormous amounts of kinetic energy are released;
- ▶ thermal energy is produced both during the compression stage and the relaxation phase of the cratering process;
- ▶ impact occurs into all kinds of terranes – basement or supracrustals; however, it is essentially a surface process and where it occurs into sedimentary rocks, vast amounts of fluids may be activated – vaporized or heated;
- ▶ the structure of an impact crater lends itself to the formation of hydrothermal systems – as, e.g., recently demonstrated for the case of the Haughton crater in Arctic Canada;
- ▶ the impact cratering process leaves huge volumes of deformed (fractured, brecciated) rock that provide for excellent conduits and structural traps for ore fluids and subsequent deposition, as well as hydrocarbon repositories.

How do these discussions apply to the Vredefort-Witwatersrand system? An impact origin for the Vredefort Structure had been suspected for many decades, but was only confirmed through diligent studies of the 1990s (see reviews by Reimold and Gibson, 1996; Gibson and Reimold, 2002). The size of the Vredefort impact structure was long thought to be delimited by the size of the Vredefort dome itself (40 km for the crystalline core diameter, 70 km for the entire dome, or 90 km for the dome plus surrounding synclinal structure). The more adventurous proposed 140 km as they observed the concentricity of the Rand Anticline along the northern margin of the structurally preserved Witwatersrand basin. In the late 1990s, several groups presented multiple (shock, geophysical, structural) evidence that strongly favours a 250-300 km diameter. The structure, thus, encompasses the entire extent of the Witwatersrand basin. Post-impact tectonic overprint, especially during the Kibaran, is called upon to explain the NE-SW extended current shape of the basin.

The gold fields of the Witwatersrand basin form the so-called Golden Arc around the Vredefort dome. Already in 1986, McCarthy and co-workers concluded from a regional structural and erosion study that the gold-bearing strata of the basin had been preserved from erosion due to downfolding into the Potchefstroom Synclinorium and because of cover by younger strata in the environs of the dome. What the process was that led to this condition, was not known at the time. When examining the possible impact that the Vredefort event could have had on the Witwatersrand ore resources, a first-order question is that of the timing of gold deposition. This has been the subject of a century-long debate between supporters of the placer, epithermal or modified-placer theories (e.g., Robb and Robb, 1998). However, since the time of the impact event and associated regional deformation (such as occurrences of impact-related pseudotachylitic breccia throughout the Witwatersrand basin; basin-wide deformation overprint on Transvaal strata) has been well constrained at 2023 ± 5 Ma, a time marker with respect to the formation of gold-sulphide mineralization has been provided. Several groups in recent years have made use of this. General findings include that, while there is strong evidence for synsedimentary gold deposition and diagenetic mineralization, most gold reefs show extensive authigenic/hydrothermal mineralization. The timing of this has been strongly debated, with

periods between 2.5 and 2.0 Ga having been proposed by various workers. However, the most detailed studies of recent time have shown evidence for gold mobility during both a pre-impact, peak metamorphic event, and a post-impact, retrograde event. Pseudotachylitic breccia associated with both the Ventersdorp Contact Reef and the Kimberley Reefs crosscut peak-metamorphic assemblages. Assemblages of alteration minerals after pseudotachylitic breccia matrix occur paragenetically with gold. Some workers have related the peak metamorphic, pre-impact event to the emplacement of the Bushveld Complex at 2.06 Ga, whereas the later retrograde event has been associated with the Vredefort impact and impact-triggered processes. Against this scenario, the Witwatersrand ores must be classified as progenetic ore in the Vredefort-Witwatersrand impact structure, with local evidence of epigenetic processes that had both pre-impact and impact-related causes.

The extent to which the Vredefort impact event affected the whole region of the Witwatersrand basin, both structurally as well as thermally/hydrothermally, must still be modelled in detail. However, the acceptance of an impact event at 2.02 Ga and of regional importance provides new impetus and strategies for future Witwatersrand studies.

REFERENCES

- Gibson & Reimold, 2002, The Vredefort impact structure, South Africa, Council for Geoscience, Pretoria, Memoir 92.
Grieve & Masaitis, 1994, Int. Geol. Rev. 36, 105-151.
McCarthy et al., 1986, Trans. Geol. Soc. S. Afr. 89, 311-324.
Reimold, 1996, The Earth, Moon and Planets 70, 21-45.
Reimold & Gibson, 1996, J. Afr. Earth Sci. 23, 125-162.
Robb & Robb, 1998, The Mineral Resources of South Africa, Council for Geoscience, Pretoria, pp.294-349.

ENVIRONMENTAL ASPECTS ASSOCIATED WITH THE PAST, PRESENT AND FUTURE MINING OF THE CENTRAL RAND

N.F. MPHEPHU and M.J. VILJOEN

Centre for Applied Mining and Exploration Geology; School of Geoscience

University of the Witwatersrand; P/Bag X3; WITS; 2050 Tel: (011) 717-6571

Fax: (011) 339-1697.

e-mail: 065dweli@cosmos.wits.ac.za

SYNOPSIS

Since the discovery of gold in the Central Rand in 1886, up to and including the present, mining activities has been the backbone of economic development in the Johannesburg area. This has happened in stages, from earlier underground mining, present reclamation of gold-bearing mine tailings to the potential future mining of remaining deep and shallow gold resources. These activities have impacted and will continue to impact on the environment on the Central Rand. This paper evaluates environmental impacts of these stages of mining on the Central Rand.

INTRODUCTION

The discovery of gold in the Central Rand south of Johannesburg led to the economic development of South Africa. The Central Rand also served as a nucleus for mining expansion to the East and West Rands. As the Central Rand is where mining first took place in the Witwatersrand basin, this also led to these mines closing earlier (in the mid-seventies) than mines on the East and West Rands.

Mining started with underground mining and this continued to a depth approaching 3000m. From the 1980's until now, the ongoing mining activity has been the reclamation of gold-bearing mine tailings. The recent documentation by a team from the Centre for Applied Mining and Exploration Geology (CAMEG) of a remaining shallow gold resources has led to new mining opportunities using opencast and selective underground mining methods.

All of the mining activities have had impacts on the environment both positive and negative. This paper documents and evaluates the existing as well as the envisaged future impacts of these mining activities.

RESULTS AND DISCUSSION

Study area

The study was based on the mines "3C's", of the Central Rand viz Consolidated Main Reef (CMR), Crown Mines and City Deep. The Central Rand forms part of the northern fringe of the Witwatersrand basin, and is bounded on the east by East Rand and on the West by West Rand. Geologically, the lowermost West Rand Group overlies granitoid rocks with greenstone schists. The overlying Central Group consists of Johannesburg Subgroup at the base, overlain by the Turffontein Subgroup, the contact marked roughly by the position of the Kimberley Reef (Figure 1). The Central Rand Group consists predominately of coarse-grained subgreywacke with minor conglomerate, quartz arenite. Most of the economic reef horizons in the Witwatersrand basin are present in this succession (Robb et al., 1995).

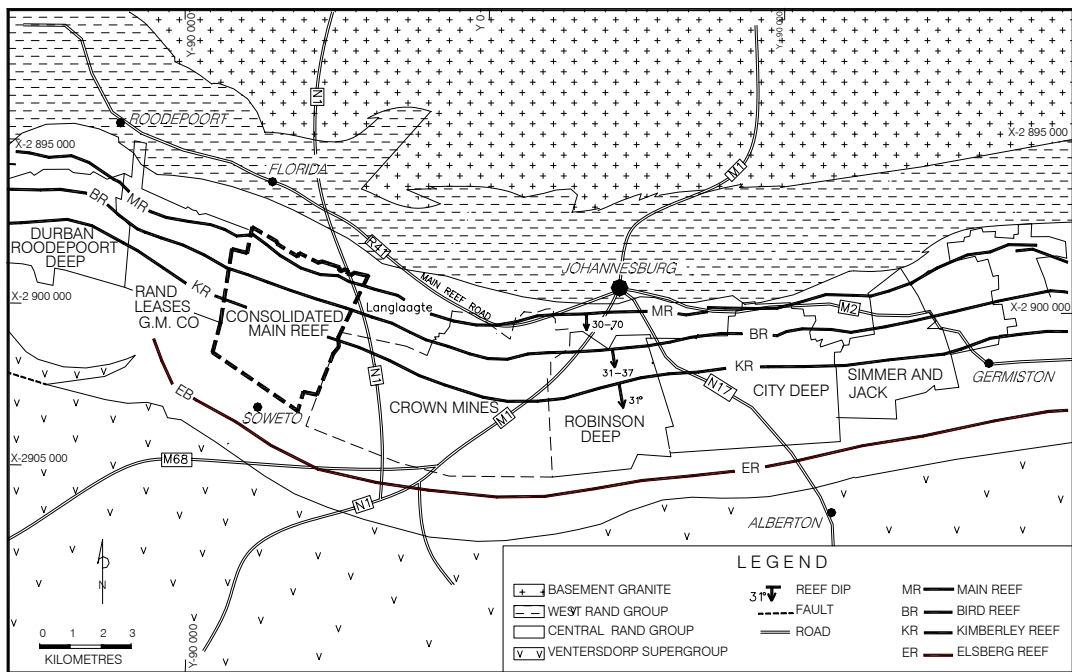


Figure 1. Central Rand goldfield, geology and mining leases

Past underground mining activities

Since its discovery in 1886, the Witwatersrand basin has produced nearly 48,000 tons of gold. There is, however, a legacy of various environmental problems. The major impacts include air (dust) pollution, surface and groundwater pollution and the limitation on land use potential. The major impacts are mainly due to the establishment of mine tailings dams and the presence of shallow underground stopes. When mining activities ceased in the mid-seventies there was little environmental legislation in place, and any limited rehabilitation was not properly done. The impacts also led to the moral degradation of people living close to the area. This has led to an ongoing court case between interested and affected parties and the Department of Environmental Affairs and Tourism, Department of Minerals and Energy Affairs and mining companies. There was an attempt during early years to revegetate the mine dumps, initiated by Chamber of Mines, and this proved successful in preventing pollution from mine dumps.

Reclamation of mine tailings

Since the 1980's mine tailings on the Central Rand have been removed as part of the process of reclaiming remaining gold. This can be attributed to the improvement in extraction technology. Crown Gold Recovery Pty (Ltd.) are reclaiming the gold bearing mine tailings, many of which have values of 0.5 to 0.7 g/t of gold. The reclamation process has exposed dump material to wind and water erosion, which has led to dust and water pollution. After the mine tailings have been reclaimed, the tailings footprints need to be rehabilitated and prepared for further land use development. In the interim, paddocks are laid out on the surface to prevent possible polluted water runoff. The reclamation process has exposed land available for development in areas where there are no shallow workings or radioactive contaminated soil under permissible standards.

Future mining activities

Gold resource evaluation done by CAMEG has established the presence of a substantial gold resource which can be mined by opencast and near surface underground mining of ore shoots which have been defined (Mphephu et al., 2001). These mining activities will serve as a trigger for

mining and land development at a later stage. These potential mining activities will have to take into consideration the environmental and social concerns of nearby residential and industrial areas from the commencement of operations. Appropriated geotechnical engineering will be required to prepare land for future land use opportunities.

CONCLUSION

The legacy of the old underground mining activities has led the degradation and pollution of the environment on the old mining base areas of the Central Rand. However reclamation of mine tailings and mining of remaining resources could bring positive spin-offs for the Central Rand. These include elimination of mine tailings, stabilization of shallow undermined ground, creation of jobs and rehabilitation of land for further innovative land use options.

REFERENCES

- Legal Resources Centre, 2000. *Environmental problems caused by various gold mine tailings dams and sand dumps in the Greater Johannesburg area*. Unpublished letter to the Department of Environmental Affairs and Tourism and Department of Minerals and Energy. Pretoria
- Mphephu, N.F. and M.J. Viljoen (2001). *Gold resource re-evaluation and environmental issues associated with the Central Rand goldfield; Johannesburg; South Africa*. Proceedings of the Conference on Environmentally Responsible Mining in Southern Africa. Muldersdrift, Johannesburg, South Africa, 25 - 28 September 2001, pp. 6c-1-6c-11.
- Scott, R. (1995). *Flooding of Central and East Rand goldmines: An investigation into Controls over the inflow rate, water quality and the predicted impacts of flooded Mines*. Water Research Commission, No. 224/1/72.
- Robb, L.J & Meyer, F.M. (1995). *The Witwatersrand Basin, South Africa: Geological framework and mineralization processes*. Ore Geol.Reviews, **10**, 67-94.

6. OTHER MINERALIZATION

GEOLOGY OF THE “ROUND MOUNTAIN” GOLD MINE IN NEVADA, UNITED STATES OF AMERICA, AND POTENTIAL FOR EXPLORATION OF SIMILAR DEPOSITS IN THE ANDES

ALBERTO LOBO-GUERRERO

Economic Geology Research Institute, University of the Witwatersrand,
Private Bag 3, Johannesburg, 2050, South Africa
e-mail: ageo@iname.com

SYNOPSIS

Round Mountain is one of the world's largest volcanic rock-hosted gold deposits, of the disseminated, low-sulfidation epithermal type. This article offers a brief version of the mine's more relevant issues and some comments on the exploration of similar deposits in the Andean Cordillera. *Round Mountain's* reserves amount to more than 500 tons of metallic gold. Permeable pyroclastics bound by impermeable rocks host mineralization and alteration. Mineralizing fluids migrated along concentric and radial fractures related to a caldera. Mineralization and alteration processes took significantly less than 500,000 years. Case studies in Quaternary to upper Tertiary volcanic edifices n the Colombian, Ecuadorian and Peruvian Andes contain disseminated gold mineralization in porous-permeable pyroclasts bound by impermeable lavas and/or welded tuffs.

Round Mountain is one of the world's largest volcanic rock-hosted gold deposits. It is located in the Basin and Range geological province of the south-western United States of America, between the towns of Tonopah and Austin, Nevada. Some authors consider the mine to be a typical epithermal low sulfidation deposit. It has been mined since 1905, and its reserves amount to more than 500 tons of metallic gold.

Gold content at this deposit is in the order of ten parts per billion, and the lowest economic concentration is 0.2799 gAu/ton. Miocene, porous and permeable tuffs (aquifers) bounded by impermeable welded tuffs and crystalline basement (aquitards) host mineralization. Concentric fractures related to caldera margins and radial fractures of the same caldera served as routes for mineralized fluid flow; hydrothermal alteration and mineralization extends outward from these thin mineralized fractures along the porous, permeable tuffs limited by impermeable units in a “sandwich” fasion (Figs. 1, 2). Fig. 3 presents a typical low-sulfidation epithermal gold deposit model; note the way in which mineralization and alteration extend along favorable, permeable layers to produce disseminated precious metal concentration. Round Mountain is one of the best examples of this type of mineralization.

Alteration types are propylitic, phyllitic, silicification and argillization, and there is no direct relationship between ore grade and alteration. Based on radiometric dating, all mineralization and alteration at *Round Mountain* lasted between 50,000 and 500,000 years; it is thought to have taken considerably less than 500,000 years to form (HENRY et al [1997]). Establishing average gold grade in this type of deposits requires detailed studies, since grade may vary up to four orders of magnitude within 10 centimeters. Occasional gold nuggets (some of which weigh over one pound) are found along intersection of main fractures and are sought with metal detectors.

The mine uses novel, re-usable heap leaching pads.

Colombia, Ecuador and Perú have a reasonable potential for gold deposits hosted in volcanic strata such as those present at *Round Mountain*. Repetitive explosive composite volcanic activity

in southern Colombia has exposed numerous mineralized tuffs and ash layers. Galeras Volcano, one of the best studied in the region, expels 0.5 kg of gold per day to the atmosphere in its fumaroles, and is probably depositing more than 0.06 kg Au/day in the volcanic edifice (GOFF et al [1994]). If such rates remain constant, a moderately sized gold deposit (more than 200 tons of contained gold) may form in only 10,000 years. If an equivalent amount is left behind in porous volcanic rocks, a short lapse of hydrothermal activity may produce deposits such as *Round Mountain*. These observations do not take into account moments of great activity and explosive vulcanism, when fumarolic activity increases and several type of hydrothermal breccia are formed.

Nevado del Ruiz, in the axis of the Colombian Central Cordillera, is another Quaternary volcanic system studied by the author. It contains important epithermal gold dissemination associated with tuff layers limited by andesite lava aquiclude. Mineralization is conditioned to more than eight porous, permeable, pumice-rich pyroclastic layers. The system is of the high sulfidation type, since alunite conforms a large portion of the matrix in breccias and mineralized tuffs.

Ecuador also has numerous recent volcanic edifices, that are well exposed by lateral explosions. Several volcanoes in the Interandean Graben, such as Hilaló and Guagua-Pichincha are open to the west due to preferential collapse of volcanic edifices in that direction, where unidirectional wind regimes tend to erode away the ash and other components. Cerro Bravo and Nevado del Ruiz volcanoes in Colombia display clear evidence of lateral explosions.

Large extensions of Eocene to Oligocene volcanic rocks outcrop in the Peruvian Andes. They are older, display more erosion than their counterpart in the Northern Andes, and in some cases offer ideal conditions for entrapment of precious metals in *Round Mountain* style. Numerous high explosivity rhyolitic events, intercalated with pyroclastic, cineritic and welded tuff events produced monotonous sequences of porous and non-porous volcanic rocks.

REFERENCES

- EKSTROM, R [1999] "Geology of the *Round Mountain* Mine", presentation at the mine site during technical visit of Queen's University M.Sc. Program in Mineral Exploration, May 5th.
- GERIKE, GN [1997] *Stable Isotope Systematics of Hydrothermal and Oxidation Minerals at Round Mountain, Nevada; Conditions of Gold Deposition and Remobilization*, M.Sc. thesis, Southern Illinois University, Carbondale, Illinois, 109 p.
- GOFF, F, STIMAC, A, LAROCQUE, CL, HULEN, JB, McMURTRY, GM, ADAMS, AJ, ROLDAN M, A, TRUJILLO, PE, COUNCE, D, CHIPERA, SJ, MANN, D & HEIZLER, M [1994] "Gold Degassing and Deposition at Galeras Volcano, Colombia", *GSA Today*, Geological Society of America, v. 4 No. 10, pp. 241-247.
- HAYBA, DO, FOLEY, NK & HEALD-WETLAUFER, P [1986] "Characteristics that Distinguish Types of Epithermal Deposits", en Conference on Volcanic-Hosted Precious Metals, *Journal of Geochemical Exploration*, 25, pp. 231-260.
- HEDENQUIST, JW, ARRIBAS, A & GONZALEZ-URIEN, E [2000] "Exploration for Epithermal Gold Deposits", *Society of Economic Geologists Reviews*, 13, 245-277.
- HEDENQUIST, JW, IZAWA, E, ARRIBAS, A & WHITE, NC [1996] *Epithermal Gold Deposits: Styles, Characteristics and Exploration*, Resource Geology Special Publication No. 1, Society of Resource Geology, Tokio, 18 p + poster.
- HENLEY, RW [1991] "Epithermal Deposition of Gold During Transition from Propylitic to Potassic Alteration at *Round Mountain*, Nevada – A Discussion", *Economic Geology*, 86, 892-894.

HENRY, CD, ELSON, HB, McINTOSH,WC, HEIZLER,MT & CASTOR,SB [1997] "Brief Duration of Hydrothermal Activity at *Round Mountain*, Nevada, Determined from $^{40}\text{Ar}/^{39}\text{Ar}$ Geochronology", *Economic Geology*, 92, 802-826.

LOBO-GUERRERO, A [2001] "Geología de la Mina de Oro "*Round Mountain*" en Nevada, Estados Unidos de América y Potencial de Exploración de Yacimientos Similares en los Andes", *Boletín de la Sociedad Geológica del Perú*, 92, 43-56.

MILLS, BA, BODEN DR & SANDER MV [1988] "Alteration and Precious Metal Mineralization Associated with the Toquima Caldera Complex, Nye County, Nevada", en Schafer, RW, Cooper, JJ & Vikre, PG (eds.) *Bulk Mineable Precious Metal Deposits of the Western United States*, Symposium Proceedings, Geological Society of Nevada, Reno, Nevada, pp. 303-331.

ROBERT, F, POULSEN, KH & DUBE, B [1997] "Gold Deposits and Their Geological Classification", article 29 in Gubins, AG, (ed.) *Proceedings of Exploration 97: Fourth Decennial International Conference on Mineral Exploration*, pp. 209-220.

ROUND MOUNTAIN GOLD CORPORATION [1999] *Round Mountain Gold – An Introduction for Visitors*, revised in March 1999, photocopies, 38 p.

SANDER MV [1988] "Geologic Setting and the Relation of Epithermal Gold-Silver Mineralization to Wall Rock Alteration at the *Round Mountain* Mine, Nye County, Nevada", in Schafer, RW, Cooper, JJ & Vikre, PG (eds.) *Bulk Mineable Precious Metal Deposits of the Western United States*, Symposium Proceedings, Geological Society of Nevada, Reno, Nevada, pp. 375-416.

SANDER, MV & EINAUDI, MT [1990] "Epithermal Deposition of Gold During Transition from Propylitic to Potassic Alteration at *Round Mountain*, Nevada", *Economic Geology*, 85, 285-311.

SANDER, MV & EINAUDI, MT [1991] "Epithermal Deposition of Gold During Transition from Propylitic to Potassic Alteration at *Round Mountain*, Nevada – A Reply", *Economic Geology*, 86, 894-897.

SHAWE, DR [1988] "Complex History of Precious Metal Deposits, Southern Toquima Range, Nevada", in Schafer, RW, Cooper, JJ & Vikre, PG (eds.) *Bulk Mineable Precious Metal Deposits of the Western United States*, Symposium Proceedings, Geological Society of Nevada, Reno, Nevada, pp. 333-373.

SHAWE, DR, MARVIN, RF, ANDRIESSEN, PAM, MEHNERT, HH & MERRITT, VM [1986] "Ages of Igneous and Hydrothermal Events in the *Round Mountain* and Manhattan Gold Districts, Nye County, Nevada", *Economic Geology*, 81, 388-407.

SILLITOE, RH [1993] "Epithermal Models: Genetic Types, Geometrical Controls and Shallow Features", in Kirkham, RV, Sinclair, WD, Thorpe, RI & Duke, JM, eds. *Mineral Deposit Modelling*, Geological Association of Canada, Special Paper 40, pp. 403-417.

SILLITOE, RH [1997] "Characteristics and Controls of the Largest Porphyry Copper-Gold and Epithermal Gold Deposits in the Circum-Pacific Region", *Australian Journal of Earth Sciences*, 44, pp. 373-388.

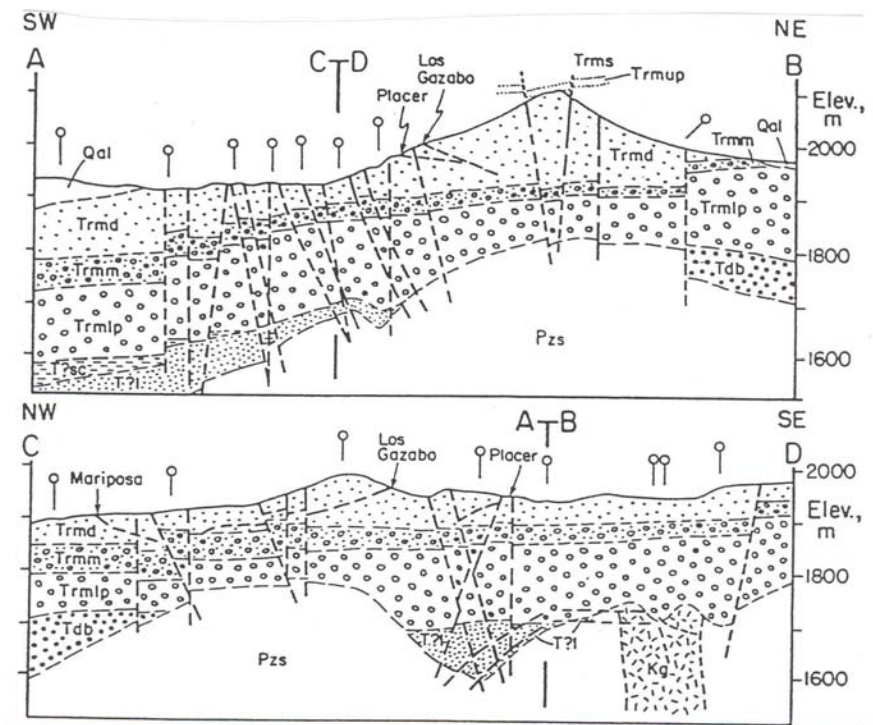


Fig. 1 Cross sections through the *Round Mountain* deposit.

Trmlp is a non-welded tuff limited by welded tuffs above and impermeable crystalline basement below. It hosts a large portion of the mine's ore. Thin fractures served as feeders for mineralization that spread out along permeable beds. (From SANDER et al [1990])

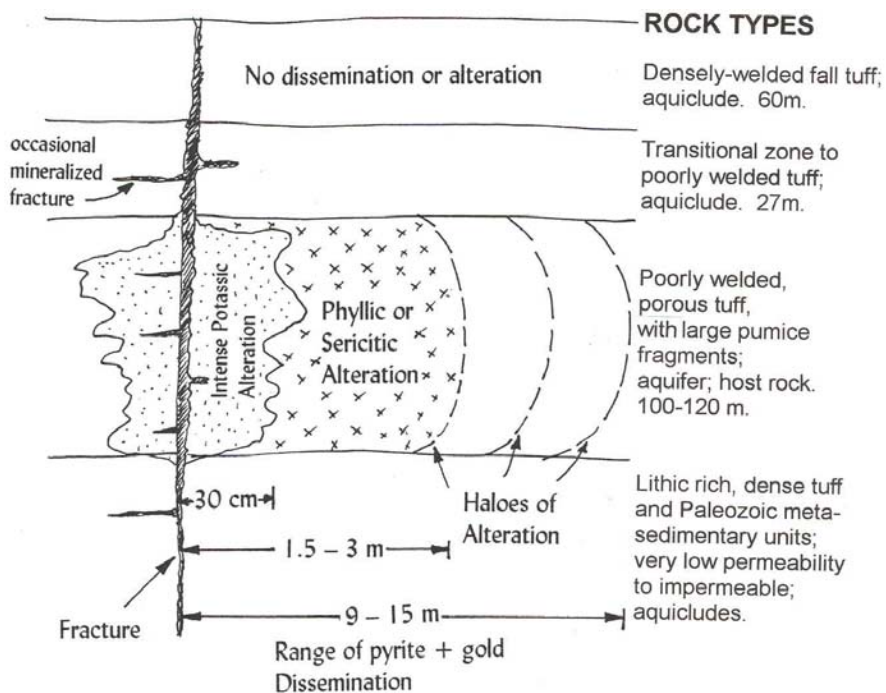


Fig. 2 Ranges of alteration in different types of rock at the *Round Mountain* mine.

Hydrothermal fluids migrated along thin fractures and away from them along permeable tuffs to produce alteration and gold dissemination. Pyrite and precious metals mineralization is found up to fifteen meters away from individual fractures. Note that Trmlp from Fig.1 is the poorly welded porous tuff. (LOBO-GUERRERO [2001])

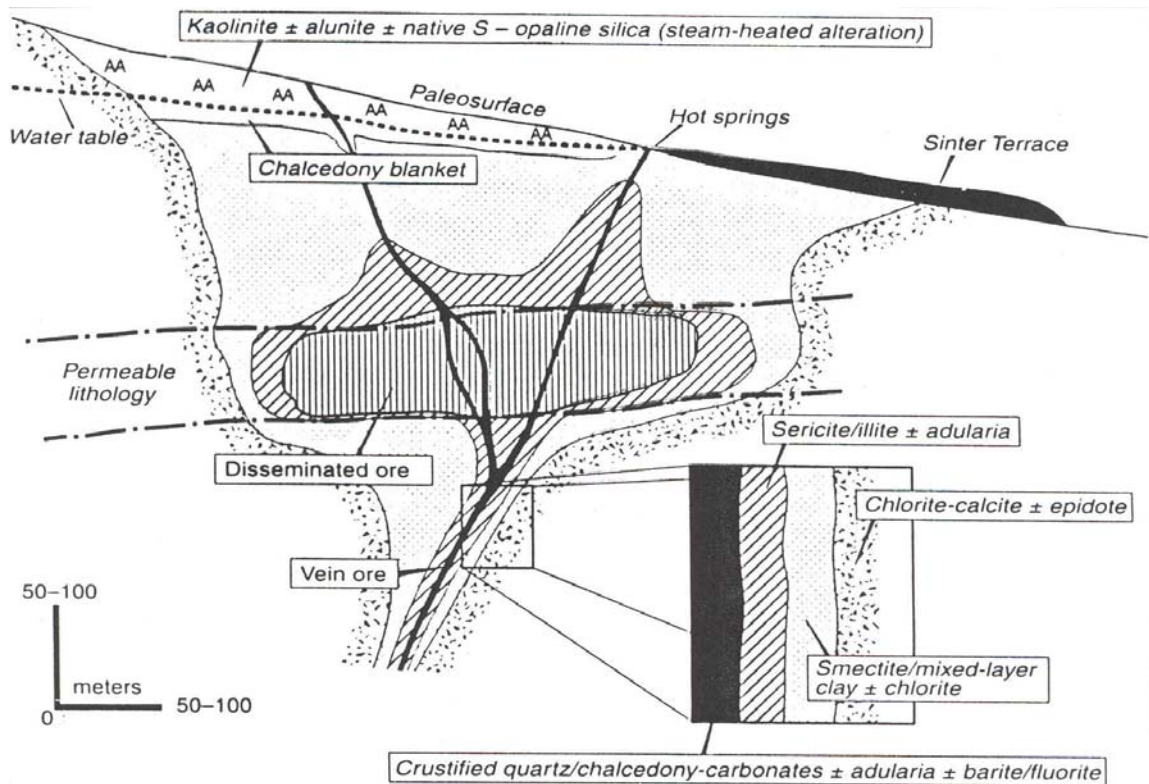


Fig. 3 Generalized schematic section of alteration patterns in a low-sulfidation epithermal system. Note widening of alteration and mineralization that takes place along favorable host rock lithology. The *Round Mountain* case is one of the best examples of this feature. The section shows variations along depth, typical hydrothermal alteration including distribution of sinter, advanced argillic alteration (AA), alteration produced by hot springs, and silicification associated with water table. Geological variations in specific deposits offer multiple deviations from this model. (Modified from HEDENQUIST et al [2000])

GEMSTONES OF SOMALILAND: SUSTAINABLE DEVELOPMENT OF THE SMALL-SCALE MINING SECTOR

JUDITH A. KINNAIRD

Department of Geology, University of Witwatersrand, Private Bag 3, Wits 2050, South Africa

SYNOPSIS

Gem-quality minerals such as emerald, aquamarine, ruby, sapphire, opal, garnet and amethyst have been produced in Somaliland for almost a decade. Emerald and aquamarine are derived from pegmatitic host rocks that are related to late granite intrusions in the Mozambique orogenic belt. Emeralds occur in pegmatites which crosscut biotite and amphibole schists, whereas aquamarines are more common in pegmatites hosted by migmatites and granite gneisses. Hessonite garnets originate from calc-silicates whereas opals occur in Miocene volcanics in the west of the country. Most gemstones are being extracted from solid unweathered rock and recovery methods are unsophisticated. However, the development of a small-scale mining sector is of major economic significance in rural areas. The importance of gems in the Mozambique orogenic belt has previously been noted within Kenya, Tanzania, Sri Lanka, India and Madagascar. The recognition of the Mozambique belt into Somaliland is therefore of considerable interest as it means there is a potential for the production of a wide-range of gemstones, although the gem producing potential has not been fully assessed. Sustainable development of natural resources is being investigated and the gemmological potential of Somaliland may provide important for income generation in this country where many will earn <US \$20 per month.

INTRODUCTION

The discovery of gemstones in Somaliland and their subsequent recovery began in 1990. It is surprising, considering the widespread distribution and range of gemstones, that they were not noted during field mapping undertaken by the Geological Survey Department during colonial rule. Sustainable development of natural resources is being investigated and the gemmological potential of Somaliland may provide an important income generation in this country where many currently earn <US \$20 per month.

BACKGROUND

Somaliland gained independence from Britain in 1960, and joined with the former Italian protectorate to the south to form the new State of Somalia, but civil war between the two factions soon followed. In 1991 NW Somalia declared independence from southern Somalia and restored the old colonial name of Somaliland. Although in the last 10 years there have been local disputes and occasional upsurges in clan-related violence, the country is now quite stable. However the economy is only now recovering from the debilitating effects of the civil war and the dissipation of a widely scattered population that fled to Canada, USA, Scandinavia, UK and elsewhere in Europe. Many expatriate Somalis have gained a good education in these countries and are now returning home with entrepreneurial skills and a keenness to invest foreign income and set up businesses.

The prolonged war has left the Somaliland infrastructure including health, education, communications, banking, and industry in disarray. However, because of the unilateral declaration of independence, Somaliland is not recognised as a separate country and suffers from a substantial lack of foreign aid, although a number of non Governmental Organisations are providing support. In the early 90's, the European Union (EU) initiated several small-scale projects that could provide employment and empowerment to communities, which included supporting a henna industry and increasing frankincense production. During these early project developments, several gemstones were brought to the EU office, including sapphire and emerald, which prompted an investigation, funded by the EU to assess, whether there were gemstone deposits in Somaliland with a potential for development.

GEMSTONE POTENTIAL OF SOMALILAND

An EU-funded, initial assessment of gemstone prospects proved that there were substantial emerald and aquamarine-bearing pegmatites related to late granite intrusions in the Mozambique orogenic belt (Kinnaird and Jackson, 2000). These pegmatites occur in two sectors in an east-west zone. In the western sector, emeralds occur in pegmatites that cross-cut biotite and amphibole schists in a zone that

is approximately 30 km wide x 100 km long, and which extends from Bawn to northwest of Hargeisa. The eastern sector which lies between Hargeisa and Berbera, and is approximately 30 km wide and 50 km long, produces mainly aquamarines from pegmatites hosted by migmatites and granite gneisses. However, a variety of gem minerals were produced by various traders including amethyst, garnet in a wide range of colours, corundum varieties and opal generally from white through cream to orange and brown in colour. However it was very clear that there was a poor understanding of the characteristics of gemstones and identification of minerals was also poor, so that reported 'tanzanite', was either purple fluorite or lilac vesuvianite, some emerald was quartz coloured green by secondary copper minerals, reported green tourmaline was frequently epidote, diopside or peridot. There is also a widespread belief that there is an abundance of diamonds in the country, based on the mis-identification of quartz infilling small cavities in rocks.

ARTISANAL MINING

Emeralds and aquamarines were being extracted from hard unweathered pegmatites, often with primitive tools (Fig. 1). In each of the two producing areas, particularly Aliheley, there is a plethora of pits on the hillsides dotted over several kilometres. Mining of emeralds in particular proceeds in a disorganised way following irregular thin fingers of aplite or pegmatite into the softer schists. Pits are developed along the strike of the pegmatitic body and the close proximity of pits may cause waste material from one to fall into an adjacent producing pit. Slopes are usually unstable, and coupled with occurrence of minor earth tremors at regular intervals, there is a significant safety hazard. There is no history of mining in Somaliland so there is an absence of inherited wisdom about production and safe procedures.

TRAINING AND DEVELOPMENT

The positive assessment of gem deposits in Somaliland prompted the EU to invest in training courses for groups of miners. Suitable participants were selected from different areas where gem minerals were being produced, for an intensive week-long training course, which included not only mineral identification techniques, but also basic geological skills, safe mining practises and general basic safety considerations and first aid. Each participant was given a hammer, chisel, gloves and hardness testing kit, together with some simple optical equipment, to assist them with mineral identification and safer gem production.

On-site visits were made to provide advice on various aspects of gem production. The positive result of these efforts is that attention has now been drawn to the gemstone sector and investment is beginning in one of the two main emerald producing areas. The most encouraging aspect is the much of this investment is coming from Somalis, either businessmen in established sectors within the country or from Somali expatriates around the world.

There have been considerable technical and financial constraints, but new localities for emeralds are still being found, and development is still at a fairly rudimentary stage. It is likely however that the production will remain artisanal and sustainable for many decades. These projects will bring income and stability to a rural area where the agrarian economy is dependent on sheep and goats. The next phase will be to establish recognised formal routes to international markets that will produce an income for government from gem sales, as well as finance further development and support the miners continuing developments. Inter-clan rivalries, suspicion of government, general gemstone smuggling across borders, and unwillingness to pay for prospecting and exporting licences combine to make the creation of a Gem Bourse a difficult task. More training is also needed in mining procedures, and on minimising risk and recording production.

FUTURE POTENTIAL

Since the initial discoveries of gemstones a decade ago, the variety of gem quality minerals has broadened considerably. In addition to expansion of the emerald-producing sector (Fig. 2.), other minerals deserve increased attention. Only recently has the quality of hessonite garnets from calc-silicates of the Mora Complex been appreciated. These calc-silicates which are widely distributed, although individually quite small in size, are host to orange coloured hessonite that may occur in monomineralic patches up to 1 m across accompanied by coarse vesuvianite, diopside, calcite and epidote (Fig. 3). The hessonite, which produces excellent faceted stones, is currently collected only from the surface. Green grossular garnets (tsavorite) also occur, but so far crystals are <4 mm in size. Other garnets of pyrope-almandine composition are also widespread but of a different paragenesis.

Opals may also have an exciting future. These occur as nodules in Miocene rhyolitic horizons close to the

border with Ethiopia. The opals are found as nodules ranging from 1 - 5 cm in size and range in colour from white to yellow, orange, red or chocolate brown and may be transparent to translucent. Orange-coloured fire opal show a little colour play but it is the chocolate brown material that displays the most striking play of colours, with intense flashes of red and green and more rarely, royal blue (Fig. 4). Tens of kilos of rough nodules have been examined, less than half of is of gem quality and only around 5% has a good play of colours. Stability of this brown gem material is good, and water content of one precious brown opal is 5%. What make the Somaliland gem opals of such interest are the size, unusual colour and availability of the gem material. The nodular form of the chocolate-brown gem opals means that when nodules with a good play of colours are found, large cabochons can be cut. Again current production is of nodules collected from the surface rather than from any production pits.

CONCLUSIONS

The gem deposits of the Mozambique belt in Kenya and Tanzania have been well documented by Keller (1992). Malisa and Muhongo (1990) have noted the extent of the Mozambique belt in eastern Gondwana and highlight the gem occurrences within Sri Lanka, India, and Madagascar. The recognition of the extension of the Mozambique belt into Somaliland is therefore of considerable interest as it means that there is a potential for the production of a wide range of gemstones. This has important implications for the Somaliland economy. The positive contribution of academic geologists in deposit evaluation, basic mineralogical education and advice has provided much-needed impetus and encouragement to the gemmological industry of Somaliland. So much attention is usually given to large ore deposits, however in terms of the beneficial effect to local economies of small-scale developments such as these, perhaps more attention should be paid to small ore deposits.

REFERENCES

- Keller, P.C. 1992. Gemstones of East Africa. Geoscience Press, Phoenix, Arizona. 144pp
Kinnaird, J.A. and Jackson, B. 2000. Somaliland - a potential gem producer in the Mozambique belt. *J. Gemm.* **27**: 3, 139-154.
Kinnaird, J.A. 2002. Chocolate-brown opals associated with volcanic rocks in Somaliland. *J. Gemm.* **28**, 2, 81-84.
Malisa, E and Muhongo, S. 1990. Tectonic setting of gemstone mineralisation in the Proterozoic metamorphic terrain of the Mozambique belt in Tanzania. *Precambrian Research*, **46**, 167-176

Figures:

Fig. 1 Artisanal workers extracting emeralds from pits in the Simodi area.

Fig. 2 Emerald crystal from the Alaak area, 3-4 mm across.

Fig. 3 Monomineralic patch of hessonite (grossular) garnet with associated vesuvianite from north of Hargeisa.



Fig. 4. Chocolate opal from Somaliland showing play of red, blue and green. This opal is 65 carats in weight and over 5 mm in thickness.

PLATINUM-GROUP MINERALOGY IN THE KATINNIQ AND ZONE 2 OREBODIES, RAGLAN NI-CU-(PGE) SULPHIDE DEPOSIT, CAPE SMITH, CANADA.

CHARLIE L. SEABROOK

Department of Geology, University of the Witwatersrand, PO Wits 2050, South Africa

HAZEL M. PRICHARD and P. C. FISHER

Department of Earth Sciences, University of Cardiff, P.O. Box 914, CF10 3YE, Wales, UK

SYNOPSIS

At least ten different platinum-group minerals (PGM) have been located and identified in samples from the Katinniq and Zone 2 ore bodies in the Raglan deposit. The most abundant PGM is sudburyite, (in terms of grain counts) comprising a third of all PGM located in both the Zone 2 and Katinniq ore. Overall, sperrylite and merenskyite make up the majority of the remaining PGM with michenerite, moncheite, temagamite and two unnamed minerals ($\text{PdPb}(\text{TeBi})_3$ and $(\text{Rh,Pt})(\text{Fe,Ni})\text{AsS}$) as single occurrences. In addition, palladium was found in solid solution within niccolite. The majority of PGM are associated with the sulphide minerals, in particular, chalcopyrite, either completely enclosed within sulphides, or at a sulphide/silicate boundary. However, remarkable amounts of PGM are associated with carbonates, particularly within Zone 2. These relationships suggest that PGM formation is the result of a polyphase process, with PGE fractionating into, and crystallizing from a Cu-rich, late-magmatic immiscible liquid. Later alteration and transport of PGE (mainly Pd) occurred in low temperature aqueous solutions with subsequent redeposition of PGM occurring in fluid flow pathways such as secondary veins and shear zones. Pd also entered niccolite during this late stage mobilization.

REGIONAL GEOLOGY

The Raglan Ni-Cu-(PGE) sulphide deposit is located in the New Quebec region of northern Canada, on the Ungava Peninsula. Twenty distinct mineralized regions, each comprising a number of ore lenses, lie within metamorphosed subvolcanic sills or intrusive-extrusive komatiitic to tholeiitic basalts of the Cape Smith Belt. This is a Proterozoic thrust belt that was preserved as part of the foreland thrust belt to the Ungava Orogen. The Raglan Formation that hosts the orebodies lies at the boundary between the Povungnituk and the Chukotat Groups, which comprises a series of thick ultramafic complexes (Lesher 1999).

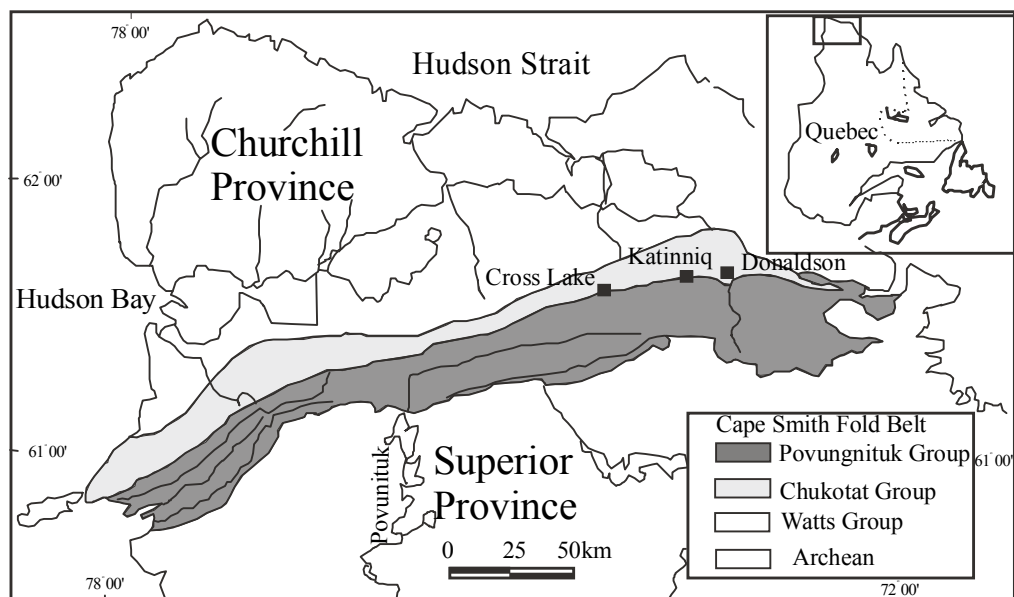


Figure 1. Geological map of the Cape Smith Belt, New Quebec, Canada

Nine peridotitic flow bodies containing economically significant mineralization occur over a distance of 55 kilometers and are generally situated in footwall embayments (channels and troughs) at the base of the flow units. PGE in the Raglan area were studied by Dillon-Leitch *et al.* (1986). They described PGE distribution as well as Cu, Ni and associated Au, Ag, Te, Sb, Bi, Co and As minerals from the Donaldson West deposit (figure 1). Recovery optimization of PGM prompted a mineralogical study within the Raglan ore bodies to the west. This study focuses on the Katinniq (underground) and Zone 2 (open pit) ore bodies, from where hand specimens were taken from massive, net-textured, reverse net-textured and chalcopyrite vein ores. PGM were located using an SEM and some of the larger ones were quantitatively analyzed using Oxford Instruments AN10000 EDX analyser attached to the SEM.

THE KATINNIQ AND ZONE 2 ORE LENSES

The Katinniq deposit consists of over 20 discrete lenses that vary in size from 10,000 tonnes to 1.4 million tonnes.. The lenses extend along 1,400 meters of strike length and dip to the northwest at 45°-50°.The Katinniq and Zone 2 bodies display a series of lithologies, distinguished by a range of sulphidic textures created as the result of magmatic segregation. Massive ores typically comprise pyrrhotite and pentlandite with some chalcopyrite, magnetite and minor PGM and occur at the base of footwall embayments. These horizons typically vary in thickness between 30cm and 10m. Overlying net-textured ore comprises some 40-70% sulphide (pentlandite, pyrrhotite and chalcopyrite), occurring between olivine pseudomorphs and partially or completely enclosing them. Reverse net-texture may be present above the net-textured horizons and has been interpreted as a secondary metamorphic texture (Gillies 1993). Disseminated ore is found above the net-textured ores and typically comprises 2-15% sulphides, occurring as lobate, fine-grained (0.1-0.3mm) pentlandite and pyrrhotite located between olivine oikocrysts. In addition, chalcopyrite-rich veinlets occur parallel to layering, Cu-rich massive sulphide veins and remobilized stringers are present below the basal massive sulphide within the Katinniq gabbro footwall. The veins occur as cusps or notches, sometimes perpendicular to the basal massive sulphide contact and sometimes elongated parallel to a fault and can be several meters in length and up to 1m wide. Veins comprise zones of sulphides, with chlorite and carbonates. Nickel arsenide (niccolite) is also a common feature in the Katinniq vein samples, as well as minor cobaltite, galena and lead and silver tellurides.

PGM MINERALOGY

Sperrylite is the dominant phase in terms of grain size, yielding some of the largest PGM grains – up to 40 microns. These crystals are enclosed by a variety of host minerals and occur in Cu-rich veins and massive sulphide ores. Sperrylite that occurs in vein samples is euhedral, cubic and associated with chalcopyrite, whereas grains found in massive ores are associated with pyrrhotite, occurring in small groups of up to five grains, isolated within an olivine- sulphide matrix. Rarely, sperrylite is seen to cross-cut pyrrhotite and frequently cross-cuts altered olivine. Sudburyite occurs in vein and net-textured ores. Vein ore grains are irregular, anhedral and occur at the boundary between olivine and pyrrhotite. Vein sudburyite is also strongly associated with niccolite. The niccolite-bearing ores display high average abundances of PGM and SEM probe analysis of the niccolite shows that it consistently contains up to 1% Pd in solid solution. Pentlandite contains no detectable Pd. Sudburyite grains also occur at the boundary between olivine and pyrrhotite in net-textured ore. These grains are highly irregular in shape and show evidence of alteration by a secondary silicate phase, possibly during regional metamorphism. Merenskyite is the only other major PGM phase and is present as anhedral blebs that are completely enclosed within magnesian calcite or chalcopyrite. Michenerite, maslovite, moncheite and two unknown minerals occur infrequently within Cu-rich vein ores and in samples from deformed, sheared areas of Zone 2.

MAGMATIC FRACTIONATION OF PGE

The separation of immiscible sulphide liquids from silicate magmas leads to the production of a monosulphide solution (MSS) during subsequent cooling, and a fractionated Cu-rich sulphide liquid (Mostert *et al.* 1982) that leads to the crystallization of an intermediate solid solution (ISS) (Skinner *et al.* 1976). Pt, Pd, Au and Cu are incompatible elements and are not retained during crystallization of MSS from a sulphide liquid. PGM in the Katinniq and Zone 2 lenses reflects these associations. Pentlandite and pyrrhotite, which were the first to exsolve from the MSS, host predominantly Pt-bearing PGM, including sperrylite. These minerals reflect the PGE that were held in the MSS and not fractionated into the Cu-rich liquid. Conversely, Cu-rich veins and cusps contain predominantly Pd-bearing minerals, indicating a strong association between Pd-bearing PGM and a residual chalcopyrite assemblage. Although platinum is also present in evolved Cu-rich sulphides, the Pt in massive sulphides suggests that some Pt was retained in the MSS and not fractionated into the Cu-rich liquid.

During crystallization of an immiscible sulphide liquid Cu fractionates from Ni, but also Te, Bi and Sb fractionate and predominantly concentrate in the Cu-rich liquid. They form Te-, Bi- and Sb-bearing minerals, especially PGM, at the edges of sulphides, principally chalcopyrite. Although the solubility of PGE in sulphides decreases with temperature, it is not clear whether the PGM at Katinniq and Zone 2 formed during late stage magmatic crystallization associated with late magmatic concentrations of As, Te, Bi and Sb or formed in solid solution in the sulphides and were expelled during cooling to form discrete PGM.

LOW TEMPERATURE HYDROTHERMAL REMOBILIZATION

Textural observations indicate alteration and remobilization of PGM by a low-temperature hydrothermal fluid. Extensive silicate alteration to tremolite and biotite, and serpentinite and the abundance of chlorite (frequently associated with sperrylite), talc and niccolite (strongly associated with sudburyite), as well as textural features, suggest the presence of a low-temperature fluid. In terms of PGM, merenskyite and sudburyite are frequently associated with Mg-rich calcite and are concentrated in sheared zones (predominantly in the Zone 2 pit). PGM that occur enclosed within carbonates may be relict minerals that have been surrounded by the carbonates, or recrystallized from a circulating fluid in fluid flow pathways. PGM that occur infrequently throughout the rest of the Raglan deposit are most prolific in secondary veins and sheared zones. These ores show the greatest diversity in PGM, although these are predominantly Pd-bearing. Pd is generally considered more mobile than Pt and this is reflected in the distribution of Pd-bearing PGM in relation to sperrylite, the main Pt-bearing PGM at Raglan. The more heavily faulted areas such as Zone 2 are likely to contain more Pd antimonides and tellurides locked in carbonate gangue, whereas PGM in less sheared orebodies such as Katinniq, have a stronger association with sulphides.

Pd also entered niccolite during late stage mobilization. The association of sudburyite with NiAs may suggest that Pd was released from solid solution in the niccolite. However, the presence of Pd remaining in solid solution indicates a separate phase of discrete mineralization i.e. the associated sudburyite minerals did not exsolve from Pd in the NiAs. The complete absence of any other PGE with niccolite may suggest that Pd is more mobile at low temperatures. The presence of this particular phase may have been responsible for the “fixing” of sudburyite at this point, in close association with Pd-bearing niccolite. This fixing in itself suggests mobilization of Pd subsequent to magmatic crystallization. PGM formation in the studied Raglan lenses was the result of a polyphase process, controlled by magmatic fractionation and late-stage alteration and remobilization by a low-temperature hydrothermal fluid.

REFERENCES

- Dillon-Leitch H. C. H., Watkinson D. H. and Coats C. J. A. 1986. The distribution of platinum-group elements in the Donaldson West deposit, Cape Smith Belt, Quebec. *Economic Geology* **81**, 1147-1158
- Gillies S. L. 1993. Physical volcanology of the Katinniq peridotite complex and associated Fe-Ni-Cu (PGE) mineralization, Cape Smith Belt, Northern Quebec. Unpublished M.S.c Thesis, University of Alabama, Tuscaloosa, 146.
- Lesher C. M. 1999. Regional Stratigraphic, Structural and Metamorphic Setting of the East Central Cape Smith Fold Belt. Chapter 2 in Lesher (editor), Komatiitic-Peridotite-Hosted Ni-Cu-(PGE) Deposits of the Raglan Area, Cape Smith Belt, New Quebec. Guidebook Series, v. 2, Mineral Exploration Research Centre, Laurentian University, Sudbury, 17-34.
- Mostert A. B., Hofmeyr P.K. . and Potgieter G. A. 1982. The platinum-group mineralogy of the Merensky Reef at the Impala Platinum Mines , Bophuthatswana. *Economic Geology* **77**, 1385-1394
- Skinner B. J., Luce F. D., Dill J. A., Ellis D. E., Hagan H. A., Lewis D. M., Odell D. A., Sverjensky D. A. and Williams N. 1976. Scientific Communications. Phase Relations in ternary portions of the system Pt-Pd-Fe-As-S. *Economic Geology*, **71**, 1469-1475.

7. GENERAL

H₂O: A FUNCTIONAL ANALOGUE FOR CONTINENTAL MARGIN RIFT TECTONICS?

STEPHEN A. PREVEC

Economic Geology Research Institute - Hugh Allsopp Laboratory, University of the
Witwatersrand, PO WITS 2050, Johannesburg, South Africa, e-mail:
006spa@cosmos.wits.ac.za.

SYNOPSIS

Rifted continental margins are an important facet of craton development and evolution. Two relatively well-studied rifts, the Palaeoproterozoic Huronian rift (Canada), and the Jurassic Lebombo rift (South Africa) are summarized to demonstrate both the insights and limitations of our understanding of rift evolution, particularly in terms of magmatic evolution. The use of Icelandic glacial outbursts (*jökulhlaups*) as an analogue model provides a fresh perspective on crustal extension and associated magmatic development. Specifically, the nature of stress development, fracture propagation and dyke, pluton and extrusive development may be examined in light of a ice-water analogue, where existing geochemical models and geochronology are insufficient to provide unambiguous solutions.

INTRODUCTION

Aspects of large-scale geological phenomena such as rates of process and chronological sequence must be inferred from resultant phenomena, or quantitative evaluation of individual aspects of fortuitously preserved stages. In general it is with some difficulty that we can reproduce the physical processes taking place and thus derive information directly rather than inferring it. In scale models, all key parameters are represented in the model in order to replicate the natural environment, as reflected by a single or specific prototype case. Typically this is impractical, and compromises must be reached by compensating 'realistic' values of some key parameters by varying others. Ultimately, models which obey 'similarity of process', but are not based on a specific physical prototype and are therefore not quantitatively constrained in terms of process, are referred to as 'analogue' models (Peakall et al., 1996).

Tectonic analogue models require a rigid, brittle crust overlying more buoyant liquid of the same average composition, but where the interactions occur on a time scale conducive to study. This environment exists in the case of ice layers underlain by water, providing us with a natural analogue model for silicate crust. The brittle ice sheet provides downward thrust, by gravity, onto incompressible liquid water trapped below. This circumstance exists on Iceland, a particularly well-studied example, where glacial ice sheets are underlain by magmatic heat sources. In this study, the behaviour of water in glacial ice is examined, and compared with our understanding of silicate systems in the form of continental rift zones. One ancient and one recent example are presented; the Palaeoproterozoic Huronian rift in Canada, and the Jurassic Lebombo rift in South Africa, respectively.

RIFTING OF CONTINENTAL CRUST

Ancient rifting: ca. 2500 Ma Huronian volcanism, magmatism and sedimentation, Canada.

The Huronian sequence represents the southern boundary of the Archaean Superior Province, central Canada. The Huronian comprises a sequence of continental flood basalts, associated with lesser rhyolitic lavas and tuffs, and a suite of leucogabbroic plutons and sills, and with granitic plutons, locally, cut by late dolerites. Ultramafic rocks are essentially absent. The sequence is interpreted as a rift zone resulting from doming and rifting, such that a radiating dyke swarm to the north, represents the aulacogenic failed north-south arm of the rift.

In spite of extensive field mapping and petrographic study, geochemical and isotopic studies, and an extremely thorough and up-to-date (U-Pb zircon) geochronological database, the emplacement sequence and the genetic relationships between the rift constituents remains ambiguous. Field relationships could not clearly distinguish the chronological relationship between the Superior Province granites and greenstones, the Huronian basalts, and the leucogabbroic plutons. The derivation of models is further

complicated by syn-emplacement crustal assimilation and the difficulty in establishing parental magma compositions.

Juvenile rifting: ca. 200 Ma Karoo sedimentation, volcanism and magmatism, South Africa.

The Lebombo 'monocline' represents the eastern boundary of the Karoo province of sediments, volcanics, and intrusive dykes. The magmatic and volcanic rocks are on the aulacogenic side of the rift, associated with post-Gondwanaland breakup, of which the rifting event is a part. The existing 'monocline' consists of a bimodal volcanic sequence, consisting mainly of picritic to tholeiitic basaltic and rhyolitic rocks, with minor volumes of nephelinitic rocks present. There are minor gabbroic rocks intrusive into the basaltic pile, and the host rocks and volcanics are cut by dolerite dykes.

Investigation of the magmatic rocks of the Lebombo has provided genetic models for each component based on fractionation of distinct mantle sources and subsequent minor syn-emplacement fractionation and contamination. At least three different mantle sources plus metasomatic enrichment have been suggested for the magmatic rift components. Few systematic genetic relationships are apparent on this basis. Age constraints on this sequence are limited to Rb-Sr whole-rock dates, plus a very few recent unpublished zircon dates. The result is a poorly-constrained overall time-span for rifting and age dates which, in some instances, contradict field relationships.

RIFTING OF ICE SHEETS

Ice-fracturing during glacial outburst floods, or jökulhlaups, provide well-studied examples of extensional environments near the margins of thick sheets of ice, underlain by upwelling, low viscosity compositional equivalents. Hydraulic pressure is built up beneath the glacier by flooding. Water can subsequently extrude via two mechanisms; it can traverse the bedslope, and eventually extrude along a linear fracture system parallel to the glacier margin, and water can ascend existing fractures or create new ones (hydrofractures) and extrude as non-linear, localised outbursts.

Roberts et al. (2000) depict various manifestations of characteristic supraglacial fracture patterns from water extrusion, including features analogous to doming (albeit by reverse faulting as opposed to ductile uplift), caldera collapse (brittle, as normal-faulted gräbens, as well as more ductile sinking), normal-faulted half-gräbens, and chaotic fracturing from a single feeder outlet ascending into a veined network.

Flood hydrographs (showing discharge volumes against elapsed time) typically indicate that a disproportionately large component of the discharge in the first half of the total discharge time. On the basis of sediments deposited by ascending water dykes, Waller et al. (2001) identify two discrete stages of extrusion. First, there is an early low-energy, steady, laminar flow phase, associated with irregular fracture pathways. This is followed, and crosscut, by a more active, high flow, actively erosional (turbulent) phase, directed through major, linear channels, and containing xenoliths from the glacier bed. This appears to represent the main phase of eruption, prior to a further, discrete waning phase.

DISCUSSION

Multi-component magmatic suites are relatively complex systems. The components of these suites are complicated by local assimilation of host rocks, different crystallisation histories and degree of preservation. Identification of parental compositions and resultant magmatic reconstructions are potentially very model-dependent and subjective. Mafic rocks are less conducive to high-precision geochronology, and the felsic components are volumetrically less and consist largely (if not exclusively) of remelted pre-rifted crust, leading to large xenocrystic contributions. Ultimately, for even relatively well-studied, tectonically well-constrained rift environments, the emplacement sequence and magmagenesis remain largely incoherent.

Relating the processes involved in ice-fracturing to the rifts may significantly clarify the evolutionary process. The ascent mechanisms involved in hydraulic fracturing, whether applied to ice (e.g., Roberts et al., 2000), or to studies of silicate dyke propagation mechanisms (e.g., Pollard, 1987), are based on the same precepts of propagating fractures through an elastic medium. A sequence may therefore be envisioned in which mantle melting produces a buoyant reservoir of magma, pooling at the base of the crust (whether associated with a plume or induced by crustal extension should be irrelevant). Ascent of the magma into brittle, elastic crust exploits existing zones of weakness where possible, and where it is not, creates new ones by hydraulic fracturing. Random networks of 'dry' fractures ahead of the advancing dyke tips could ultimately provide reservoirs for magma chambers. The chambers would be both fed by

and cross-cut, after ‘freezing’, by ascending dykes. This is post-dated by extrusion of liquid being fed by the magma source, with changes in source, assimilant content and composition and (partial) remelting contributions being dictated by the flow style as buoyant pressure (periodically) waxes and wanes.

CONCLUSIONS

Our grasp of even well-studied rift systems is limited by restrictions of preservation, exposure, scale, and methodological criteria. While the application of fluid dynamic theory and fracture propagation to interacting liquids and solids is well-developed in geology, glacial ice tectonic analogues evolve rapidly and cause and effect are more readily apparent. It is likely that a great deal of complementary and perhaps new information may be derived by further examination of ice and silicate analogues.

ACKNOWLEDGEMENTS

Philip Marren is acknowledged for his advice, assistance, and Icelandic expertise donated to the author.

REFERENCES

- Peakall, J., Ashworth, P. and Best, J. (1996) Physical modelling in fluvial geomorphology: principles, applications and unresolved issues in *The Scientific Nature of Geomorphology. Proceedings of the 27th Binghamton Symposium in Geomorphology* (edited by B.L. Rhoads and C.E. Thorn): 221-253.
- Pollard, D.D. (1987) Elementary fracture mechanics applied to the structural interpretation of dykes in *Mafic Dyke Swarms*, Geological Association of Canada Special Paper 34 (edited by H.C. Halls and W.F. Fahrig): 5-24.
- Roberts, M.T., Russell, A.J., Tweed, F.S. and Knudsen, Ó (2000) Ice fracturing during jökulhlaups: implications for englacial floodwater routing and outlet development. *Earth Surface Processes and Landforms*, 25: 1429-1446.
- Roberts, M.T., Russell, A.J., Tweed, F.S. and Knudsen, Ó (2001) Controls on englacial sediment deposition during the November 1996 jökulhlaup, Skei_arárjökull, Iceland. *Earth Surface Processes and Landforms*, 26: 935-952.
- Waller, R.I., Russell, A.J., Van Dijk, T.A.G.P. and Knudsen, Ó. (2001) Jökulhlaup-related ice fracture and supraglacial water release during the November 1996 jökulhlaup, Skei_arárjökull, Iceland. *Geografiska Annaler*, 83A: 29-38.

JIGSAW BRECCIAS

AN INTRODUCTION TO HYDROTHERMAL BRECCIAS

ALBERTO LOBO-GUERRERO

Economic Geology Research Institute, University of the Witwatersrand,
Private Bag 3, Johannesburg, 2050, South Africa
e-mail: ageo@iname.com

SYNOPSIS

Field identification of hydrothermal breccias constitutes a useful tool for mineral exploration geologists, especially given the number of metallic mineral deposits in magmatic arcs that are associated with brecciod rocks. Hydrothermal breccias are among the most favorable host rocks to contain hydrothermal orebodies of any size. Their classification and description is complex, and working knowledge of these rocks is not widely spread among practicing geologists in many parts of the world. Breccias generally grade from one type to another, displaying a wide range of fragmentation and displacement of their angular clasts. Distinguishing a breccia contributes to identify the geological environment in which it formed, and helps to build a model of eventual mineral deposits. This article briefly summarizes the concepts of breccia, hydrothermal breccia, intrusive breccia, matrix and fragments. It details the geometry of several types of hydrothermal breccias, with emphasis on description and characterization of mosaic breccias (or jigsaw breccias), special type of rock where fragments could be “put back together” again if the matrix was removed. A systematic methodology to describe hydrothermal breccias is described. Finally the methodology is shortened into a table or checklist with the suggested order of terms to be used in the field and/or rock laboratory for rocks that may be hydrothermal breccias.

Most of the hydrothermal deposits in magmatic arc environments are genetically associated with brecciod rocks. Porphyry copper, sediment-hosted gold (incorrectly so-called “Carlin-style” or “Carlin-type”), high and low sulfidation, some mesothermal, and of course subvolcanic breccia pipe deposits in Cordilleran environments display clear relationships with these rocks (For examples, see CARRILLO [2000] and SILLITO [1985]). There is a large variety of breccia types, intimately related with one another, that change radically when mapped in the field (Fig.1); their field recognition is an important tool for exploration geologists. This paper will deal with the classification and description of *jigsaw breccias* that occur as part of magmatic hydrothermal (Fig.1), phreatomagmatic or phreatic breccias (See CORBETT & LEACH [1996] for description of these types of breccias). Some of the best host rocks for low-grade hydrothermal ore deposits are breccias, because they occur at the precise point of second boiling of hydrothermal systems. This occurs where mineralizing fluids precipitate after sudden pressure changes produced by relief in pressure during the explosive fragmentation of rocks.

The instantaneous fragmentation of rock produces a significant release of energy in magmatic systems. BURNHAM [1985] clearly explains the process and the formation of stockworks in hydrothermal systems. HEDENQUIST & LOWENSTEIN [1994] also describe the process.

Brecciation of any origin generates open space because there is an inherent volume increase. Hydrothermal explosion breccias are prime candidates for the infiltration of hydrothermal solutions, because breccias are the “sponges” that “suck” mineralizing fluids. The ore load carried by mineralizing fluids is precipitated in pores of the breccias and reactive surfaces of the fragments. As might be expected, hydrothermal breccias are especially characteristic of epithermal precious metal ore deposits.

Breccias associated with porphyry systems form at greater depths and are more likely generated by hydraulic fracturing than by explosion (See BURNHAM [1985]). Hydrothermal breccias are often confused with tuffisites (Francis [1989]) and with other extrusive volcaniclastic rocks (HIBBARD [1995], LASNICKA [1988] and CAS & WRIGHT [1987]).

"A breccia is a clastic rock composed of fragments held together by a matrix and containing cavities filled by post-brecciation hydrothermal minerals" (CORBETT & LEACH [1996 p. 45]). Intrusive breccias are a "heterogeneous mixture of angular to rounded fragments in a matrix of clastic material, which has been mobilized and intruded into its present position along pre-existing structures" (JACKSON [1997 p. 333]). They are commonly hydrothermally altered. Fragments or broken rock become progressively milled with increased brecciation. Matrix is the fine rock material between the fragments and, depending on the degree of milling, may grade into fragments. Breccias are either matrix or fragment supported. The majority of the mineralized component of breccias is introduced as hydrothermal fluid and so occurs within the matrix; but sometimes breccia fragments react with mineralizing fluids and can host ore. A mineral cement holds fragments and matrix together. Cavities develop during breccia formation and are filled by hydrothermal minerals including metallic mineralization; cavities then are an integral part of the brecciation and mineralization processes (CORBETT & LEACH [1996, p. 45] and JACKSON [1997, p.82]).

A jigsaw breccia is one in which the fragments can be fitted back together by removal of the matrix (JACKSON [1987], CAS & WRIGHT [1987]). A commonly used synonym is mosaic breccia. It is characterized by fragments that "fit" together as a result of minor expansion without significant rotation, reactive replacement along a network of fractures (called crackle breccia), or mechanical repacking of angular fragments (LAZNICKA [1988], HIBBARD [1995 p. 401]). Stockworks are a variety of jigsaw breccia, formed chiefly by reactive replacement in crackle breccia. Thus, jigsaw breccias exhibit no input of exotic fragments and little fragment rotation or rounding. The matrix tends to be composed substantially of introduced hydrothermal components and not of locally derived milled material. There is obviously an overlap between the use of the terms dilatational and jigsaw breccias (CORBETT & LEACH [1996]). It seems logical that higher-pressure environments such as those in which copper porphyry systems form are less likely to have rotated and displaced fragments. Nevertheless, the Brady Breccia at El Teniente Mine in Rancagua, Chile, contains fragments that are the size of an entire one-floor family house (personal experience of the author).

Accurately mapped field descriptions of breccias serve as an aid to location within a mineralised system. Extreme care should be placed on interpretation. For example, a jigsaw breccia in the carapace to an intrusion (Fig. 1) may be barren and not vector towards higher grade mineralization in the same manner as a jigsaw breccia in a high sulfidation system. Nevertheless, identifying the rock precisely will greatly aid in interpreting the geological environment, and help piece the model of the eventual ore deposit.

If a simple maxim is to be remembered from this paper it could be: *Description of breccias should be objective*. Descriptive terms are more useful to qualify breccias than genetic terms. This is especially true during initial field mapping. Hypothesis on the genesis of a given breccia may be kept on field notes or on reports, but descriptions should always be as objective as possible to allow for future interpretation. The method of multiple working hypothesis (CHAMBERLIN [1897]) should be applied word by word.

There is abundant literature to aid in description of brecciod rocks and their textures. A working group at the University of Queensland, Australia has made significant contributions in this respect. See for example DOND, MORRISON & JAIRETH [1995], MORRISON [1999], MORRISON, DOND & JAIRETH [1999]. JEBAK [1992] is also a very helpful publication to aid in field description of breccias and vein systems as well as on their genesis.

Precise data should be collected, to be able to identify and correlate different types of hydrothermal breccias. In general, they should be described following the procedure described on the table below. In order to obtain better results, fresh cut surfaces should be sought, and observed while wet.

PROCEDURE TO DESCRIBE HYDROTHERMAL BRECCIAS DURING FIELD WORK

PARAMETER	NOTES
Polymictic/oligomictic fragments	Differing compositions rare, describe each & relative percentages of abundance.
Fragment shape	Rectangular, regular or aleatory, "honey-comb", etc.
Fragment size/shape gradation	Directional (If suitable, statistical description of size and angularity, think in terms of stresses). Lateral variation along the longest direction of the brecciod body.
Fragment rotation	Approximate amount, if any. Evidence of advance direction?
Matrix- or grain-support	Percentage of each in the whole rock
Matrix composition	Crystals, smaller fragments, glass, etc. Evaluate relative proportions of each component and describe as a tuff (see HIBBARD [1995] and CAS & WRIGHT [1987]).
Cement of matrix	Opaline silica, quartz, albite, K-feldspar, alunite, dolomite, etc.
Vugginess	%, type, size, shape
Mineralization	Type and location (in matrix, fragments or both)
Alteration	Whole rock, gradual away from matrix, etc.

Brecciod bodies should be delimited in the field as far as possible. Normally jigsaw breccias will grade from moderately fresh, unfractured rock on one side, through fractured rock and jigsaw breccia, to completely fractured and remobilized breccia on the other. Sometimes the remobilized side is missing, and it is represented by a fault or a later intrusive body (Fig.1). If possible, such contacts must be literally followed step-by-step by trenching, to produce an accurate depiction the system.

Another important cartographical aspect is that the allochtony or autochtony of the brecciod rock as a whole should be established in the field. Repetitive explosive events may have remobilized the bodies. Transported jigsaw breccias will be less significant as guides to ore than in-situ jigsaw breccias. At a map scale, gradation of the character of jigsaw breccias that are in place will serve as a powerful exploration tool.

REFERENCES

BURNHAM, CW [1985] "Energy Release in Subvolcanic Environments: Implications for Breccia Formation", *Economic Geology*, v. 80, pp. 1515-1522.

CARRILLO L, VM [2000] "Brechas de Atrición y Mineralizaciones Auríferas en las Minas de Miraflores (Quinchía, Risaralda) y su Relación con un Cuerpo Tipo 'Brecha-Pipe'", *Boletín de Geología*, Bucaramanga, Colombia, v. 22, 37, pp. 28-38.

CAS, RAF & WRIGHT, JV [1987] *Volcanic Successions Young and Ancient*, Allen and Unwin, London, 528 p.

CHAMBERLIN, TC [1897] "The Method of the Multiple Working Hypothesis", *Journal of Geology*, v. V, pp. 837-848, reprinted in Mather, KF & Mason, SL, *A Source Book in Geology 1400-1900*, Harvard University Press, Cambridge, Massachusetts, pp. 604-812.

CORBETT, G & LEACH, T [1996] *Southwest Pacific Rim Gold-Copper Systems: Structure, Alteration, and Mineralization*, workshop presented for SEG/SME at Phoenix, Arizona, 8-11

March, 400 p. Document corrected and re-edited in 1998 as *Special Publication No. 6*, Society of Economic Geology.

DOND, G, MORRISON, G & JAIRETH, S [1995] "Quartz Textures in Epithermal Veins, Queensland – Classification, Origin, and Implication", *Economic Geology*, v. 90, 1841-1856.

FRANCIS, EH [1989] "Tuffisite" and "Volcanic Neck" in Bowes, DR editor, *The Encyclopedia of Igneous and Metamorphic Petrology*, Encyclopedia of Earth Sciences, Van Nostrand Reinhold, New York, p. 574-575, p. 603-605.

HEDENQUIST, JW & LOWENSTEIN, JB [1994] "The Role of Magmas in the Formation of Hydrothermal Ore Deposits", *Nature*, v. 370, 18, pp. 519-526.

HIBBARD, MJ [1995] *Petrography to Petrogenesis*, Prentice Hall, Englewood Cliffs, N.J., 587 p.

JACKSON, JE [1997] *Glossary of Geology*, 4th ed., American Geological Institute, Alexandria, Virginia, 769 p.

JÉBRAK, M [1992] "Les Textures Intra-Filoniennes, Marqueurs des Conditions Hydrauliques et Tectoniques", *Chronique de la Recherche Minière*, 506, pp. 25-35.

LASNICKA, P [1988] *Breccias and Coarse Fragmentites, Petrology, Environments, Associations, Ores*, Elsevier, New York, 488 p.

MORRISON, G [1999] *Describing and Understanding Veins and Breccias*, short course notes, James Cook University, Townsville, Queensland, Australia, 24 p.

MORRISON, G, DOND, G & JAIRETH, S [1999] *Textural Zoning in Epithermal Quartz Veins*, Klondike Exploration Services, Townsville, Queensland, Australia, 33 p.

SILLITOE, RH [1985] "Ore-Related Breccias in Volcanoplutonic Arcs", *Economic Geology*, v. 80, pp. 1467-1514.

WRIGHT, AE [1989] "Breccia Pipe" and "Diatreme" in Bowes, DR editor, *The Encyclopedia of Igneous and Metamorphic Petrology*, Encyclopedia of Earth Sciences, Van Nostrand Reinhold, New York, p. 64, p. 123-125.

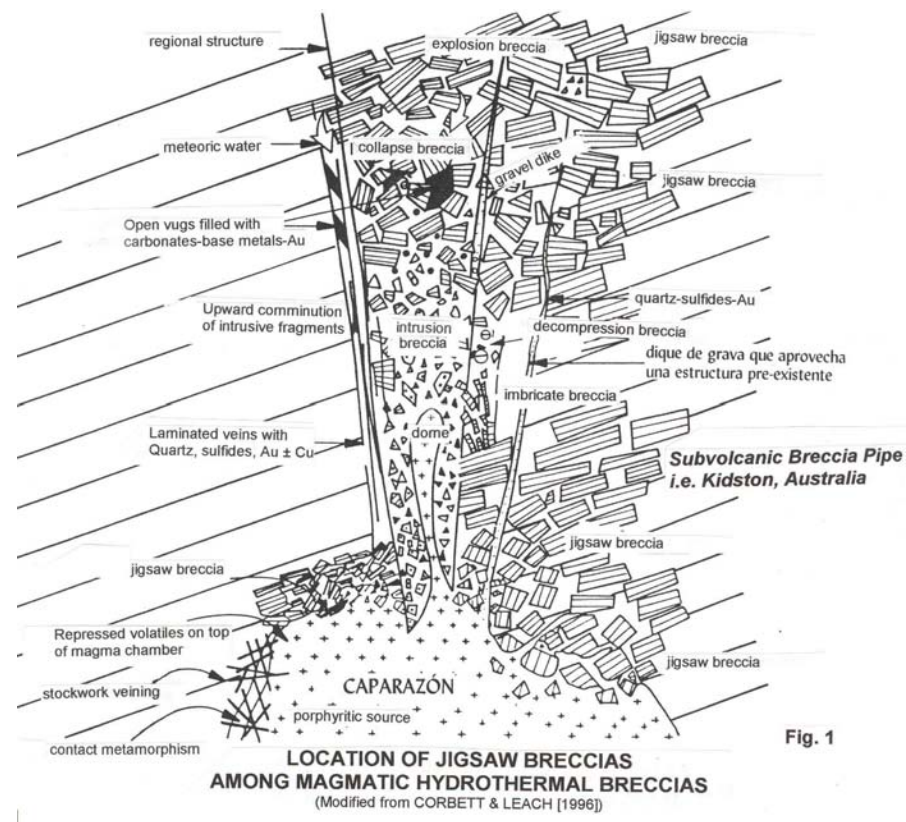


Fig. 1 Location of Jigsaw Breccias Among Magmatic Hydrothermal Breccias.
Example from a subvolcanic breccia pipe in the Kidston deposit, Australia. Note that jigsaw breccias grade into different types of breccias depending on their specific location in the magmatic system.

GEOLOGY AND STRUCTURAL SETTING OF THE JAMIESON WINDOW, MT USEFUL SLATE BELT, VICTORIA AUSTRALIA

F. WIELAND

Impact Crater Research Group, School of Geosciences, University of Witwatersrand,
Private Bag 3, P.O. Wits 2050, Johannesburg
e-mail: wielanf@science.pg.wits.ac.za

SYNOPSIS

The Jamieson Window represents one of four structural windows within the Mount Useful Slate Belt at the eastern margin of the western sub-province of the Lachlan fold belt in SE Australia. The area is part of the Mount Wellington Fault Zone and records a history of complex deformation and tectonism during Paleozoic times. A Cambrian greenstone sequence forms the core of the Jamieson Window. It comprises andesitic to felsic lava, breccias and volcaniclastic rocks and minor andesitic lavas. Geochemical data indicate that these volcanic rocks are related to a calc-alkaline series and derived from a magmatic arc in a subduction-related setting. The margin of the window is a shear zone, separating the Cambrian greenstones from a sequence of siliciclastic meta-sedimentary rocks of Ordovician to Devonian age. Metamorphism in and around the Jamieson Window is low grade, characterized by prehnite-pumpellyite mineral assemblages. At least four deformation events can be recognized. D1 produced a pervasive cleavage (S1), which is developed throughout the whole window. A crenulation cleavage (S2) related to the second deformation event (D2) shows the same pattern in distribution and development as the S1 cleavage. The D3 deformation phase is related to a regional shearing and thrusting event. A fracture cleavage (D4) has been observed only in some parts of the window. This non-pervasive deformational event produced rare open and upright folds. A last stage of deformation is related to the uplift of the area since Mesozoic and involved block-faulting and vertical off-sets within the stratigraphic units. A model of backthrusting is proposed to account for the current structural set-up of the Jamieson Window. This involves a) regional scale low-angle thrusting towards the east and b) a large scale-assymmetric fold related to a back-thrust towards the west. Other models are currently debated.

The Lachlan Orogen in southeastern Australia comprises a major fold belt with a present length of approximately 700 km, which formed along the Pacific margin of Gondwanaland in Palaeozoic time (Coney et al., 1990). It consists of three subprovinces, known as the western, the central and the eastern subprovinces, which differ in rock types, metamorphic grades, geological history and tectonic evolution.

The Mt Wellington Fault Zone is a 20 km wide and 135 km long, north-northwest-striking zone (Gray and Foster, 1998) that belongs to the eastern part of the Melbourne Zone, which itself forms the eastern margin of the western subprovince of the Lachlan Orogen.

Within this fault zone there are a number of fault-bounded blocks comprising Cambrian volcanics, volcaniclastics and minor intrusives (Cherry, 1999). The Jamieson Window represents one of four structural windows within the Mount Useful Slate Belt at the eastern margin of the western subprovince of the Lachlan fold belt. The northwest-southeast elongated pattern of the fault-bounded window reflects the regional northwest trend. The Jamieson Window can be divided into two domains. In the western domain structural features, S₁ foliation and S₂ crenulation cleavage, are very regular, but in the eastern part the deformation intensity increases and the structure becomes more complex. A Cambrian greenstone sequence forms the core of the Jamieson Window. It comprises andesitic to felsic lava, breccias and volcaniclastic rocks, and minor andesitic lavas.

The Cambrian volcanic rocks of the Jamieson Window show effects of two phases of metamorphism: an earlier stage of burial metamorphism followed by regional metamorphism. The geochemistry of the volcanic rocks has been modified by low-grade metamorphism and hydrothermal alteration. The bulk of the greenstones has been affected by upper zeolite to lower greenschist facies, characterized by prehnite-pumpellyite mineral assemblages. Typical minerals reflecting this assemblage are quartz,

albite, chlorite, calcite and epidote. Geochemical data indicate that these volcanic rocks are related to a calc-alkaline series and derived from a magmatic arc in a subduction-related setting. The margin of the window is a shear zone, separating the Cambrian greenstones from a sequence of siliciclastic meta-sedimentary rocks of Ordovician to Devonian age.

A minimum of four deformation events have been recognized that affected the rocks in the Jamieson Window. The first deformation phase produced a pervasive cleavage (S_1) which is well developed and is evident throughout the whole window. A crenulation cleavage is related to the second deformation event showing the same pattern in distribution and development as the S_1 cleavage. Due to the strong weathering and unsuitable outcrop conditions, only F_2 axis directions could be measured. A third type of fracture cleavage is present in some parts of the project area and is related to the third deformation phase, D3, that is related to a regional shearing and thrusting event. This weaker deformational event produced rare open and upright folds. A last stage of deformation is related to the uplift of the area since Mesozoic times and involved block-faulting and vertical off-sets within the stratigraphic units.

The complexity of structural features and inadequate outcrop conditions in the Jamieson Window renders any interpretation of the structural development of the area difficult. The few existing studies of the Jamieson Window and their various interpretations of the structural setting further complicate the assessment of the structural development of this area.

A model of backthrusting is proposed to account for the current structural set-up of the Jamieson Window. This involves a) regional-scale low-angle thrusting towards the east and b) a large scale-asymmetric fold related to a back-thrust towards the west. Other models are currently debated.

ACKNOWLEDGEMENTS

This work is based on the author's M.Sc. project carried out at the University of Heidelberg, Germany, under supervision of Prof. R.O. Greiling and in Australia at the Monash University of Melbourne, under supervision of Dr. F. Bierlein.

REFERENCES

- Cherry, D.P., 1999. The Cambrian Jamieson Volcanics, Geology and Mineralisation, Barkly River Greenstone Belt, Eastern Victoria, B.Sc. (Hons.) Thesis, University of Tasmania (unpubl.)
- Coney, P.J., Edwards, A., Hine, R., Morrison, F. and Windrum, D., 1990. The regional tectonics of the Tasman Orogenic System, eastern Australia. *Journal of Structural Geology*, v. 12, p. 519-543.
- Gray, D.R., 1997. Tectonics of southeastern Australian Lachlan Orogen: structural and thermal aspects. In: *Orogeny through time*, eds. J.P. Burg and M. Ford. Geological Society of London Special Publication, 121, pp. 149-177.
- Gray, D.R. and Foster, D.A., 1998. Character and Kinematics of faults within the turbidite-dominated Lachlan Orogen: implications for tectonic evolution of eastern Australia: *Journal of Structural Geology*, Vol. 20, No. 12, pp. 1691-1720.
- VandenBerg, A.H.M., Wilman, C.E., Hendrickx, M., Bush, M.D. and Sands, B.C., 1995. The geology and prospectivity of the 1993 Mount Wellington Airborne Survey area. Geological Survey of Victoria VIMP Report No. 2, Melbourne.
- Wieland, F. 2001. Geology and Structural Setting of the Jamieson Window, Mt Useful Slate Belt, Victoria, Australia, M.Sc. (Diploma) Thesis (unpubl.).

REUNITING LOST CONTINENTS – FOSSIL REPTILES FROM THE ANCIENT KAROO AND THEIR WANDERLUST

BRUCE S. RUBIDGE

Bernard Price Institute for Palaeontological Research, School of Geosciences,
University of Witwatersrand, Johannesburg, P.O. Wits 2050, South Africa.

SYNOPSIS

Fossil discoveries from South Africa have greatly expanded knowledge of the development of life on Earth. In particular the enormous palaeontological wealth of the Karoo, covering a period of at least 80 million years from the Permian to the Jurassic, has enhanced understanding of the evolution of important tetrapod lineages, and ultimately mammals and dinosaurs as well. These fossils provide the best record of continental Permian to Jurassic faunal biodiversity patterns, and have been crucial to understanding of the nature of the Permo-Triassic extinction in the continental realm as well as giving insight on other extinction events. Recent studies of stratigraphic and geographic distribution patterns of Karoo fossils have enhanced biostratigraphic resolution and global correlation of vertebrate faunas from the Permian to the Jurassic. This in turn has led to a better understanding of biodiversity across Pangaea, and also the places of origin and initial diversity of early reptile evolutionary lineages. Many of these originated in the southern African portion of the Gondwanan continent. Combination of palaeontological and sedimentological studies has led to new basin development models and solved problems which each discipline in isolation could not have achieved.

INTRODUCTION

The main Karoo basin of South Africa is a Late Carboniferous-Middle Jurassic retroarc foreland fill in front of the Cape Fold Belt in relation to subduction of the palaeo-Pacific plate underneath the Gondwana plate. Subsequent to the early Permian glaciation, global temperatures increased during the middle Permian to provide ideal conditions for the radiation of reptiles. Because of their largely continuous depositional record the rocks of the Karoo, which contain an abundance of fossils, provide the best record of the extended history of the development of Pangaean continental life. Although the initial amniote radiation took place in the northern hemisphere, later radiation occurred in Gondwana as well and many important reptilian lineages had their origins on this supercontinent. The end of Karoo sedimentation early in the Jurassic, midway through the reign of the dinosaurs, coincided with the fragmentation of Pangaea and massive outpourings of basaltic lava.

FOSSILS

When the oldest rocks of the Karoo (Dwyka Group) were deposited the only vertebrates in existence were fish and amphibians, although reptiles had recently made their appearance in the northern hemisphere. With the retreat of the Dwyka glacials, the climate in Gondwana warmed and the continent became populated by a great variety of fish, amphibians and reptiles. Numerous important new fossil discoveries have recently been made in the Karoo and have greatly clarified the early evolution and diversification of reptiles. These discoveries include distant ancestors of dinosaurs, tortoises and most importantly, of mammals.

FAUNAL DIVERSITY PATTERNS

Because of the very extensive and long fossil history represented by the rocks of the South African Karoo, coupled with the abundance of fossil forms, it has been possible to subdivide the rocks biostratigraphically based on their fossil content, and assign ages to each of the past faunal eras in the Karoo. The uniquely complete fossil record of the Karoo has enabled the correlation of rock units from all over the world with those of South Africa, based on their fossil content.

Because radiometric markers are scarce in the Karoo, chronostratigraphic dating of the fossils relies on correlation of the fossil faunas of South Africa with better dated rocks elsewhere in

Pangaea. The time scales for the Permian and Triassic are very largely based on marine deposits, containing invertebrate fossils from Euramerica. As temnospondyl amphibians often occur in both marine and nonmarine deposits, they are very useful for correlation and dating, and have increasingly played a greater role in the correlation of Karoo sequences with those of other parts of the world.

GONDWANAN ORIGINS

Numerous amniote evolutionary lineages originated in the southern African portion of Gondwana. The distribution of tetrapod taxa present in both South Africa and other Pangean countries has allowed speculation as to possible routes of migration of early tetrapods around the world.

Stereospondyl amphibians - The presence of the most primitive stereospondyl amphibians only in Gondwana and nowhere else in the world strongly suggests that their initial radiation occurred in Gondwana and possibly in southern Africa. By the Triassic stereospondyls had a global distribution, but it is not yet clear whether this radiation occurred in the late Permian or early Triassic.

Anapsids - Although pareiasaurs and procolophonids have a global distribution across Pangaea, the oldest pareiasaurs and procolophonoids are from the lower Beaufort of South Africa. Optimisation of Gondwanan and Euramerican distributions of anapsid reptiles suggests that they diversified initially in the Gondwanan portion of Pangea.

Synapsids - Previous accounts favoured a Laurasian origin for therapsids, which then came to southern Africa via overland migrations. The discovery of a primitive therapsid fauna at the base of the Beaufort Group has led to a re-thinking of the place of origin of therapsids. Currently it is apparent that, apart from the Biarmosuchia, and possibly some of the dinocephalia, the most primitive therapsid radiations occurred in South Africa rather than Russia.

Diapsids - Younginiforms were the only diapsids in the Permian of South Africa, but the end Permian extinction allowed for the radiation of archosaurs and ultimately dinosaurs, in the early Triassic. Because of the depositional hiatus between the Beaufort and the overlying rocks of the Molteno Formation, coupled with the fact that the Molteno rocks generally do not preserve fossil tetrapods, almost nothing is known of the fauna of southern Africa during Carnian times save for footprints of theropod dinosaurs in the upper Molteno which are among the oldest remains of dinosaurs known. This was a crucial time in the evolution of the earliest dinosaurs, as by the time that the earliest fossil bearing rocks of the overlying Elliot Formation were being deposited, several different lines of dinosaurs were already well established.

Palaeobiogeographic and phylogenetic evidence suggests that in the early and middle Permian there was recognisable provincialism among parareptiles and therapsids, then the dominant amniote clades. This provincialism compromised during the Late Permian, so that by the Triassic there was global distribution of similar tetrapods. These ideas emphasise the very important part the South African rock record has played in elucidating the ancestry and biogeographic spread of the different tetrapod lineages.

EXTINCTION EVENTS – OPPORTUNITIES OR THREATS?

Gross generic level calculation of genera in the Karoo indicates marked faunal changes in the Karoo at the end of the *Tapinocephalus*, *Dicynodon* and *Euskelosaurus* zones. The first of these is the subject of a current study by the author and records the global extinction of the dinocephalia. The end-*Dicynodon* Assemblage Zone faunal turnover corresponds with the Permo-Triassic extinction, which was responsible from the decimation of 70 %? of animals on land and 90%? of marine organisms. The Beaufort Group preserves one of the best terrestrial records of this event and has been the subject of numerous studies recently. Of the 44 “reptilian” genera in the *Dicynodon* Assemblage Zone only three are among the 20 genera in the *Lystrosaurus* Assemblage Zone. The third extinction corresponds with the Triassic-Jurassic boundary and has been recognised as a global extinction event. In South Africa there is a

changeover from large prosauropod dinosaurs such as *Euskelosaurus* to small forms such as *Massospondylus*.

ENVIRONMENTAL RECONSTRUCTION

Tetrapod fossils have been useful in elucidating the palaeoenvironment of the Ecca-Beaufort palaeoshoreline contact around the basin. Stratigraphically higher in the Beaufort high-resolution taphonomic studies of fossils have enabled delineation of the spatial aspects of floodplain subenvironments within the lower Beaufort. More recently taphonomic studies have greatly assisted with environmental interpretation at the time of the Permo-Triassic turnover. In the Late Triassic-Jurassic Elliot Formation fossils have also been used in palaeoenvironmental interpretation, while palaeosol studies in the *Tritylodon* Acme Zone led to the recognition of regional base level changes in the Early Jurassic.

BASIN DEVELOPMENT STUDIES

Dated periods of compressional deformation in the Cape Fold Belt, the southern margin of the Karoo basin, led to sedimentary responses in the Karoo basin. Enhanced biostratigraphic subdivision has improved time resolution for the subaerial continental deposits of the basin. Recent research has suggested that the Karoo behaved as a partitioned basin with reciprocal proximal (foredeep) and distal (forebulge) deposition across the basin hingeline and has led to improved basin development models.

CONCLUSION

The enormous fossil richness of the Karoo is of particular importance in understanding the evolution of important tetrapod lineages, and ultimately dinosaurs and mammals. These fossils demonstrate Permian - Jurassic faunal biodiversity patterns and have been crucial to understanding of the nature of the end Permian extinction on the continental realm. Greater understanding of stratigraphic and geographic distribution patterns of these fossils has enhanced biostratigraphic resolution and global correlation of vertebrate faunas from the Permian to the Jurassic. This in turn has led to a better understanding of biodiversity distribution patterns across Pangaea, and also the places of origin and initial diversity of early tetrapod lineages.

The combination of multidisciplinary palaeontological and sedimentological studies has been of great use in basin development studies and have solved problems which each discipline in isolation could not have achieved. South Africa occupied a central position on the Gondwanan portion of Pangaea. Because of its uniquely extensive record, both in time and geography, the unravelling of the South African Karoo record is essential for further understanding of the development of Gondwana and indeed the entire Pangaean world.

oOo
